INVESTIGATIONS OF β-DIKETOENOLATO METAL COMPLEXES

ABSTRACT

The solution properties of a series of diamagnetic metal acetyl - acetonates have been investigated using several spectroscopic techniques. In the concentration range in which absorption spectra are readily measurable, i.e. 10^{-5} to ca. 10^{-3}M, it is shown that many of the metal acetylacetonates exhibit marked deviations from Beer's Law. These deviations are qualitatively interpreted in terms of an ionic model in which the complexes dissociate in ethanol solution: solvolysis of the acetylacetonate anion leads to the formation of free acetylacetone and the appropriate metal ethoxide or hydroxide.

All of the metal acetylacetonates examined phosphoresced in ethanol glasses at 77K. Although there are only minor differences in the emission spectra, a significant ordering of the measured lifetimes is observed consistent with the ionic model for the complexes. A heavy atom effect is discounted as an important process except with complexes containing very heavy metal ions. Non - exponential luminescence decays are found with the Group Ia and Group IIa metal acetylacetonates and these are explained by the presence in solution of the coordinated complex and the uncoordinated acetylacetonate anion.

The trend in relative ionic character of the metal acetylacetonates is corroborated by nmr spectral studies obtained in a variety of suitable solvents. The coordinating solvent DMSO - D6 gives the most complete series of results and the ratio of the ligand methyl and ring proton resonances is found to be 6:1 for each complex. The largest chemical shifts are observed with complexes such as $Al(AA)_3$ where the charge / radius ratio of the metal ion is large whereas the smallest chemical shifts are observed with complexes such as Cs(AA) where the charge / ionic radius ratio is small.

The possible self - association of some metal acetylacetonates has been investigated using molecular weight and nmr studies. The results suggest that the lanthanide complexes exist as dimers in non - polar solvents, that both monomers and dimers coexist in polar, weakly coordinating solvents and that solvated monomers are the sole solution species in strongly coordinating solvents. It is probable that a similar situation exists in solutions of some Group IIa metal acetylacetonates.

The fluorescence quenching of some protonated molecules by inorganic ions has been studied. Although it is not possible to unequivocally assign specific mechanisms, it is probable that anionic quenching occurs by charge transfer processes whereas cationic quenching occurs by energy transfer processes. An intermolecular energy transfer mechanism has similarly been ascribed to the phosphorescence quenching of the ligand triplet state of $Al(AA)_3$ by other $M(AA)_n$ complexes.

INVESTIGATIONS OF β-DIKETOENOLATO METAL COMPLEXES

A Thesis

presented for the degree of

MASTER OF SCIENCE

in the Faculty of Science of the

University of St. Andrews

by

James Albert Kemlo

United College of

St. Salvator and St. Leonard,

St. Andrews.

December 1976

Th 8888

DECLARATION

I declare that this thesis is my own composition, that the work of which it is a record has been carried out by me, and that it has not been submitted in any previous application for a Higher Degree.

This thesis describes results of research carried out at the Department of Chemistry, United College of St. Salvator and St. Leonard, University of St. Andrews, under the supervision of Dr. T.M. Shepherd since the 1st of October 1972.

J.A. KEMLO

CERTIFICATE

I hereby certify that James A. Kemlo has spent seven terms of research work under my supervision, has fulfilled the conditions of the Resolution of the University Court 1972 No. 2 (St. Andrews) , and is qualified to submit the accompanying thesis in application for the Degree of Master of Science.

T.M. Shepherd

Director of Research

ACKNOWLEDGMENTS

I should like to thank Dr. T.M. Shepherd for his continued interest, help and encouragement during the course of this work. My thanks are also due to J.D. Neilson and R.N. Napier for their cooperation in several projects, to Mrs. M. Smith for cheerfully operating the nmr spectrometer, to J. Bews for analysing all the samples used in the course of this work and to all my friends and colleagues too numerous to mention by name.

I am indebted to the University Authorities for allowing me to carry out this research and to Professor Lord J.M. Tedder and Professor P.A.H. Wyatt for permitting me to use the facilities of the Chemistry Department.

Finally, I should like to thank my wife and family for their love, patience and understanding.

CONTENTS

SUMMARY

The solution properties of a series of diamagnetic metal acetyl - acetonates have been investigated using several spectroscopic techniques. In the concentration range in which absorption spectra are readily measurable, i.e. 10^{-5} to ca. 10^{-3}M, it is shown that many of the metal acetylacetonates exhibit marked deviations from Beer's Law. These deviations are qualitatively interpreted in terms of an ionic model in which the complexes dissociate in ethanol solution: solvolysis of the acetylacetonate anion leads to the formation of free acetylacetone and the appropriate metal ethoxide or hydroxide.

All of the metal acetylacetonates examined phosphoresced in ethanol glasses at 77K. Although there are only minor differences in the emission spectra, a significant ordering of the measured lifetimes is observed consistent with the ionic model for the complexes. A heavy atom effect is discounted as an important process except with complexes containing very heavy metal ions. Non - exponential luminescence decays are found with the Group Ia and Group IIa metal acetylacetonates and these are explained by the presence in solution of the coordinated complex and the uncoordinated acetylacetonate anion.

The trend in relative ionic character of the metal acetylacetonates is corroborated by nmr spectral studies obtained in a variety of suitable solvents. The coordinating solvent DMSO - D6 gives the most complete series of results and the ratio of the ligand methyl and ring proton resonances is found to be 6:1 for each complex. The largest chemical shifts are observed with complexes such as $Al(AA)_3$ where the charge / radius ratio of the metal ion is large whereas the smallest chemical shifts are observed with complexes such as Cs(AA) where the charge / ionic radius ratio is small.

The possible self - association of some metal acetylacetonates has been investigated using molecular weight and nmr studies. The results suggest that the lanthanide complexes exist as dimers in non - polar solvents, that both monomers and dimers coexist in polar, weakly coordinating solvents and that solvated monomers are the sole solution species in strongly coordinating solvents. It is probable that a similar situation exists in solutions of some Group IIa metal acetylacetonates.

The fluorescence quenching of some protonated molecules by inorganic ions has been studied. Although it is not possible to unequivocally assign specific mechanisms, it is probable that anionic quenching occurs by charge transfer processes whereas cationic quenching occurs by energy transfer processes. An intermolecular energy transfer mechanism has similarly been ascribed to the phosphorescence quenching of the ligand triplet state of $Al(AA)_3$ by other $M(AA)_n$ complexes.

CHAPTER 1

AN INTRODUCTION TO PHOTOCHEMICAL AND PHOTOPHYSICAL PROCESSES

Photochemistry has been defined by Wayne as " the study of interactions between light and matter and is concerned both with chemical changes brought about by the absorption of light and with the emission of radiation from energy - rich species " [1].

Essential to all photochemical processes is the absorption of a quantum of light: a photon. When a photon is absorbed by a molecule, an electronic transition may occur which usually involves the promotion of an electron in a bonding or non - bonding molecular orbital to an antibonding orbital (Figure 1.1).

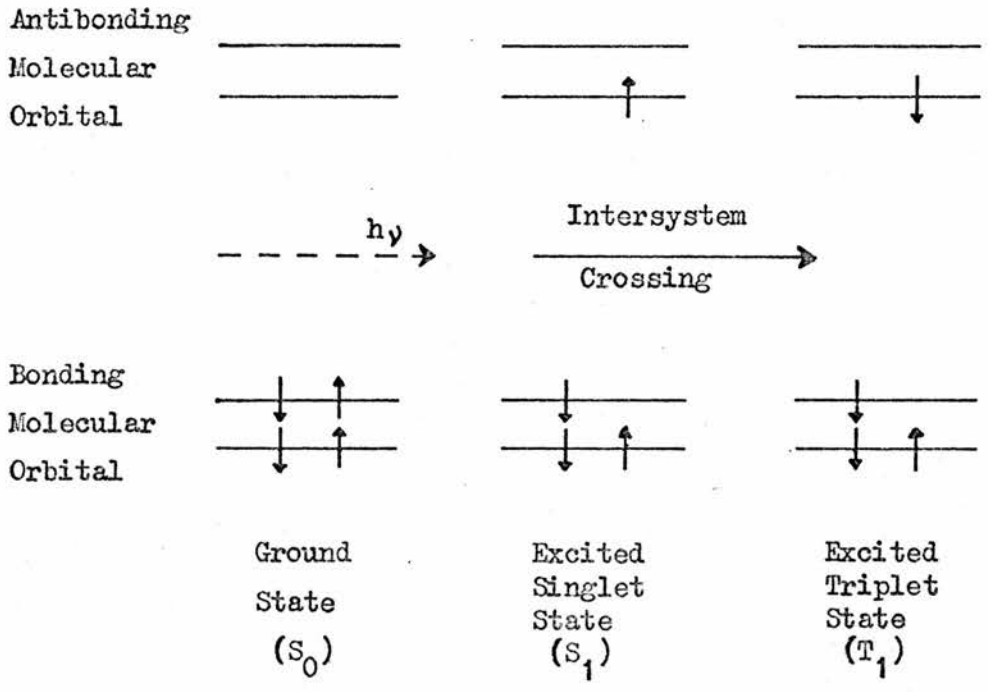

Figure 1.1 Molecular Orbital Representation of Excited States

The molecule is thus raised to an electronically and usually vibrationally excited state from which a photochemical and / or photo - physical process may occur. In general, there will be a number of such possible excited states for any molecule. For example, naphthalene possesses two distinct absorption bands in the near ultraviolet, corresponding to two different electronic transitions from the ground state[2].

The ground states of most organic compounds have all electrons paired and the resultant spin (S) therefore equals zero and the multiplicity (M, defined as 2S + 1) is unity. Using the convention introduced by Terenin[3] and Lewis et al.[4,5], a ground state with M = 1 is designated a singlet state (S_0). Since spin is usually conserved in an electronic transition, the resulting excited states will also be singlets with no net spin and may be designated S_1 , S_2 , etc.

For every excited singlet state there will be a corresponding state where the excited electron has its spin parallel with the electron in the highest ground state orbital. The total spin in this case is therefore one, the spin multiplicity is three and the state is referred to as a triplet state[3,4,5]. According to Hunds first rule, these triplet states will be lower in energy than the corresponding excited states.

(a) THE NATURE OF ELECTRONIC TRANSITIONS AND STATES

Many useful notations to describe the difference between the ground and excited states of a molecule have been developed based on the bonding properties of electrons before and after excitation. Only the classification of transitions introduced by Kasha[6] will be considered

here although others have been introduced and are reviewed by Mulliken[7] and Platt[8].

In a typical organic molecule there may be up to three " types " of electrons present: namely those occupying

(i) sigma bonding orbitals (σ),

(ii) pi bonding orbitals (π),

and (iii) non - bonding orbitals (n).

Excitation of any of these electrons will place it in a higher energy orbital. In the case of polyatomic molecules, this higher energy orbital will normally be a σ^* or π^* antibonding molecular orbital.

Clearly, the " type " of electron promoted and the higher energy orbital involved will have a profound effect on the electronic distribution and energy of the excited state. As frequent reference will be made in subsequent chapters to π, π^* and n, π^* transitions, they are discussed in more detail below.

π, π^* Transitions

A π, π^* transition is represented in Figure 1.2 using a carbonyl chromophore as the example.

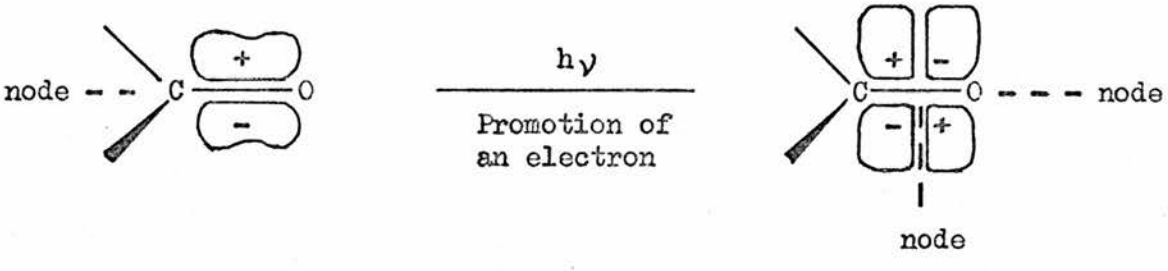

Figure 1.2 Molecular Orbital Representation of the π, π^* Transition

The π^* state orbital differs from the ground state π orbital in that it has an additional nodal plane perpendicular to the bond axis giving it antibonding character. There is considerable overlap

between the π and π^* states leading to a low energy, high intensity ($\varepsilon_{max} \sim 10^4$ to 10^5 $dm^3mol^{-1}cm^{-1}$) transition since the spin and symmetry rules are obeyed.

Both $S_1 \longleftarrow S_0$ and $T_1 \longleftarrow S_0$ π,π^* transitions are well documented for aromatic hydrocarbons. However, the singlet-triplet splitting of the π,π^* states is generally large and the emission process from S_1 usually competes with intersystem crossing. This in turn results in relatively large fluorescence yields (Φ_f) compared with phosphorescence yields (Φ_p).

n, π^* Transitions

There is very little overlap between the non-bonding (n) and antibonding (π^*) orbitals of a chromophore such as the carbonyl oxygen (Figure 1.3). Therefore, when an electron is promoted from the n to the π^* orbital, the transition probability is generally low ($\varepsilon_{max} < 2000$ $dm^3mol^{-1}cm^{-1}$).

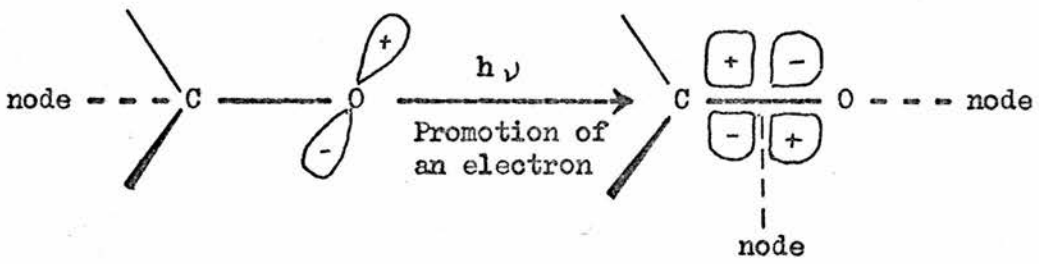

Figure 1.3 Molecular Orbital Representation of the n, π^* Transition

Due to this small orbital overlap, the deactivation transition ($\pi^* \longrightarrow$ n) will have a relatively long lifetime and will be more susceptible to non-radiative transitions than the $\pi^* \longrightarrow \pi$ transition. Intersystem crossing will become an important deactivation process due to the long lifetime of the n, π^* state, and the small singlet-triplet

n,π^* splitting. Phosphorescence is usually the predominant radiative process associated with n,π^* states[9].

In molecules where both n,π^* and π,π^* transitions are possible (e.g. benzophenone) the first excited singlet state (S_1) is usually an n,π^* state[9].

(b) QUANTUM EFFICIENCY

The concept of quantum efficiency (Φ), sometimes known as quantum yield, was introduced by Einstein[10]. The parameter Φ may be used to describe both photophysical and photochemical processes and several definitions of Φ have been discussed by Parker[11], Wayne[1] and Leermakers[12]. In photophysical processes, i.e. where the exciting radiation does not result in any ultimate chemical change, Φ generally refers to either the fluorescence quantum efficiency (Φ_f) and/or the phosphorescence quantum efficiency (Φ_p) of the lowest excited singlet and triplet states respectively, where

$$\Phi_f = \frac{\text{Number of photons emitted by } S_1 \longrightarrow S_0}{\text{Total number of photons absorbed}} ,$$

$$\Phi_p = \frac{\text{Number of photons emitted by } T_1 \longrightarrow S_0}{\text{Total number of photons absorbed}} , \text{ and}$$

$$\Phi_f + \Phi_p \leq 1$$

In photochemical processes the quantum efficiency may exceed unity. The experimental measurement of Φ_f and Φ_p has been reviewed by Crosby et al.[13].

(c) LIFETIMES OF EXCITED STATES

Theoretically, radiational lifetimes (τ_{FM}) are related to the degree of allowedness of an electronic transition which is experimentally obtainable from the absorption band area. The relationship 1.1 may be derived for atomic spectra for transitions between two states and this may be used as a reasonable approximation for molecular band emission.

$$\frac{1}{\tau_{FM}} = 3*10^{-9} n^2 \nu_0^2 \int \varepsilon \, d\nu \qquad 1.1$$

where n = refractive index, ν_0 = wavenumber of band centre and ε = molecular extinction coefficient.

The above equation does not take account of statistical weight factors which are present if there is a change in multiplicity. However, if there is such a change in multiplicity, the " forbidden " nature of the transition usually makes the band area difficult to measure accurately. Variations on the above formula have been proposed to allow for the widths of absorption and emission bands and these are discussed by Birks and Munro[14].

The experimental fluorescence lifetime (τ_M) is the reciprocal of k_M, the total first order rate parameter for the decay of emission from an isolated excited molecule. k_M is the sum of the rates of all the competing processes operating in parallel and includes k_{FM}, ($\frac{1}{\tau_{FM}}$), the excited molecule radiative transition probability.

The experimental lifetime only equals the radiative lifetime if the quantum yield is unity, otherwise the measured lifetime is shorter by the factor of the yield. This relationship may be expressed by

$$\frac{\tau_M}{\tau_{FM}} = \Phi \qquad 1.2$$

While fluorescence lifetimes for solutions of organic molecules are of the order of 10^{-8} seconds, phosphorescence lifetimes are 10^{6} to 10^{9} times longer due to the forbidden nature of the transitions involved. Phosphorescence lifetimes are easily measured but the quantum yields of phosphorescence necessary to calculate the radiational lifetimes are difficult to obtain experimentally, mainly due to errors associated with measurements involving solid solutions at low temperatures.

(d) PRIMARY PHOTOPHYSICAL PROCESSES

The definition by Wayne[1] has indicated that the essential feature of photochemistry is the participation of excited atoms or molecules in chemical and/or physical processes. These processes have been defined by Leermakers[12] and Noyes et al.[15] respectively. Some photochemical processes have been discussed in recent papers by Day[16], Lower et al.[17], Suppan[18], Turro[19] and Swenton[20].

The primary photophysical processes may be illustrated by a Jablonski diagram[21,22] (Figure 1.4) which indicates the various intramolecular processes initiated by photon absorption.

The box beside each electronic energy level depicts the molecular orbitals of the excited states of a molecule, the lowest box indicating the highest filled molecular orbital of the ground state singlet (S_0). Only the two highest energy electrons are considered in Figure 1.4 , the others are paired in such a way that their total spin angular momentum is zero.

After absorption of a photon by a molecule, an electron is raised from the zero ground state vibrational level to a vibrational level of one of the electronic excited states. This process occurs in ca. 10^{-15} seconds and is short relative to all other radiative

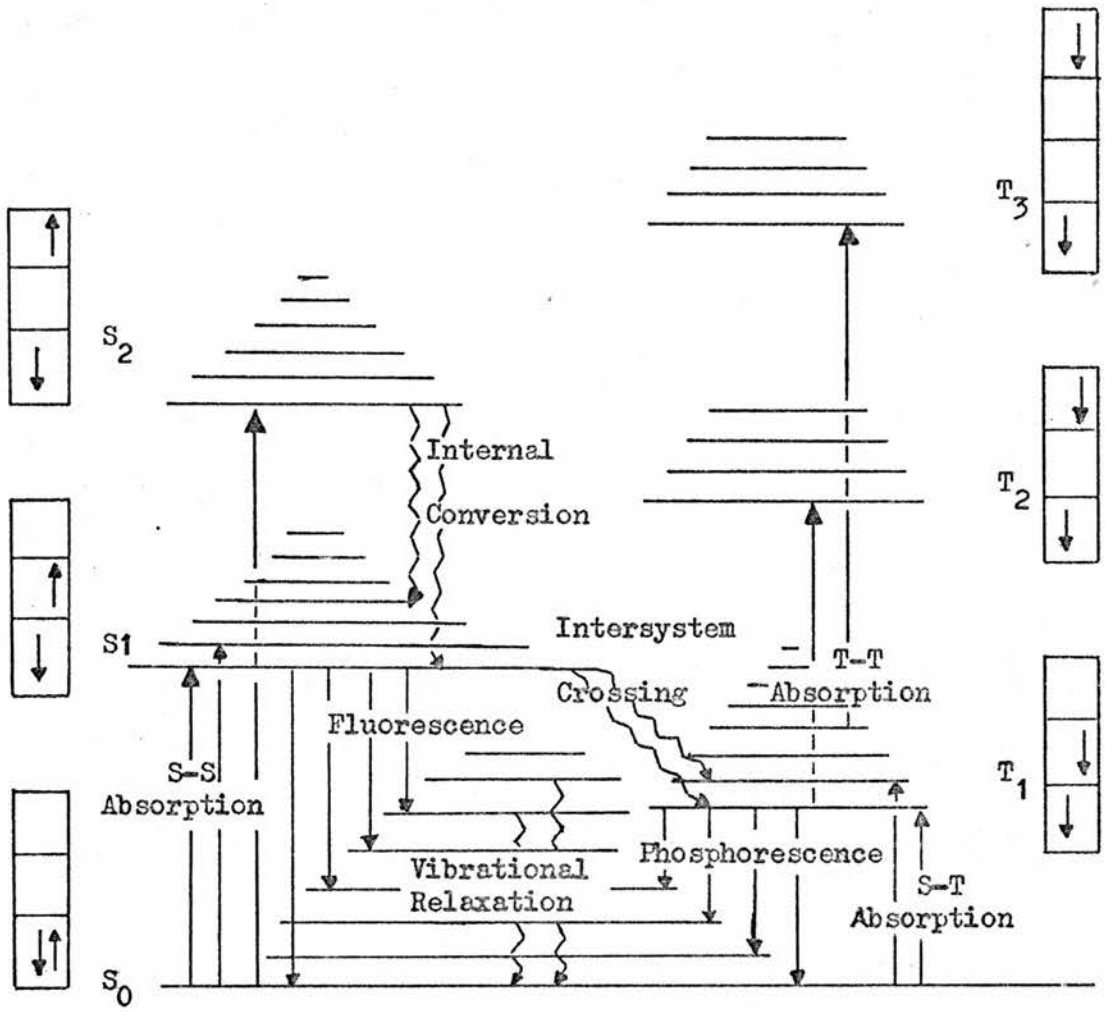

Figure 1.4 Jablonski Diagram

and non-radiative processes, a fact made use of in the Frank-Condon principle[11,21]. Absorption may occur to any of the excited singlet states (S_1 , S_2 , etc.) or to any of the excited triplet states (T_1 , T_2 , etc.) and the resulting processes are described in more detail below.

(i) Vibrational Relaxation

Absorption may give rise to an excited vibrational level of an electronically excited state. In condensed media, i.e. in solution

or in the solid state, an electron in an excited vibrational level rapidly loses its excess vibrational energy in 10^{-11} to 10^{-14} seconds[9] and returns to the zero vibrational level of the corresponding electronic state. This process is referred to as vibrational relaxation (Figure 1.4). In the gas phase, vibrational relaxation can be considerably slower.

(ii) Internal Conversion

With the exception of the S_0 and S_1 states, the energy separation between adjacent singlet states is usually small, resulting in considerable overlap of their vibrational levels. Consequently, any electron raised to an excited level above S_1 will rapidly lose its excess energy non-radiatively and return to the S_1 state. This process is referred to as internal conversion (Figure 1.4) and led to the formulation of a general rule by Kasha[6] which states " in organic molecules in condensed media, the emitting level of a given multiplicity is the lowest excited level of that multiplicity." Of the few exceptions to this rule, the only one which is well substantiated is the azulene molecule where the observed emission corresponds to the $S_2 \rightarrow S_0$ transition[23,24]; recent papers have presented evidence for $S_2 \rightarrow S_0$ transitions in other molecules[25-27].

For most molecules, the $S_1 \rightarrow S_0$ energy separation is sufficiently large to preclude internal conversion in the absence of collisional perturbation. Therefore, the internal conversion quenching rate (k_{CM}) at low temperatures will tend to zero. At any temperature, T, it is to be expected that

$$k_{CM} = k'_{CM} \exp(-w_{CM} / kT) \qquad 1.3$$

where k'_{CM} is the frequency factor and w_{CM} the activation energy of the internal conversion quenching produced by collisional solvent perturbation[28,29]. There is evidence that in certain systems[30-32] such as anthracene and pyrene in aliphatic solvents, $k_{CM} \sim 0$ even at 300K.

(iii) Fluorescence

The emission from any radiative transition where the ground state and excited state have the same spin multiplicity is defined as fluorescence, e.g. $S_1 \longrightarrow S_0 + h\nu$. The radiative lifetimes of S_1 states of organic molecules are usually within the range 10^{-6} to 10^{-9} seconds.

(iv) Phosphorescence

The emission from any radiative transition where the ground state and excited state have different spin multiplicities is defined as phosphorescence, e.g. $T_1 \longrightarrow S_0 + h\nu$ in organic molecules or the $^5D_0 \longrightarrow {}^7F_2 + h\nu$ transition of the Eu^{3+} ion. Since the radiative (and non-radiative) transitions between excited and ground states are spin forbidden in these cases, the radiative lifetimes are usually considerably longer than those described in (iii) and usually within the range 10 to 10^{-3} seconds. Due to this relatively long lifetime, the excited state is susceptible to environmental quenching and care must be taken in measuring the deactivation rate of the excited state, especially in the case of organic molecules, to eliminate possible quenching by impurities such as molecular oxygen.

(v) Intersystem Crossing

Radiative transitions between states of different spin multiplicities (e.g. between singlets and triplets) are theoretically forbidden. In practice, because of spin-orbit coupling and/or the presence of paramagnetic materials, these transitions do occur although spin-allowed transitions (e.g. between singlets and singlets) are much more probable.

Population of a triplet level by direct absorption from the ground state is a difficult process to obtain experimentally since the absorption coefficient is usually very small. However, intersystem crossing can in many cases compete successfully with the alternative deactivation routes of S_1 and, with subsequent internal conversion, produce a molecule in the zero vibrational level of T_1 (Figure 1.4). The first spectroscopic observation of a singlet - triplet transition was reported by Sklar[33].

Intersystem crossing normally occurs in ca. 10^{-8} seconds and the intersystem crossing rate (k_{TM}) at any temperature, T, may be represented by,

$$k_{TM} = k^0_{TM} + k'_{TM} \exp(- w_{TM} / kT) \qquad 1.4$$

where k^0_{TM} represents the natural intersystem crossing rate in the absence of external perturbations, k'_{TM} is the frequency factor and w_{TM} is the activation energy for the intersystem crossing quenching[14].

(vi) Delayed Fluorescence

If the T_1 state can obtain sufficient thermal energy from the environment to attain a higher vibrational level, intersystem crossing ($T_1 \rightsquigarrow S_1$) may occur. Once the S_1 state is produced,

all the above mentioned deactivation routes are available and the subsequent radiative transition $S_1 \longrightarrow S_0$ is referred to as <u>delayed fluorescence</u> [1,21,34,35] (Figure 1.5).

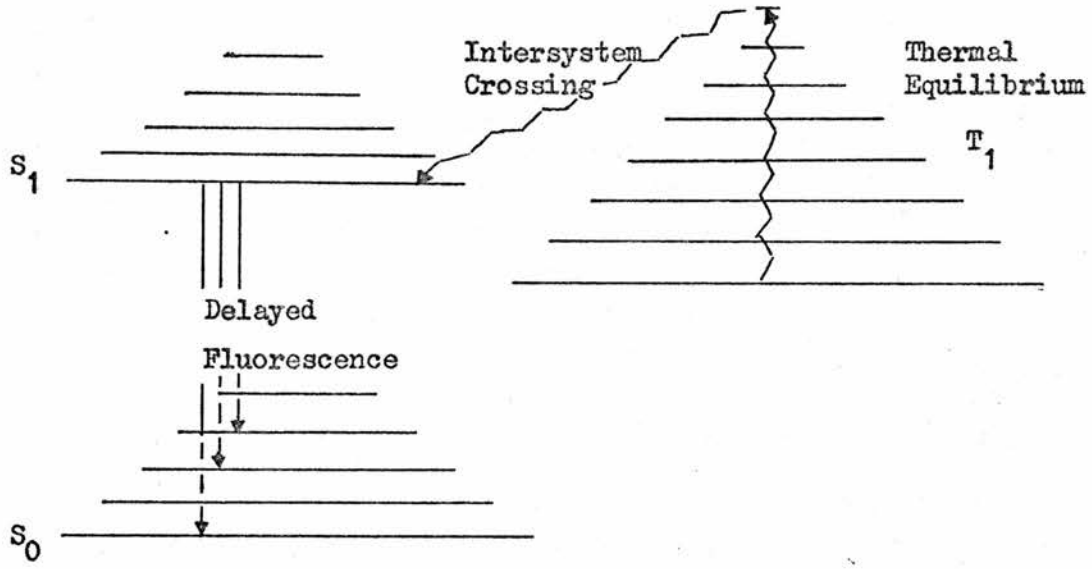

<u>Figure 1.5 Illustration of Delayed Fluorescence</u>

The primary photophysical processes which have been discussed are summarised in Table 1.1.

<u>Table 1.1 Primary Photophysical Processes</u>

Term	Definition	Rate (s^{-1})	Typical Process
Absorption	Promotion of an electron to an energetically higher level	10^{15}	$S_1 \longleftarrow S_0$
Vibrational Relaxation	Transition from a non-equilibrium vibrational energy distribution in a given electronic state to a thermally equilibrated vibrational energy distibution relative to the zero point energy of that same state	$\geqslant 10^{12}$	$S_i^1 \rightsquigarrow S_i^0$

Table 1.1 (cont.)

Term	Definition	Rate (s^{-1})	Typical Process
Internal Conversion	Non-radiative transition between two different electronic states of the same molecule which have the same spin multiplicity.	$10^{11} - 10^{15}$	$S_2 \rightsquigarrow S_1$
Fluorescence	Radiative transition between two energy levels of the same spin multiplicity.	$10^{7} - 10^{9}$	$S_1 \longrightarrow S_0 + h\nu$
Phosphorescence	Radiative transition between two energy levels of different spin multiplicity.	$10 - 10^{3}$	$T_1 \longrightarrow S_0 + h\nu$
Intersystem Crossing	Non-radiative transition from an electronic state of a given spin multiplicity to an electronic state of a different spin multiplicity.	10^{8}	$S_1 \rightsquigarrow T_1$

The intramolecular energy transfer processes available to a molecule in an excited singlet state are shown diagramatically in Figures 1.6 (a) and (b).

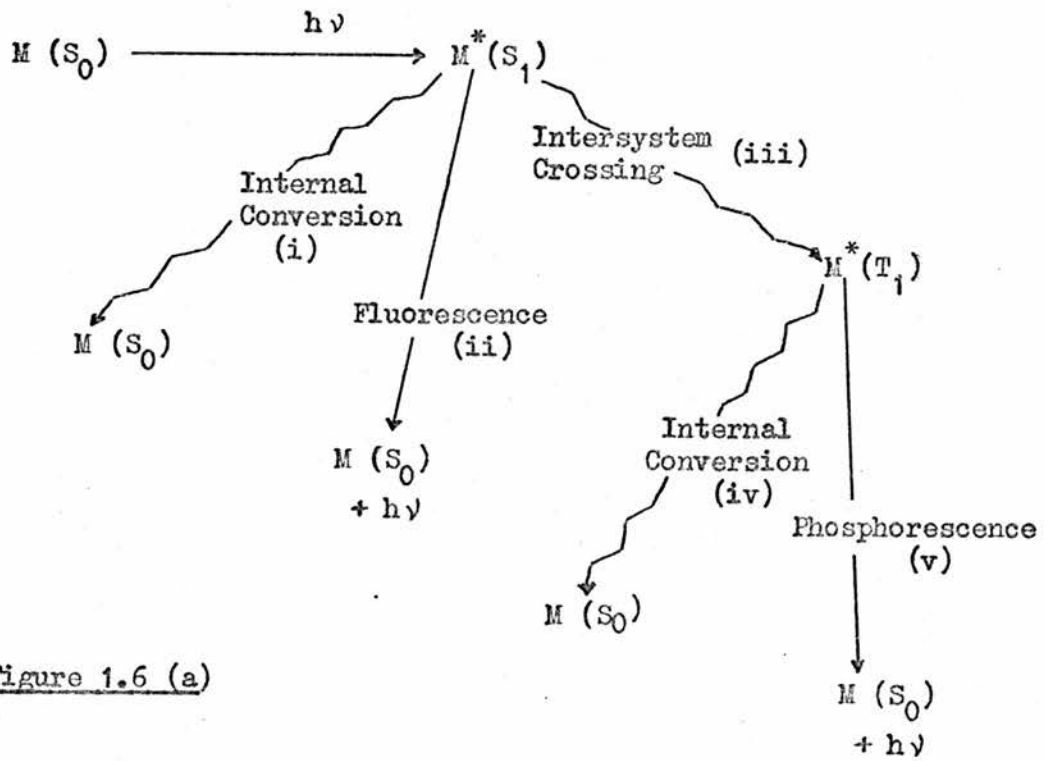

Figure 1.6 (a)

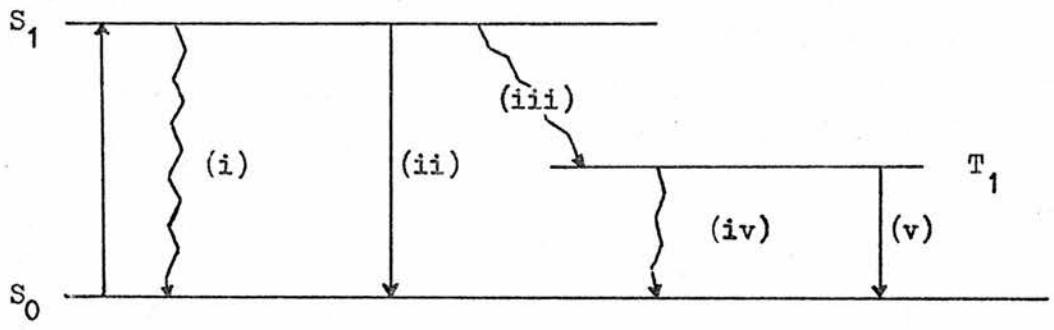

Figure 1.6 (b) Deactivation Routes

(e) IMPURITY QUENCHING

There are three principal processes by which the excited state energy of a molecule (M) may be transferred to an impurity molecule (Q), leading to impurity quenching of the emission.

(i) Static Quenching may occur through the formation of a metastable charge-transfer complex between M and Q (Figure 1.7),

$$M + Q \rightleftharpoons (MQ)^{\ddagger} \qquad 1.5$$

where $(MQ)^{\ddagger}$ indicates the metastable complex. Strictly, static quenching does not quench the excited state M^* but prevents the production of M^* from the ground state M.

(ii) Dynamic or Collisional Quenching may occur due to interaction between M^* and Q (Figure 1.7),

$$M^* + Q \longrightarrow (MQ)^* \qquad 1.6$$

where the transient $(MQ)^*$ complex may lose its excess energy by methods analagous to those available to the M^* state. In addition, photochemical reactions may occur, such as the formation of a stable (MQ) molecule or free radical formation (Figure 1.7).

The collisional quenching rate (k_Q) may be diffusion -

controlled and obeys to a first approximation the Einstein - Smoluchowski equation[36,37] which may be represented by

$$k_Q = \frac{8\,R\,T\,\rho}{3000\,\eta} \qquad 1.7$$

where ρ = the probability of quenching occurring in a collision and η = the viscosity coefficient of the solvent[14,38-40].

The kinetics of such a process in solution ideally follow the Stern - Volmer Law, which may be expressed by

$$R - 1 = K[Q] \qquad 1.8$$

where R may be either the ratio of luminescence intensity (I_0/I) or of luminescence lifetime (τ_0/τ) and [Q] is the quencher concentration. I_0 and τ_0 are the intensity and lifetime respectively of the donor molecule. From the constant K and a value of τ_0, the absolute rate (k) for the process, in units of $dm^3 mol^{-1} s^{-1}$, may be calculated from the expression

$$k = K/\tau_0 \qquad 1.9$$

The constants K and k are independent of the donor concentration.

Impurity quenching by molecular oxygen is of major practical importance since dissolved oxygen is present in all exposed solutions at room temperature. The oxygen concentration can usually be reduced sufficiently for normal fluorescence measurements by bubbling oxygen-free nitrogen through the solution. More efficient methods of oxygen removal, such as the " freeze-pump-thaw " technique[35] are required for delayed fluorescence or other triplet state measurements. The absolute quenching rate (k) of oxygen in certain systems, e.g. fluorescent molecules in organic solvents, is ca. $10^{10} dm^3 mol^{-1} s^{-1}$, which is approximately equal to the diffusion - controlled rate

for many solvents[41,42]. For some other impurity quenchers such as organometallic compounds, the rate constant has been shown to be less than the diffusion - controlled rate[43-45].

(iii) Energy Transfer Quenching may occur due to resonance interaction between M^* and Q (Figure 1.7)

$$M^* + Q \longrightarrow M + Q^* \qquad 1.10$$

The energy transferred to the quenching molecule may then be dissipated by radiative and /or non - radiative transitions in Q^* by methods analagous to those available to M^*.

Intermolecular energy transfer in solution is an important process and is widely used to excite acceptor molecules to a state of specific multiplicity. Distinctions between the physical and chemical properties of the excited states of different multiplicities may thus be studied.

Energy transfer may occur by radiative processes involving the emission of a photon by the donor molecule and its subsequent absorption by the acceptor molecule,

$$M^* \longrightarrow M + h\nu \; ; \quad Q + h\nu \longrightarrow Q^* \qquad 1.11$$

A particular case of this type of quenching is that of self-absorption of the fluorescence due to an overlap of the emission and absorption bands of a molecule. This does not modify any of the molecular absorption processes but competes with the normal emission and changes the observed values of the fluorescence lifetime and quantum efficiency. The self - absorption parameter (a) depends on the overlap of the absorption, $\leq(\bar{\nu})$, and the fluorescence spectrum, $F_M(\bar{\nu})$, on the concentration (c) and the sample thickness (x) by the equation,

$$a\,Q_M = \int_0^{\infty} F_M(\bar{\nu}) \left[1 - 10^{-\Sigma(\bar{\nu}).c.x} \right] d\bar{\nu} \qquad 1.12$$

This self absorption process or " inner-filter effect " has been widely studied[46-51]. Detailed mathematical treatments of the fluorescence lifetimes and other parameters have been reported. However, the experimental technique of viewing from the surface excited by the incident radiation (front-face illumination) surmounts many of these problems.

Non-radiative electron transfer may also occur due to

(a) Coulombic interactions[52-54],

(b) electron-exchange interactions[55-58], or

(c) exciplex formation[37,59].

(a) Coulombic interactions (e.g. dipole-dipole) may take place over distances of 2 - 6nm, which are large compared with molecular diameters. The interaction may be represented as

$$^1M^* + {}^1Q \longrightarrow {}^1M + {}^1Q^* \qquad 1.13$$

or,
$$^3M^* + {}^1Q \longrightarrow {}^1M + {}^1Q^* \qquad 1.14$$

for singlet - singlet and triplet - singlet quenching respectively. The conditions necessary for effective Coulombic transfer are that there must be an overlap of the donor emission spectrum and the acceptor absorption spectrum and an allowed transition in the acceptor.

(b) Electron - exchange interactions may take place over distances of 0.6 to 1.5nm, which are only slightly greater than the molecular diameters (ca. 0.6nm). The electron - exchange interaction may be represented by

$$^1M^* + {}^1Q \longrightarrow {}^1M + {}^1Q^* \qquad 1.15$$

or,
$$^3M^* + {}^1Q \longrightarrow {}^1M + {}^3Q^* \qquad 1.16$$

for singlet - singlet and triplet - triplet quenching respectively. The conditions necessary for efficient electron - exchange transfer are that there must be short range interaction between donor and acceptor molecules and spin conservation in the process.

(c) Exciplex formation may occur in solutions due to Coulombic, electron - exchange, exciton resonance or charge - transfer processes. The dissociation of these complexes may provide a further non - radiative transfer process as

$$ {}^1M^* + {}^1Q \longrightarrow {}^1(MQ)^* \longrightarrow {}^1M + {}^1Q^* \qquad 1.17 $$

or,

$$ {}^3M^* + {}^1Q \longrightarrow {}^3(MQ)^* \longrightarrow {}^1M + {}^3Q^* \qquad 1.18 $$

for singlet - singlet and triplet - triplet quenching respectively.

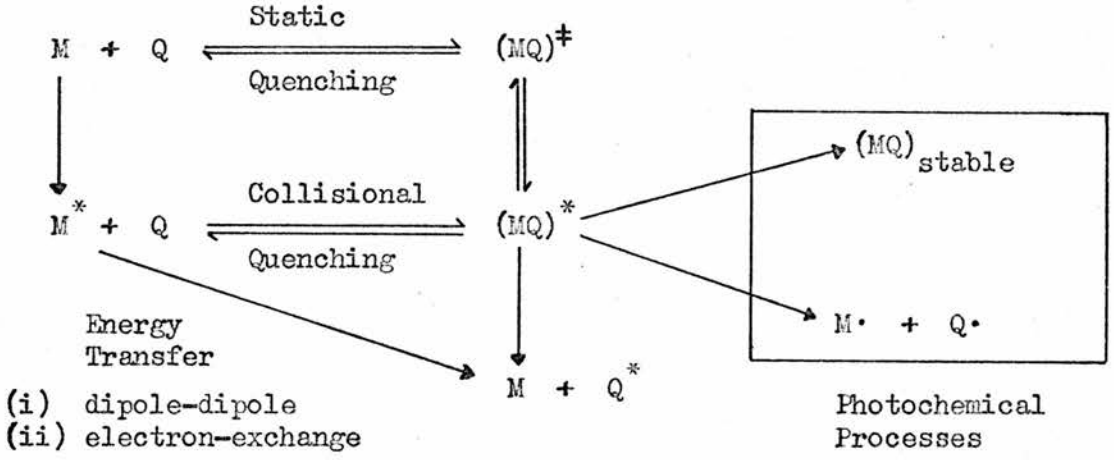

Figure 1.7 Impurity Quenching Routes

(f) CONCENTRATION QUENCHING AND EXCIMER FORMATION

Many aromatic compounds exhibit a second type of fluorescence in concentrated solution or in the crystal form known as excimer

fluorescence[60 - 64]. This originates from excited dimers (excimers) which are produced by the collisional interaction of excited and unexcited monomers as

$$M^* + M \longrightarrow D^* \qquad 1.19$$

Excimer fluorescence is normally associated with concentration quenching of the M^* fluorescence and the appearance of a structureless excimer fluorescence band at longer wavelengths, which corresponds to the radiative transition of D^* from its first π electronic excited state to the dissociated singlet ground state. Birks and Munro[14] have discussed excimer fluorescence and its characteristic parameters, including the fluorescence lifetime (τ_D) and the radiative lifetime (τ_{FD}).

CHAPTER 2

METAL β - DIKETOENOLATE COMPLEXES

(a) INTRODUCTION

A compound which has β - carbonyl groups and at least one proton on the carbon between may undergo a keto - enol tautomerism (Figure 2.1)[65].

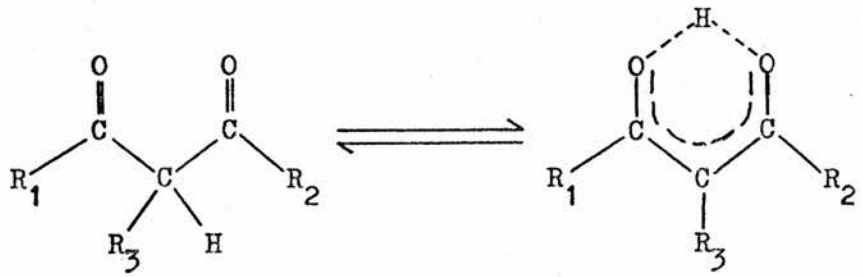

Figure 2.1 Keto - Enol Tautomerism

A wide variety of substituents R_1, R_2 and R_3 are known and abbreviations for some of the compounds referred to in this thesis are given in Table 2.1

More than one hundred compounds of this type are known and most of these may, under the appropriate conditions, exchange a labile enolic proton for a metal ion to form a metal β - diketoenolate complex (Figure 2.2). An important characteristic of this type of complex is that the ligand is attached to the metal ion by more than one donor atom in such a manner as to form a heterocyclic ring. The term chelate was first suggested by Morgan and Drew[66] to indicate the " claw - like " nature of the bonding.

Table 2.1 Abbreviations for some β - Diketoenolates

Systematic Name	Trivial Name	Abbreviation (Anion)
2,4-pentanedione	Acetylacetone	AA
1-phenyl-1,3-butanedione	Benzoylacetone	BA
1,1,1-trifluoro-4-phenyl-2,4-butanedione	Benzoyltrifluoroacetone	BTFA
1,3-diphenyl-1,3-propanedione	Dibenzoylmethane	DBM
2,2,6,6-tetramethyl-3,5-heptanedione	Dipivaloylmethane	DPM
1,1,1,5,5,5-hexafluoro-2,4-pentanedione	Hexafluoroacetyl-acetone	HFAA
1,1,1,2,2,3,3-heptafluoro-7,7-dimethyl-4,6-octanedione		FOD
1,1,1-trifluoro-2,4-pentanedione	Trifluoroacetylacetone	TFAA
1,1,1-trifluoro-4-(2-thienyl)-2,4-butanedione	Thienoyltrifluoro-acetone	TTFA

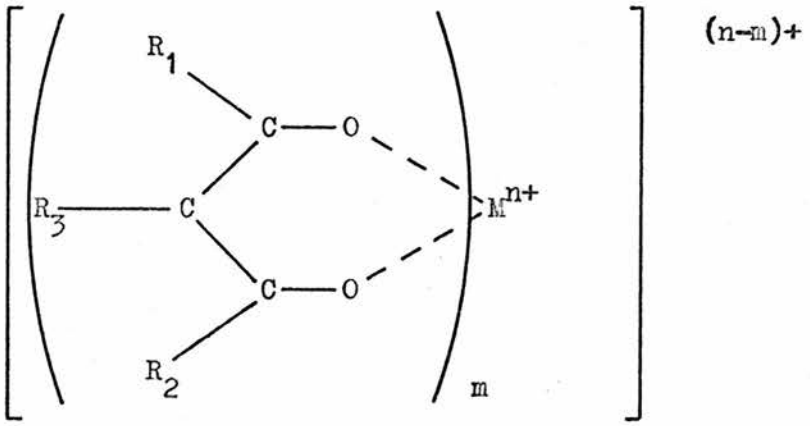

Figure 2.2 Representation of a Metal β - Diketoenolate Complex

The earliest reported preparation of a metal β - diketoenolate complex, bis (2,4-pentanedionato) beryllium (II), was made by Combes in 1887[67]. Since then, metal β - diketoenolates have been widely studied and in many cases are available commercially. Excellent reviews on the chemistry of these types of metal chelates have been compiled by Sidgwick and Brewer[68], Martell and Calvin[69], Fernelius and Bryant[70], and more recently by Harris and Livingstone[71] and Moshier and Sievers[72]. Metal chelates are now known for most of the stable metallic elements and many of the non-metals in the periodic table[73].

(b) STRUCTURE AND BONDING

In almost all the cases which have been examined, the metal - ligand bonding of the metal β - diketoenolate complexes has been shown to occur via the oxygen atoms of the ligand. The only well - authenticated exceptions to this rule are the chelates of general formula $M\left[Pt\ (AA)_2X\right]$ (where M = Mn, Fe, Co, Ni, Cu, Zn, Cd, Pd, VO, or UO_2 , and X = Cl or Br) , which have been shown to contain both metal - oxygen and metal - carbon bonds[74].

In general, metal β - diketoenolate compounds may be classified into four distinct groups depending on the degree of coordinative unsaturation. These groups are

(i) neutral monomeric species,

(ii) addition compounds (adducts),

(iii) polymeric species, and

(iv) cationic or anionic species.

(i) Monomeric Species

(a) Divalent metal ions normally react with two ligand groups to give neutral chelates in which the four donor oxygen atoms are attached to each metal ion in a tetrahedral or square planar arrangement. If the normal coordination number of the metal is four, a stable, coordinatively saturated molecule (ML_2) is formed. However, very few divalent metal ions form stable $M(AA)_2$ complexes which are monomeric both in solution and in the solid state[75,76]. The only monomeric acetylacetonate species confirmed by x-ray analysis are $Be(AA)_2$[77] and $Cu(AA)_2$[78] (Table 2.2), although the latter chelate may behave as a Lewis acid with strong bases to form adducts of general formula $Cu(AA)_2B$[79].

Due to the bulky t-butyl groups of the dipivaloylmethane ligand, stable $M(DPM)_2$ complexes may be formed with transition metal ions (Table 2.2). These monomeric chelates may have either a tetrahedral or square planar structure.

Penta-coordinate complexes which are monomeric in the solid state are rare, the only well-authenticated species being $VO(AA)_2$ which has a square pyramidal structure[80]. Basic solvents coordinate readily to $VO(AA)_2$, forming mono-adducts in which the basic group is presumably trans to the vanadium oxo-oxygen[81,82].

(b) Trivalent metal ions normally react with three ligand groups to give neutral octahedral molecules (ML_3). Boron is an exception to this rule since it is restricted to a maximum coordination number of four and tends to form cationic complexes of the type $[B(AA)_2]^+$.[117] All other trivalent metal ions which have an ionic radius less than ca. 0.9 Å generally form stable chelates which are monomeric in the solid state and in solution (Table 2.2).

Table 2.2 X - Ray Crystallographic Data

Metal Chelate	M-O[a] (Å)	O-M-O[b] (degrees)	Structure	Reference
$Be(AA)_2$	1.70	106	Tetrahedral	77
$Cu(AA)_2$	1.92	93.5	Planar	78
$Cr(DPM)_2$	1.84	94	Planar	83
$Fe(DPM)_2$	1.96	94.7	Tetrahedral	84
$Co(DPM)_2$	1.96	95	Tetrahedral	85
$Ni(DPM)_2$	1.84	94.6	Planar	86
$Zn(DPM)_2$	1.96	94.7	Tetrahedral	85
$Cu(DBM)_2$	1.91	93.2	Planar	87
$VO(AA)_2$	1.97	87.5	Square Pyramidal	80
$Al(AA)_3$	1.95	89	Octahedral	88
$Mn(AA)_3$	1.88	97.8	Octahedral	89
$Fe(AA)_3$	1.95	89.5	Octahedral	90
$Co(AA)_3$	1.88	96.7	Octahedral	91
$Ga(AA)_3$	1.95	91.3	Octahedral	92
$Rh(AA)_3$	1.99	95.3	Octahedral	93
$Er(DPM)_3$	2.21	74.4	Octahedral	94
$Zr(AA)_4$	2.20	75	Antiprismatic	95
$Nb(AA)_4$	2.13	79.8	Antiprismatic	96
$Ce(AA)_4$	2.40	72	Antiprismatic	97
$Cu(AA)_2 \cdot quin.$	N/A	N/A	See text	98
$Co(AA)_2 \cdot 2H_2O$	2.05	92	Distorted Octahedral	99
$Co(AA)_2 \cdot 2py.$	2.03	89.8	Distorted Octahedral	100
$Ni(AA)_2 \cdot 2H_2O$	2.01	92.4	Distorted Octahedral	101
$Ni(AA)_2 \cdot 2py.$	N/A	N/A	Distorted Octahedral	102
$Zn(AA)_2 \cdot H_2O$	2.02	88.3	Distorted Square Pyramidal	103
$Nd(AA)_3 \cdot 3H_2O$	2.44	N/A	Distorted Octahedral	104
$Ho(AA)_3 \cdot 4H_2O$	2.26	N/A	Dodecahedral	105
$Fe(AA)_3 \cdot AgClO_4 \cdot H_2O$	1.98	89.3	Octahedral	106
$[Li(AA)]_n$	1.95	92.2	See text	107

Table 2.2 (cont.)

Metal Chelate	M-O[a] (Å)	O-M-O[b] (degrees)	Structure	Reference
$[Co(AA)_2]_4$	2.00	91.8	See text	108
$[Ni(AA)_2]_3$	2.04	96.5	See text	109
$[Zn(AA)_2]_3$	2.00	89	See text	110
$[TiO(AA)_2]_2$	1.97	83.4	See text	111
$[Pr(DPM)_3]_2$	2.44	86.8	See text	112
$[Pr(FOD)_3.H_2O]_2$	2.42	N/A	See text	113
$Cs[Y(HFAA)_4]$	2.32	73.8	Dodecahedral	114
$Cs[Eu(HFAA)_4]$	2.38	72.5	Dodecahedral	115
$Cs[Am(HFAA)_4]$	2.41	72	Dodecahedral	115
$NH_4[Pr(TTFA)_4].H_2O$	2.45	70.8	Dodecahedral	116

(a) Average metal - ligand oxygen distance.

(b) Average angle O - M - O for each ligand group.

N/A indicates that the relevant data is not available.

In contrast, the larger lanthanide metal ions prefer to form complexes with the higher coordination numbers seven and eight[118]. Adduct formation or polymerisation of lanthanide metal chelates is thus an important process, and $Er(DPM)_3$ is the only lanthanide DPM-chelate reported as monomeric in the solid state[94], although the dipivaloylmethanates of the heavier lanthanide metals thulium, ytterbium and lutetium may have a similar structure[119,120]. $Ln(DPM)_3$ complexes have been reported as being essentially monomeric in polar and non - polar solvents[121-123].

(c) Tetravalent ions of the smaller metals tend to form cationic complexes with β - diketoenolate ligands. However, if the metal ion is sufficiently large to allow a coordination number of

eight, neutral ML_4 complexes may be formed (Table 2.2). These complexes are monomeric in the solid state and in solution and may have either a regular dodecahedral or square antiprismatic structure[124].

(ii) Addition Compounds

(a) Divalent transition metal ions usually have a coordination number towards oxygen greater than four. The neutral ML_2 molecules formed with β - diketoenolate ligands will thus behave as Lewis acids, forming addition compounds (adducts) with bases such as water, ammonia, pyridine or γ - picoline[75]. The normal preparative methods for chelates with these ions will thus give hydrates. Numerous examples of such complexes have been reported (Table 2.2) and the following series, derived from metal acetylacetonates serve as examples (Table 2.3)[125].

Table 2.3 Typical Adducts Formed by Divalent Metal Acetylacetonates

Adduct	Metal
$ML_2(NH_3)_2$	Mn, Co, Zn, Cd, Mg
$ML_2(py)_2$	Co, Ni
$ML_2(bipy)$	Mn, Co, Ni, Zn, Cd
$ML_2(phen)$	Mn, Co, Ni, Zn, Cd

The first adduct to be isolated was the quinoline adduct of $Cu(AA)_2$, obtained by the crystallisation of the complex from quinoline[126]. This complex has a square pyramidal structure confirmed by x-ray analysis (Figure 2.3)[98]. The product from the reaction of bases with the β - diketoenolates of Ni(II), Co(II) and Fe(II) is

normally the bis- adduct ML_2B_2[125,127]. Crystal structure determinations have shown that these adducts have a trans- octahedral configuration (Figure 2.4)[99-102].

$Zn(AA)_2.H_2O$ has been examined by x-ray analysis (Table 2.2)[103]. The zinc atom in this complex is penta- coordinate, the oxygen atoms being arranged in a distorted square pyramid with all Zn-O linkages equal (Figure 2.5). Reaction of this complex with heterocyclic bases gives compounds of general formula $Zn(AA)_2.B$ (B = py., γ-pic.) which are only slightly dissociated in non - polar solvents and are presumably penta- coordinate[128]. Hexa- coordinate complexes have also been obtained, e.g. $Zn(AA)_2.2\gamma$-pic., which dissociates in benzene solution with the loss of one of the molecules of γ - picoline[125,128].

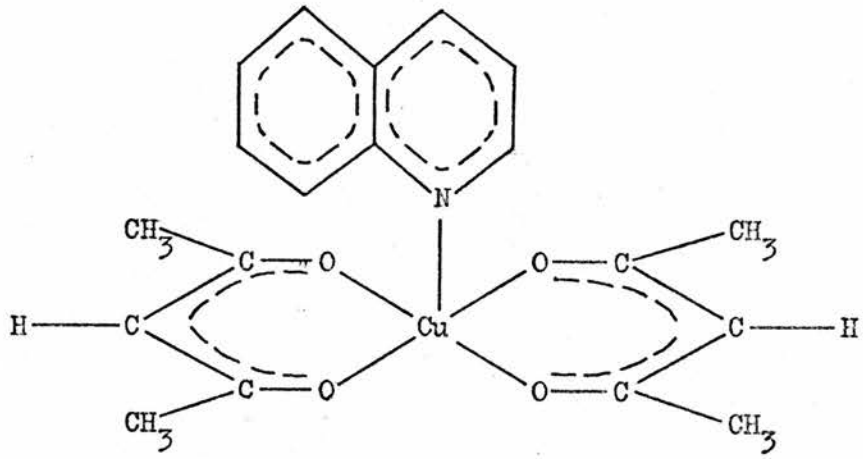

Figure 2.3 Square Pyramidal Structure of $Cu(AA)_2.quin.$

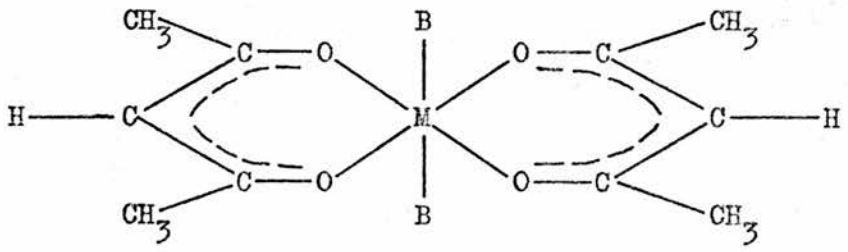

Figure 2.4 Trans- Octahedral Base Adducts of Ni, Co and $Fe(AA)_2$

(M = Ni, Co, Fe : B = H_2O, py.)

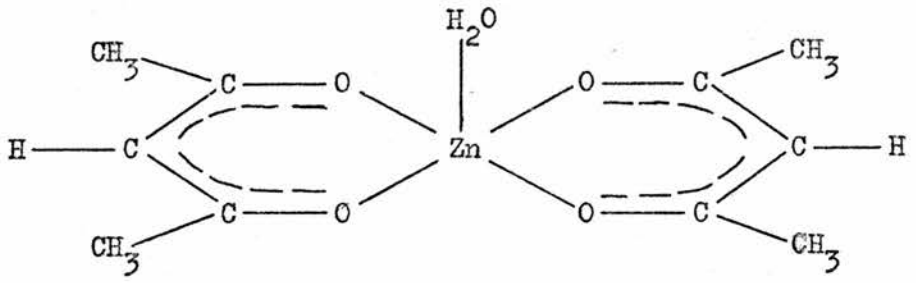

Figure 2.5 Distorted Square Pyramidal Structure of $Zn(AA)_2.H_2O$

(b) The ready solvation of lanthanide tris- acetylacetonates indicates that these complexes react as Lewis acids. Mono-, di- and tri- hydrates of general formula $Ln(AA)_3.nH_2O$ have been characterised[129], and the dihydrates have been shown to be distorted dodecahedra (Table 2.2). Attempts to prepare anhydrous chelates have been unsuccessful except in the cases where the ligand is sterically hindered, e.g. dipivaloylmethane[119].

Adduct formation between $Ln(DPM)_3$ or $Ln(FOD)_3$ complexes and basic substrates has been extensively used in recent years to induce shifts in the nmr spectra of the organic substrates[130].

(iii) Polymeric Species

Removal of water from hydrated β- diketoenolate complexes or of base from base adducts leaves the anhydrous chelate ML_2 or ML_3 as a highly reactive Lewis acid. The chelate also contains oxygen atoms which are potential Lewis bases, and varying degrees of self-association have been observed in which the coordination number of the ion is increased[75,131,132]. Evidence for polymerisation in solution has been obtained from molecular weight determinations[133,134] and by observing variations in magnetic and spectroscopic properties[130,135]. Polymerisation in the solid state, which is suggested by the greater

heats of sublimation of certain complexes compared with others in which the metal ion is coordinatively saturated[121,136], has been confirmed by x-ray analysis in some cases (Table 2.2). The structures of some of these complexes are shown in Figures 2.6 to 2.11.

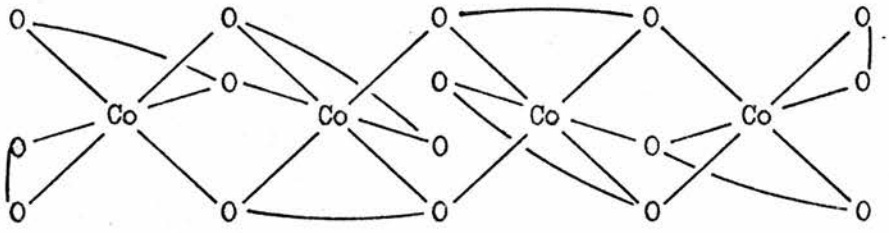

Figure 2.6 Tetrameric Molecule of $[Co(AA)_2]_4$

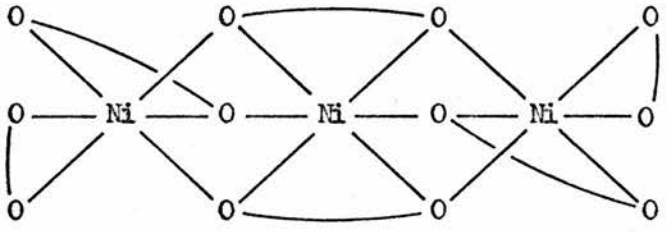

Figure 2.7 Trimeric Molecule of $[Ni(AA)_2]_3$

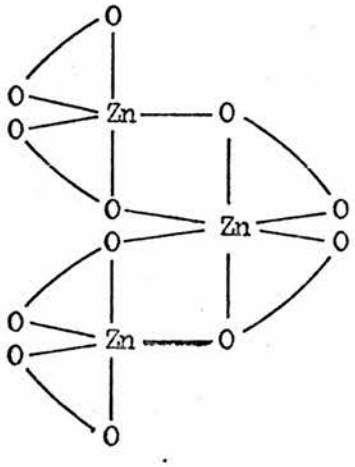

Figure 2.8 Trimeric Molecule of $[Zn(AA)_2]_3$

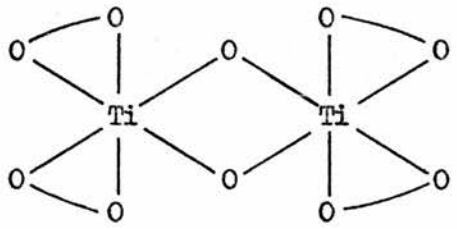

Figure 2.9 Dimeric Molecule of $[TiO(AA)_2]_2$

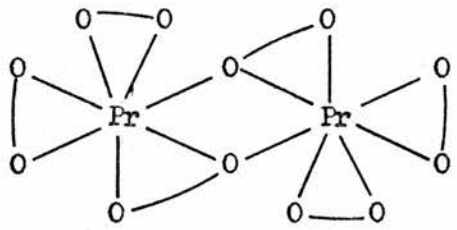

Figure 2.10 Dimeric Molecule of $[Pr(DPM)_3]_2$

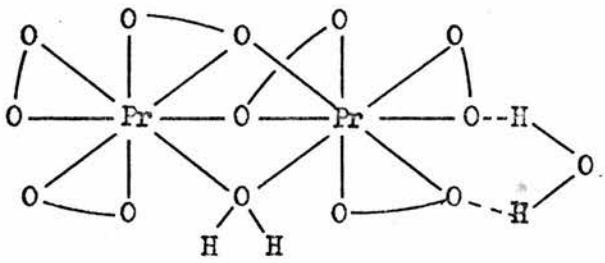

Figure 2.11 Dimeric Molecule of $[Pr(FOD)_3.H_2O]_2$

(iv) Cationic and Anionic Species

Since the coordination number of boron is restricted to four, cationic complexes of the type $[BL_2]^+$ are formed when boron trichloride is added to the ligand[117]. If boron trifluoride is used, neutral complexes of general formula BF_2L are formed in which the fluorine atoms presumably occupy two of the tetrahedral " sites " around the metal ion[117].

Silicon(IV) has a coordination number of six and forms octahedral complexes of general formula $[SiL_3]^+$ [117,137-139]. In contrast, germanium(IV) and tin(IV) form the non - ionic species GeX_2L_2 [140] and SnX_2L_2 [141] respectively, where X = Cl or Br.

Stable tetrakis anions of the type $[LnL_4]^-$ are formed by the reaction of a lanthanide(III) salt with four equivalents of a neutralised β- diketoenol (other than acetylacetone) [142]. The structures of certain of these complexes have been determined by x-ray crystallography and show that the ligands are arranged dodecahedrally about the lanthanide ion (Table 2.2). There is evidence that lanthanide tetrakis chelates may also interact sufficiently with donor molecules to give stable adducts in which nine coordination is found [143].

(v) The Structure of Group Ia Metal Chelates

The absence of definitive structures for the Group Ia and Group IIa metal β - diketoenolates may be directly attributed to the inability to prepare suitably crystalline samples for x-ray analysis. Since these chelates decompose without melting at temperatures above 550K [73,126], it is probable that they exist in non - discrete polymeric forms. Recent confirmation of the polymeric nature of these chelates has been produced by Soling [144] and von Schroder and Weber [107] who have determined the structures of $[Cs(TTFA)]_n$ and $[Li(AA)]_n$ respectively. The predominantly ionic character of these chelates is demonstrated by their insolubility in non - polar solvents and by the fact that they are known to dissociate in water [141] and other polar solvents [145].

(c) SYNTHESIS OF METAL β- DIKETOENOLATES

Since the preparation of the first metal β- diketoenolate in 1887[67], a variety of synthetic procedures have appeared in the literature. However, much of the earlier work is of dubious value since, in many cases, methods of preparation were often vague and analytical and melting point data were not always reported.

There has been no comprehensive review of synthetic procedures since Fernelius and Bryant classified the methods available prior to 1957[70]. It is very improbable that such a review will be forthcoming since most workers are concerned mainly with the properties of a specific compound or series of compounds. It is also a common practice to find similar synthetic procedures appearing with little or no acknowledgment of the original author. The volumes of Inorganic Syntheses are, however, very useful since they contain specific preparative methods which are well authenticated and which may be suitably adapted to prepare a series of metal chelates.

One of the most common synthetic procedures is the direct reaction of a β- diketoenol with the metal salt. If the metal chelate is not particularly soluble in the solvent used, the reaction may come to equilibrium, e.g.

$$M^{n+} + m(AA)^{-} \rightleftharpoons \left[M(AA)_m \right]^{(n-m)+} \qquad 2.1$$

but will not go to completion. This disadvantage may largely be overcome by controlling the pH and one method widely used is to buffer the solution by, for example, using metal acetates[146]. Another method, which is widely used to prepare lanthanide chelates, is to gradually add a weak base such as ammonia, ensuring that the pH is maintained below the value at which the metal hydroxide precipitates,

thereby contaminating the product[147,148].

Some other general types of preparation include the reactions of the β - diketoenol with metal oxide, hydroxide, carbonate or carbonyl[70].

(i) Preparation of Lanthanide tris- Acetylacetonates

The method used to prepare lanthanide tris- acetylacetonates is capable of being adapted to prepare many related lanthanide tris- β - diketoenolates. This method was introduced by Stites et al.[147] and involves the reaction between the lanthanide chloride and the ammonium salt of acetylacetone in aqueous solution under conditions where the pH is controlled. Pope et al.[149] found that, by recrystallising the crude product from the Stites preparative method in 60% by volume ethanol solution, the appropriate lanthanide tris- acetylacetonate trihydrate was produced, confirmed by C and H analysis. Richardson et al.[129] reported that the mono- and di- hydrates of the lanthanide tris- acetylacetonates may be prepared from the crude Stites product by recrystallisation from 95% cold ethanol and acetylacetone respectively. Richardson et al.[129] also found that attempts to prepare the anhydrous compound were unsuccessful, due to decomposition of the product.

In the experimental investigations described in subsequent chapters, the trihydrates of some of the lanthanide acetylacetonates were used. These were synthesised by the method of Stites et al.[147] followed by the purification method outlined by Pope et al.[149]. The stepwise procedure employed is detailed below.

(a) Preparation of $LnCl_3.nH_2O$

The lanthanide oxides (Koch-Light, 99.9%) were converted to the hydrated chlorides by refluxing in 70% hydrochloric acid until solution was complete. The solid lanthanide chlorides were obtained by the removal of excess hydrochloric acid and water on a rotary evaporator. The solid product was redissolved in water and the water removed on the rotary evaporator. This procedure was repeated twice to remove excess acid and to prevent the formation of insoluble lanthanide oxychloride. For convenience, the lanthanide chloride was normally kept as an aqueous solution.

(b) Preparation of $Ln(AA)_3.3H_2O$

A solution of ammonium acetylacetonate was prepared by adding redistilled acetylacetone dropwise to an equivalent molar amount of ammonium hydroxide in a stirred aqueous solution. The resulting ammonium acetylacetonate solution (4.5 molar equivalents) was added dropwise to a stirred aqueous solution of the lanthanide chloride (1 molar equivalent). The pH of the stirred solution was monitored throughout and was brought to within 0.1 to 0.2 units of the pH at which the particular hydroxide precipitated (Table 2.4)[149]. The crude product was filtered, washed with water, air dried and dissolved in hot 95% ethanol. When solution was complete, a few drops of acetylacetone were added to minimise hydrolysis and the required volume of water added to produce a 60% ethanol solution.

The solution was allowed to cool slowly, the crystals which separated were filtered, washed once with 50% ethanol and once with water, air dried and stored in a tightly stoppered bottle. The resulting product was analysed for C and H and in all cases the analytical data agreed within 0.3% for the theoretical elemental percentages for the trihydrates (Table 2.5).

Table 2.4 The pH values at which $Ln(OH)_3$ begins to precipitate

pH [a]	Lanthanide
6.9	Lanthanum.
6.6	Praesodymium, Neodymium.
6.5	Samarium, Gadolinium.
6.4	Dysprosium, Holmium, Terbium, Yttrium.
6.3	Erbium.
6.1	Ytterbium.
6.0	Lutetium.

(a) Values from reference 149.

Table 2.5 Analytical Data for $Ln(AA)_3.3H_2O$ Complexes.

$Ln(AA)_3.3H_2O$	Analyses			
	Calc. %		Found %	
	C	H	C	H
La^{3+}	36.74	5.55	36.58	5.60
Pr^{3+}	36.59	5.49	36.66	5.57
Nd^{3+}	36.34	5.45	36.38	5.66
Sm^{3+}	35.96	5.43	35.89	5.42
Eu^{3+}	35.79	5.37	35.65	5.33
Gd^{3+}	35.47	5.38	35.26	5.28
Tb^{3+}	35.33	5.36	35.20	5.36
Dy^{3+}	35.06	5.26	35.03	5.04
Ho^{3+}	34.89	5.25	35.16	5.33
Er^{3+}	34.74	5.21	34.72	5.20
Yb^{3+}	34.35	5.15	34.10	5.17
Lu^{3+} [a]	35.44	4.96	35.39	4.92

(a) Analyses figures for the Lu^{3+} complex correspond to the dihydrate

(ii) Preparation of Group Ia and Group IIa Metal Acetylacetonates

The methods used to prepare M(AA) and $M(AA)_2$ complexes were developed from the general method of Job and Goissedet[150] involving the reaction between the metal hydroxide and acetylacetone. Some of these chelates, e.g. Na(AA), have also been prepared by the reaction between the metal and acetylacetone[151] in an inert medium but this method has not been extensively adopted due to the extreme reactivity of certain of the metals, e.g. caesium.

(a) Preparation of M(AA) Complexes

The metal hydroxide (Fisons A.R. or Koch-Light) (1 molar equivalent) was dissolved in the minimum amount of water and this solution was added dropwise to a stirred ethanolic solution of redistilled acetylacetone (1.2 molar equivalents). Crystals of the desired product were formed immediately or, in the case of the Rb and Cs complexes, were precipitated on standing. The crude product was filtered, washed with very little water and dried in vacuo.

(b) Preparation of $M(AA)_2$ Complexes

An ethanolic solution of ammonium acetylacetonate was prepared by adding concentrated ammonium hydroxide solution to an equivalent molar amount of acetylacetone in ethanol. Ethanol was added as required to obtain complete solution. The resulting ammonium acetylacetonate solution (2.4 molar equivalents) was added dropwise to a stirred aqueous solution of the metal chloride (1 molar equivalent). Crystals of the desired product were formed immediately or on standing. The crude product was filtered, washed with very little water and dried in vacuo.

(c) Purification of M(AA) and $M(AA)_2$ Complexes

The crude product from the preparation (a) or (b) above was dissolved in the minimum amount of hot 95% ethanol and, when solution was complete, a few drops of acetylacetone were added to minimise hydrolysis. The solution was allowed to cool slowly, the crystals which separated were filtered, washed with very little water and air dried. The recrystallised product was then dried in a vacuum oven at 373K for twelve hours and stored in a tightly stoppered bottle in vacuo.

The products were analysed for C and H and only in the cases of Li(AA) and $Mg(AA)_2$ did the analytical data show satisfactory agreement with the theoretical percentages for the anhydrous acetylacetonate (Table 2.6). For most of the complexes, the analytical results could be interpreted in terms of the hygroscopic nature of the complexes and further evidence for this came from the analyst who reported difficulty in weighing the samples, due to weight gains. The results for the Cs and Rb complexes could not be interpreted in this way and it is necessary to consider the possibility of metal hydroxide being present as contaminant (Table 2.6). Further recrystallisation of the Cs and Rb complexes did not improve the analytical results.

(d) Preparation of Rb(AA) and Cs(AA)

- Dry Box Technique

Dry methanol was added to freshly ground metal hydroxide (1 molar equivalent) and the suspension stirred. Freshly distilled acetylacetone (1.5 molar equivalents) was added dropwise and stirring continued for ca. 5 hours. Excess methanol was allowed to evaporate, the crude precipitate was then filtered, washed with a little methanol and pumped dry. The crude product was dissolved in redistilled

Table 2.6 Analytical Data for M(AA) and $M(AA)_2$ Complexes

Metal Complexes	Analyses			
	Calc. %		Found %	
	C	H	C	H
Li(AA)	56.63	6.65	56.22	6.55
[a] $Na(AA).1.6H_2O$	39.79	6.81	39.91	6.74
[a] $K(AA).0.9H_2O$	38.89	5.74	38.62	5.43
[b] $Rb(AA)_{0.7}(OH)_{0.3}$	26.28	3.28	24.66	3.52
[b] $Cs(AA)_{0.8}(OH)_{0.2}$	22.28	2.71	22.61	2.68
$Mg(AA)_2$	53.97	6.34	53.64	6.19
[a] $Ca(AA)_2.0.5H_2O$	48.57	6.11	49.02	5.45
[a] $Sr(AA)_2.1.5H_2O$	38.39	5.48	38.36	5.62
[a] $Ba(AA)_2.0.7H_2O$	34.80	4.50	34.52	4.29

(a) C and H calculated on the basis of hydrates.

(b) C and H calculated on the basis of non- stoichiometric amounts of M(AA) and M(OH).

ethanol, filtered to remove insoluble material and the excess ethanol allowed to evaporate. The crystals were filtered, washed with a little ethanol, dried in a vacuum oven at 373K for ca. 12 hours and stored in a tightly stoppered bottle in vacuo. The products were then analysed for C and H (Table 2.7).

The Cs(AA) prepared by this method was more stable than that obtained by the aqueous method and contained only a small amount of Cs(OH). The Rb(AA) prepared by this method was unstable and gave very poor analytical results. Further recrystallisation of Cs(AA) or Rb(AA) did not improve the analytical results.

It is probable that this preparative method is only suitable for the Cs(AA) complex due to the strongly basic character of the Cs(OH) which dissociates in methanol. The crucial step in this preparation

Table 2.7 Analytical Data for Cs(AA)

Metal Complex	Analysis			
	Calc. %		Found %	
	C	H	C	H
Cs(AA)	25.88	3.04	25.30	2.98

is the evaporation, which pushes the equilibrium

$$Cs(OH) + HAA \rightleftharpoons Cs(AA) + H_2O \qquad 2.2$$

to the right since methanol and water will be removed more easily than acetylacetone. The comparable situation for Rb(AA) does not occur to the same extent since the initial dissociation of Rb(OH) in methanol is less likely (cf. Chapter 4).

(e) General Comments on the Preparation of M(AA) and $M(AA)_2$

The hygroscopic nature of the anhydrous complexes has been shown to be very significant. Since lithium acetylacetonate has been found to exist as a long chain polymeric structure[107] it is not unreasonable to suggest that similar structures may be found for these related chelates. For example, no melting point data were obtained for any of these chelates. It is therefore significant that in no case examined did the analytical data correspond to a distinct hydrated species. There is also evidence that decomposition accompanies the acquisition of water and this necessitates the careful storage and handling of these complexes.

Since the subsequent spectral investigations of these complexes were carried out in solvents which contain significant amounts of water even when purified, e.g. ethanol, many of the results must have a considerable degree of error. The nature of the decomposition is, however, explained in Chapter 4, in which the absorption spectra of these complexes are discussed in qualitative terms.

(iii) Preparation of Other Metal Acetylacetonates

A variety of metal acetylacetonates were used in the experimental investigations described in subsequent chapters. These chelates were prepared by methods similar to those outlined in the introduction to section (c) of this chapter. The specific synthetic method for each chelate is given in Table 2.8 and in each case the purified product was analysed for C and H.

Table 2.8 Analytical Data for Metal Acetylacetonates

$M(AA)_n$ Complex	Analyses				Reference
	Calc. %		Found %		
	C	H	C	H	
$Al(AA)_3$	55.57	6.53	55.45	6.80	152
$Sc(AA)_3$	52.63	6.18	52.63	6.00	152
$VO(AA)_2$	45.28	5.28	45.09	5.45	153
$Cr(AA)_3$	51.57	6.06	51.70	6.08	154
$Mn(AA)_3$	51.13	6.01	51.24	6.28	155
$Co(AA)_3$	50.57	5.95	50.84	6.04	156
$Zn(AA)_2 \cdot H_2O$	42.70	6.11	42.69	5.93	157
$Ga(AA)_3$	49.08	5.77	49.23	5.91	152
$Y(AA)_3 \cdot 3H_2O$	40.92	6.18	40.95	6.18	147
$In(AA)_3$	43.71	5.14	43.66	4.99	152
$Th(AA)_4$	38.20	4.50	38.20	4.61	158

(iv) Preparation of 3- Substituted Aluminium Acetylacetonates

The $Al(R\text{-}AA)_3$ complexes, where R = Me, Et and Cl were prepared by an adaptation of the method suggested by Lodzinska and Rozploch[159] involving the reaction between anhydrous $AlCl_3$ and the appropriate

ligand in an inert solvent, e.g. benzene, with the evolution of hydrogen chloride gas. The ligands 3 - methyl -[160], 3 - ethyl -[160] and 3 - chloro - acetylacetonate[161] were prepared from acetylacetone.

The 3 - bromo - acetylacetonate complex was prepared by refluxing $Al(AA)_3$ in dry benzene solution in the presence of a slight excess of Br_2, until evolution of HBr was complete. The resulting solution was filtered and excess solvent removed on the rotary evaporator until the complex precipitated.

The crude products were recrystallised from 95% ethanol and air dried, and the recrystallised products analysed for C and H (Table 2.9).

Table 2.9 Analytical Data for $Al(R\text{-}AA)_3$ Complexes

Metal Complex	Analyses			
	Calc. %		Found %	
	C	H	C	H
$Al(MeAA)_3$	59.01	7.44	58.92	7.64
$Al(EtAA)_3$	61.74	8.16	61.46	8.14
$Al(ClAA)_3$	42.13	4.24	42.15	4.02
$Al(BrAA)_3$	32.11	3.23	31.89	3.15

CHAPTER 3

INSTRUMENTATION

(a) GROUND STATE ABSORPTION SPECTROSCOPY

Two spectrophotometers, a Unicam SP800 and a Perkin Elmer 402, have been used to record absorption spectra. Both are continuous scanning spectrophotometers and were used in the range 200 to 850 nm. The 402 spectrophotometer allowed repetitive scanning between selected wavelengths.

All measurements were obtained using optically balanced quartz cells with PTFE stoppers and using purified solvent as reference. All absorption spectra were recorded at the instrument temperature unless otherwise stated. Extinction coefficients are quoted in units of $dm^3 cm^{-1} mol^{-1}$.

(b) EMISSION SPECTROSCOPY

Two spectrofluorimeters have been used to obtain emission and excitation spectra in solution and in the solid state, over the temperature range 77K to ambient. These were the Perkin Elmer Hitachi MPF-2A and a locally designed high resolution spectrofluorimeter based on the Hilger Watts Monospek 1000 monochromator and using phase sensitive detection.

Comparison of corrected spectra of the same sample obtained from

both instruments showed no appreciable difference for most purposes. All preliminary experiments were carried out using the MPF-2A and the majority of emission and excitation spectra in this thesis were recorded on this instrument. However, the resolution characteristics and photomultiplier response of the high resolution spectrofluorimeter, particularly over the red region of the spectrum, are preferable in studies of the sharply structured fluorescence bands of lanthanide compounds.

(i) Perkin Elmer Hitachi MPF-2A

The MPF-2A spectrofluorimeter is shown schematically in Figure 3.1. The light source of the MPF-2A is a 150 watt Xenon lamp, giving a near continuum from 270 - 800 nm (Figure 3.2). Allowance for fluctuations in the intensity of the excitation source could be made by using the MPF-2A in the " Reference " mode. In this mode, the excitation light beam is monitored by a reference photomultiplier, the output of which inversely controls the gain of the final detection photomultiplier. The excitation light is dispersed by a 600 line mm^{-1} monochromator and focused onto the sample.

The sample emission is dispersed through a second monochromator then focused onto a standard RCA R106 photomultiplier. The output is amplified and recorded on a pen recorder.

Emission spectra were obtained by setting the excitation monochromator, adjusting the slits to give suitable light intensity and scanning with the emission monochromator. Excitation spectra were obtained in a similar manner by setting the emission monochromator and slits and scanning the excitation monochromator. In general, the excitation (or emission) monochromator was set to give maximum intensity when measuring emission (or excitation) spectra.

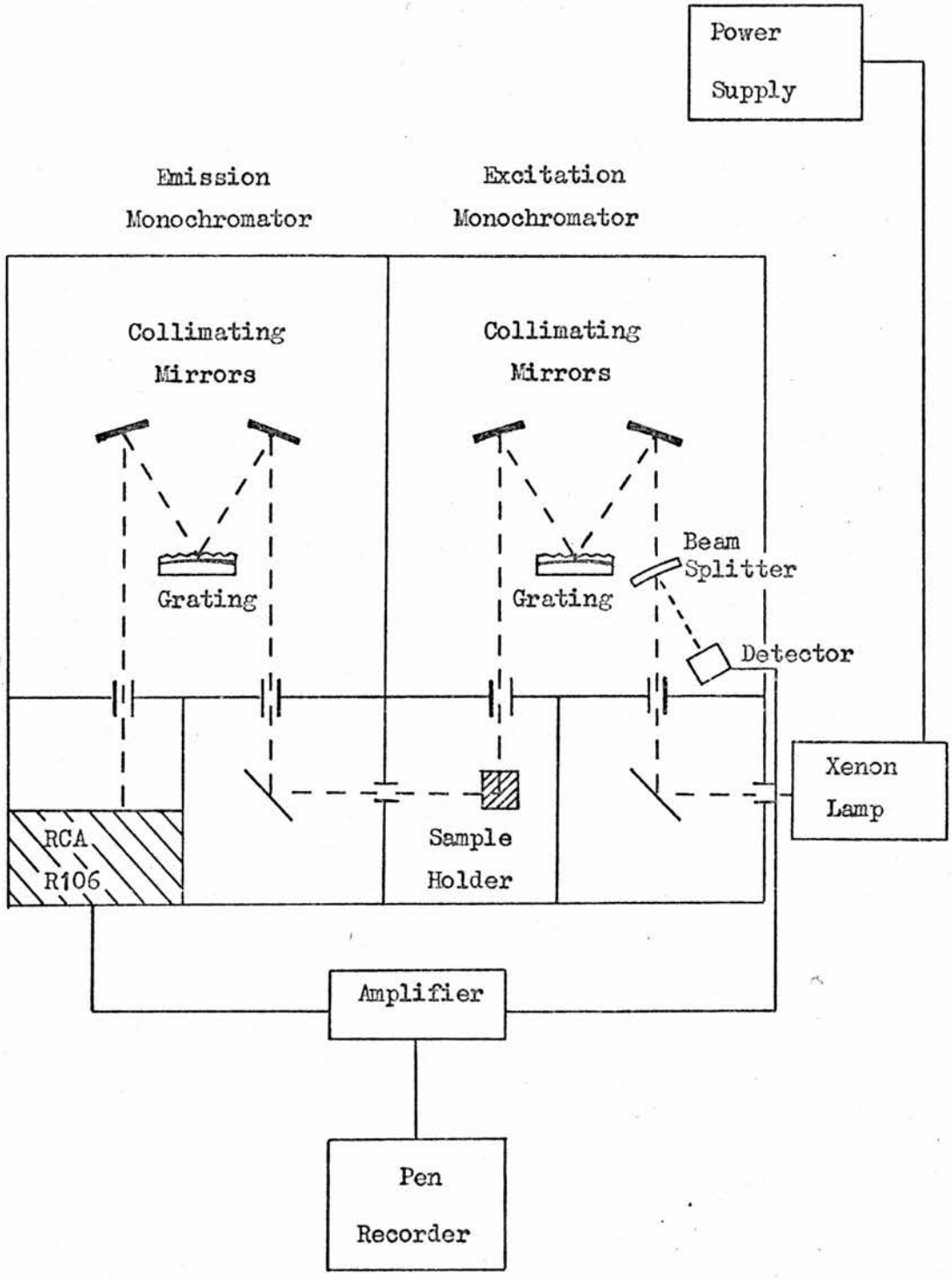

Figure 3.1 Schematic Representation of the MPF-2A Spectrofluorimeter

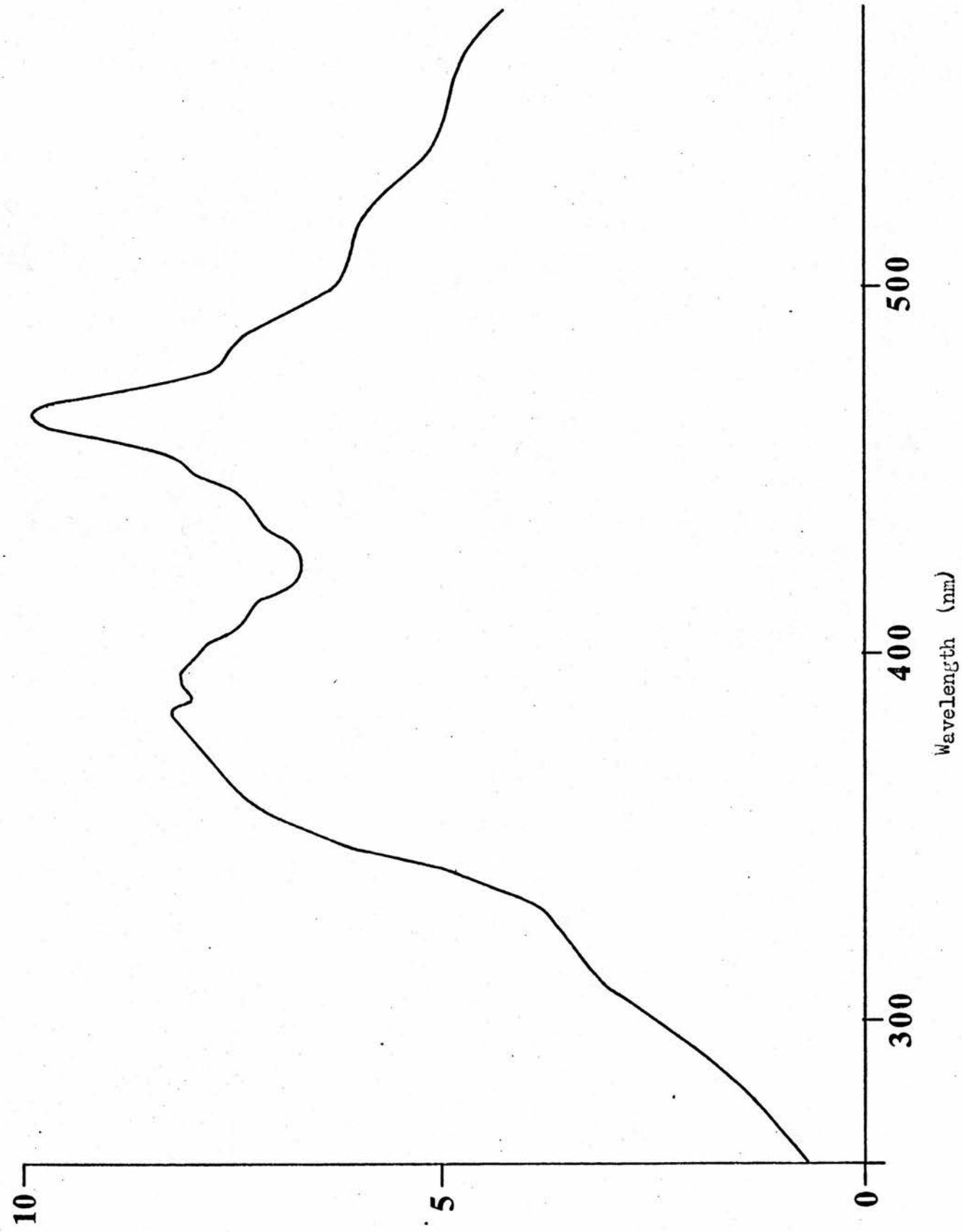

Figure 3.2 Relative Photon Yield of the Xenon Lamp of the MPF-2A

Emission and excitation spectra thus obtained are functions of photomultiplier current against wavelength. Investigations involving relative intensity measurements, such as fluorescence quenching, can usually be made with this information. However, if the absolute luminescence spectrum is required, the response characteristics of the photomultiplier, and the instrument optics must be taken into account. This is discussed in Section (b)(iv).

(ii) High Resolution Spectrofluorimeter

The high resolution spectrofluorimeter is shown schematically in Figure 3.3. It uses a Hilger Watts Monospek 1000 (1200 lines mm^{-1}) as an emission monochromator. Sampling accessories such as solid samplers, solution cells and phosphorescence attachments were modified to offer a range of facilities, and variable temperature measurements were possible over the range 77 to ca.360K.

The excitation source used was a water cooled, medium pressure mercury lamp, filtered to pass only the 365.5 nm radiation. The excitation light was focused onto the sample, the light emitted focused by a lens onto the monochromator incident slits and the dispersed light from the excident slits focused onto an EMI 9526 photomultiplier. The signal to noise ratio was improved by using a phase sensitive detector (Brookdeal Electronics) before the signal was amplified and relayed to a pen recorder (Leeds and Northrup Speedomax).

Luminescence intensity was controlled by suitable adjustment of monochromator slits and photomultiplier supply voltage, and the emission spectrum of the sample obtained by scanning over the appropriate wavelength range. The emission spectrum thus obtained could be converted to the absolute luminescence spectrum using a computer program which takes account of the response characteristics

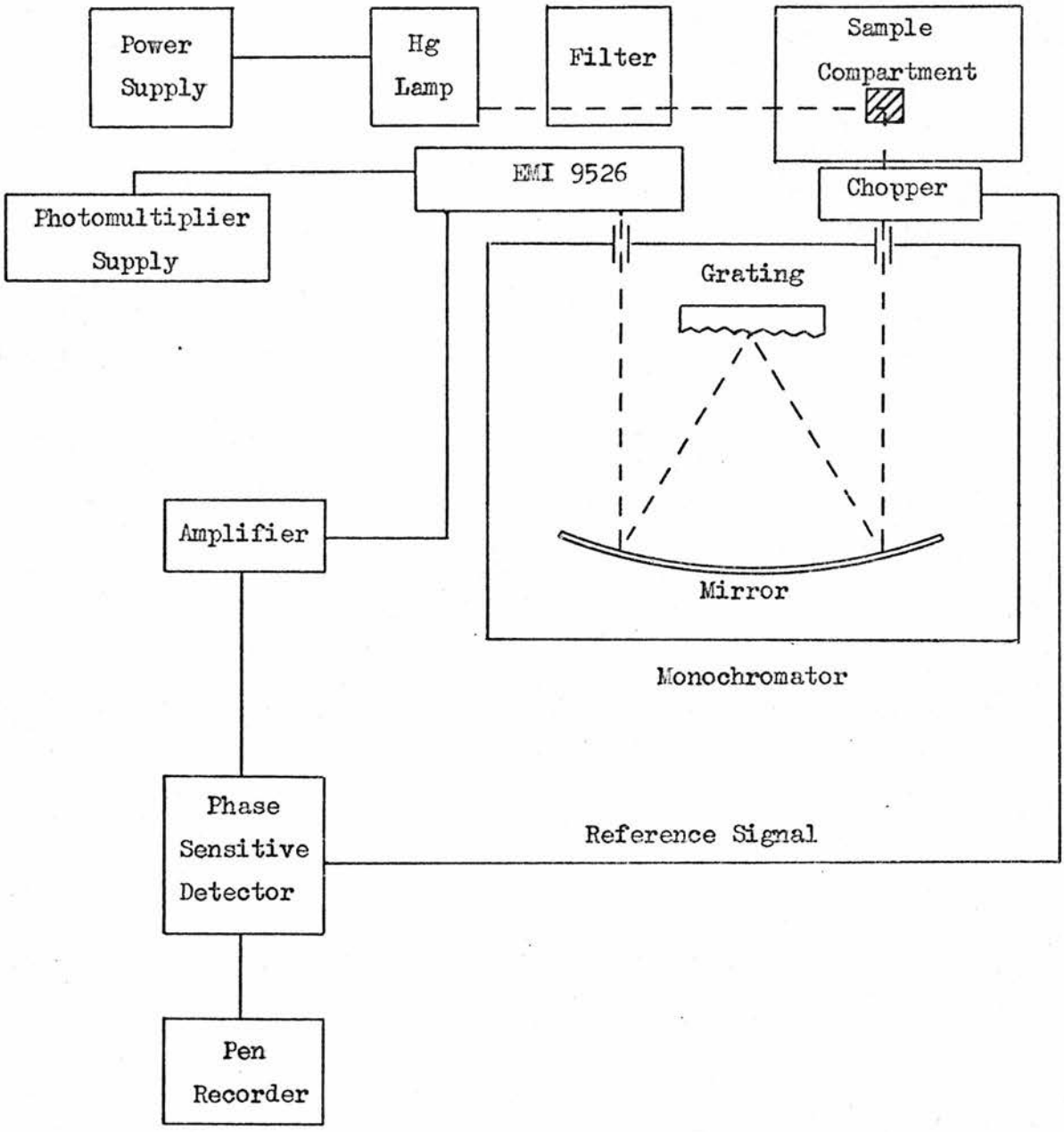

Figure 3.3 Schematic Representation of the High Resolution Spectrofluorimeter

of the EMI 9526 photomultiplier and the instrument optics. Further discussion of this is given in Section (d)(i).

(c) SAMPLING TECHNIQUES

The importance of clean apparatus, pure samples and solvents for measuring both quantitative and qualitative photophysical processes has been emphasised by Parker[11]. All glassware, cells, etc. were cleaned by immersion in chromic acid, followed by copious washing with distilled water and dried before use. Solvents and organic reagents were fractionally distilled or recrystallised from an appropriate solvent before use. All metal chelates were recrystallised and analysed for C, H and N.

(i) Solutions

Emission and excitation spectra were recorded using the right - angled viewing technique[11]. This technique minimises possible interference from the " inner - filter effect ", found with molecules where the emission and absorption bands overlap. In these circumstances, corrections have to be made if solutions with optical densities greater than ca. 0.02 are used[11]. In general, metal chelates have emission bands shifted well to the red relative to the absorption band, and no inner - filter restrictions of this type are placed on concentration.

Luminescence may be quenched by dissolved oxygen in fluid solutions and precautions are normally taken when measuring luminescence to prevent such quenching. Two methods may be used to remove dissolved oxygen from solutions,

(1) degassing by a freeze - pump - thaw process and keeping the solution under vacuum during measurements,

and (2) bubbling dry nitrogen gas through the solution to displace dissolved oxygen.

Method (1) has been used for low temperature luminescence

measurements, while method (2) has been used with the standard PTFE stoppered fluorescence cells. Comparison of quantitative measurements, such as the emission intensities and lifetimes of metal chelates, using degassed and undegassed solutions indicated that oxygen quenching was not an important deactivation process. Most investigations involving metal chelates in solution therefore did not require any deoxygenating procedures.

Front face illumination was used in investigations of energy transfer between organic molecules and metal ions and halides. This was achieved on the MPF-2A spectrofluorimeter using a solid sample holder, suitably adapted to hold a 1mm pathlength quartz cell (Figure 3.4). This cell is held at an angle of 30^{o} relative to the incident beam and the emission detected at right angles to this beam. Reproducibility was improved by placing a defocusing lens in front of the excitation beam and causing most of the sample to be illuminated. This minimised errors due to slight positional changes of the cell when removing and replacing in the holder.

(ii) Solid Solutions

Phosphorescence emission spectra of metal chelates were obtained exclusively on the Hitachi MPF-2A spectrofluorimeter using the phosphorescence attachment. Phosphorescence lifetime and quenching studies were carried out on the high resolution spectrofluorimeter. The temperature of all phosphorescence studies was 77K, maintained by immersing the sample in liquid nitrogen contained in a quartz dewar (Figure 3.5). Frosting of the quartz " windows " was eliminated by passing a stream of dry nitrogen gas through the cell compartment.

Most solvents and mixed solvents form cracked or opaque glasses

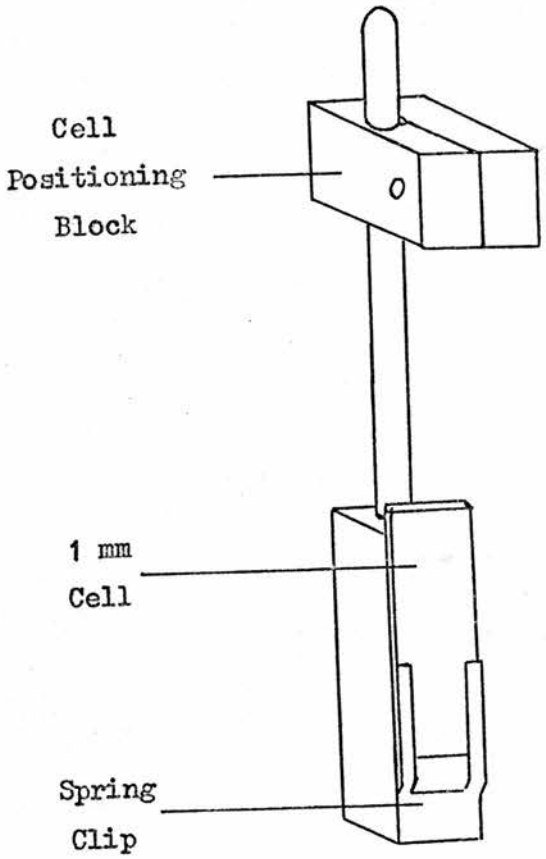

Figure 3.4

1 mm Cell Holder

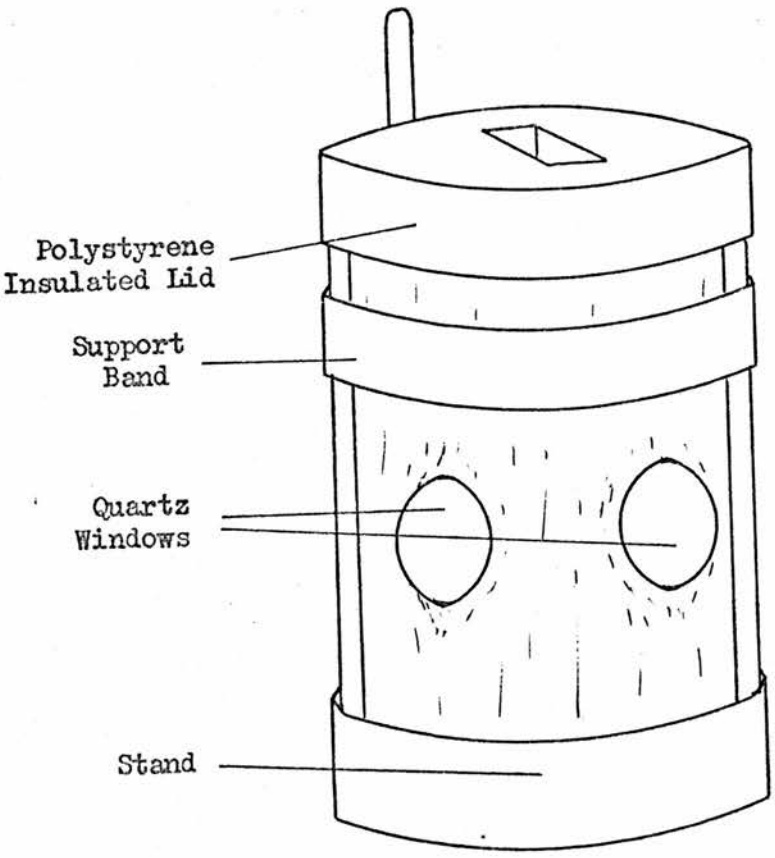

Figure 3.5

Sample Dewar

when cooled to 77K, thus making quantitative measurements extremely difficult. Even with good quality glasses, excitation light can be scattered by the sample and interfere with measurements of emission spectra and total luminescence. The scattered light effect can be largely overcome on the MPF-2A by using a chopper of variable speed which eliminates both random scattered light and short lifetime fluorescence, while allowing longer lived phosphorescence ($\tau > 0.5$ ms) to be detected. However, accurate measurement of relative quantum yields was not possible since the sample geometry was difficult to reproduce.

The solvent used throughout for phosphorescence determinations of metal chelates was ethanol, which allowed solid solution strengths of up to 10^{-1} M and also provided very good quality solid glasses.

(d) CORRECTION OF EMISSION AND EXCITATION SPECTRA

(i) Emission Spectra

An apparent emission spectrum is obtained when a spectrofluorimeter is operated at constant slit width and constant detector sensitivity. The curve obtained is a function of the observed photomultiplier output against wavenumber and this can be represented at any wavenumber ($\bar{\nu}$) by

$$A(\bar{\nu}) = \left(\frac{dQ}{d\bar{\nu}}\right).P(\bar{\nu}).B(\bar{\nu}).L(\bar{\nu}) = \left(\frac{dQ}{d\bar{\nu}}\right).S(\bar{\nu}) \qquad 3.1$$

where $A(\bar{\nu})$ is the observed photomultiplier output, $\frac{dQ}{d\bar{\nu}}$ is the fluorescence intensity, $P(\bar{\nu})$ is the output per quantum from the photomultiplier, $B(\bar{\nu})$ is the bandwidth in wavenumber units, $L(\bar{\nu})$ is the fraction of light transmitted by the spectrofluorimeter and $S(\bar{\nu})$ is the spectral sensitivity factor of the monochromator / photomultiplier combination.

The absolute fluorescence spectrum, which is a plot of the fluorescence intensity measured in relative quanta per unit wavenumber interval against wavenumber, can be obtained by division of the apparent emission spectrum point by point by $S(\tilde{\nu})$. A spectral sensitivity curve can be obtained in various ways[162-166] by taking measurements using,

(1) calibrated tungsten lamps (visible region),

(2) fluorescence screen monitors (ultraviolet region),

(3) thermopiles,

(4) fluorescence solutions which function as quantum screen counters

and, (5) reference solutions, the absolute emission spectra of which have been previously determined.

Both the MPF-2A and the high resolution spectrofluorimeter were calibrated using method (5). The compounds used in the calibrations are given in Table 3.1.

Table 3.1 Compounds used to Calibrate the Spectrofluorimeters

Compound		Solvent	Concentration (M)	Excitation Wavelength (nm)	Range (nm)	Spectrum Reference
A	2-amino-pyridine	0.05M H_2SO_4	$1.3*10^{-5}$	285	300 - 450	167
B	quinine sulphate	0.05M H_2SO_4	$1.1*10^{-5}$	366	400 - 550	162, 164
C	3-amino-phthal-imide	0.05M H_2SO_4	$6*10^{-6}$	390	450 - 630	162
D	N,N-dimethyl-m-nitro-aniline	30/70 benzene /hexane	$1.4*10^{-4}$	390	470 - 650	162

Table 3.1 (cont.)

Compound		Solvent	Concentration (M)	Excitation Wavelength (nm)	Range (nm)	Spectrum Reference
E	aluminium PBBR chelate	95% ethanol	$3*10^{-6}$M PBBR, $2.5*10^{-4}$M $AlCl_3.6H_2O$	390	580 - 700	162
F	4-dimethyl-amino-4'-nitro-stilbene	o-dichloro-benzene	$8*10^{-6}$	470	600 - 750	162

The correction factors for the MPF-2A spectrofluorimeter were found by Ireland[163], and those for the high resolution spectrofluorimeter by Dr. C.R.S. Dean. Comparison of the $S(\bar{\nu})$ values obtained for the MPF-2A and the high resolution spectrofluorimeters showed that the latter instrument had much better response in the red region, due largely to the EMI 9526 photomultiplier (Figure 3.6).

(ii) Excitation Spectra

If a solution of a pure compound is illuminated with light of wavelength λ, and intensity $I(\lambda)$, then the intensity of fluorescence reaching the detector $P(\lambda)$ in arbitrary units may be expressed by

$$P(\lambda) = K.\phi(\lambda).I(\lambda).A(\lambda) \qquad 3.2$$

where $A(\lambda)$ is the fraction of exciting light absorbed by the solution, $\phi(\lambda)$ the quantum yield at wavelength , and K a constant dependent on the geometry of the system.

Measurement of absolute quantum yields of many organic compounds in solution have been shown to be independent of the excitation

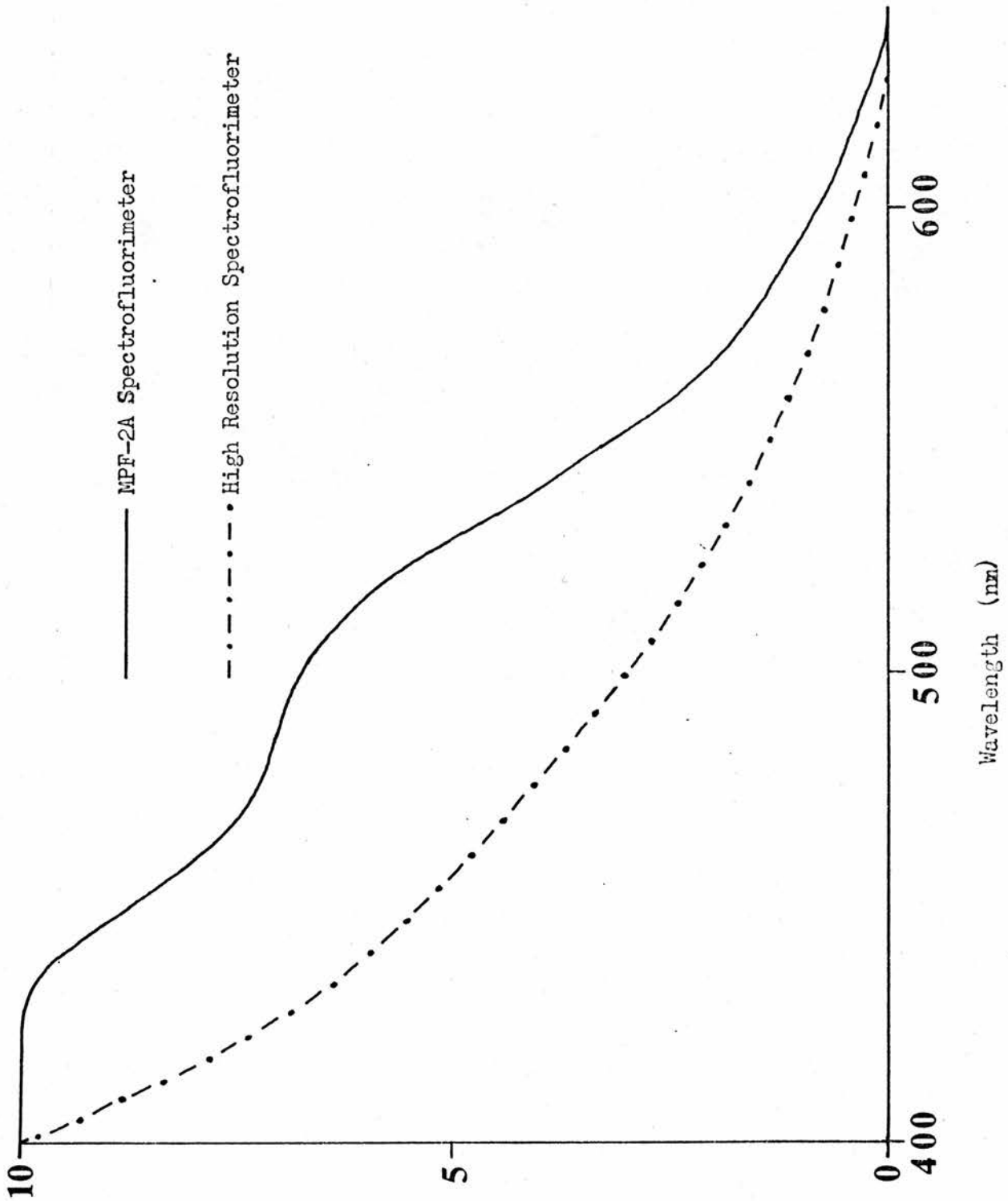

Figure 3.6 Plot of $1 / S(\bar{\nu})$ against λ

wavelength. Absorption and absolute excitation spectra are therefore identical for compounds having a constant quantum yield over any given wavelength range and equation 3.2 may be expressed by,

$$P(\lambda) = K'.I(\lambda).A(\lambda) \qquad 3.3$$

where $K' = K.\phi(\lambda)$

Comparison of the absorption and apparent excitation spectra of such compounds thus allows the spectral sensitivity factor, $S'(\lambda)$, of the source to be calculated from,

$$\frac{P(\lambda)}{A(\lambda)} = K'.I(\lambda) = S'(\lambda) \qquad 3.4$$

The corrected excitation spectrum for any solution may thus be determined by division of the apparent excitation spectrum point by point by $S'(\lambda)$.

If absolute values of the radiative output, $I(\lambda)$, of the source are required, then these may be determined by various methods using, for example,

(1) sensitive thermopiles[11],

(2) calibrated phototubes[168],

(3) ferrioxalate actinometers[169],

(4) fluorescence quantum counters[170],

and, (5) photographic methods[171].

The MPF-2A spectrofluorimeter was calibrated by a modification of method (4), described by Argauer et al.[162], and involved the comparison of the absorption and excitation spectra of dilute fluorescent solutions. The solutions used, experimental technique and results obtained in the calibration of the MPF-2A spectrofluorimeter were discussed by Ireland[163] and are summarised in Table 3.2.

The absorption and excitation spectra of the solutions used to calibrate the $S'(\lambda)$ values of the MPF-2A spectrofluorimeter are given in Figures 3.7 and 3.8.

Table 3.2 Compounds used to Calibrate the MPF-2A Spectrofluorimeter (Excitation)

Compound	Solvent	Concentration (M)	Emission Wavelength (nm)	Range (nm)	Spectrum Reference
aluminium PBBR chelate	95% ethanol	$3*10^{-6}$M PBBR $2.5*10^{-4}$M $AlCl_3.6H_2O$	600	235 - 600	162
quinine sulphate	0.5 M H_2SO_4	$1.1*10^{-5}$M	450	230 - 400	162

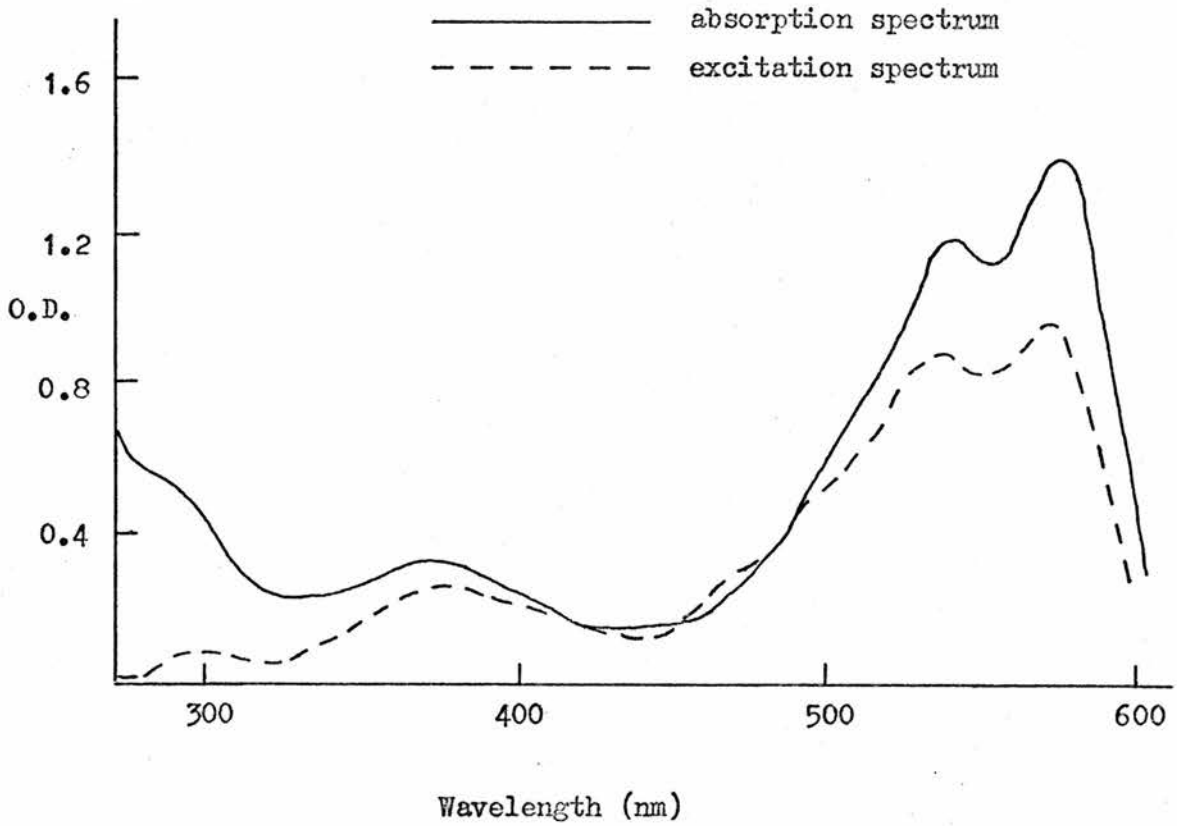

Figure 3.7 Absorption and Uncorrected Excitation Spectra of the Al-PBBR Chelate in Ethanol

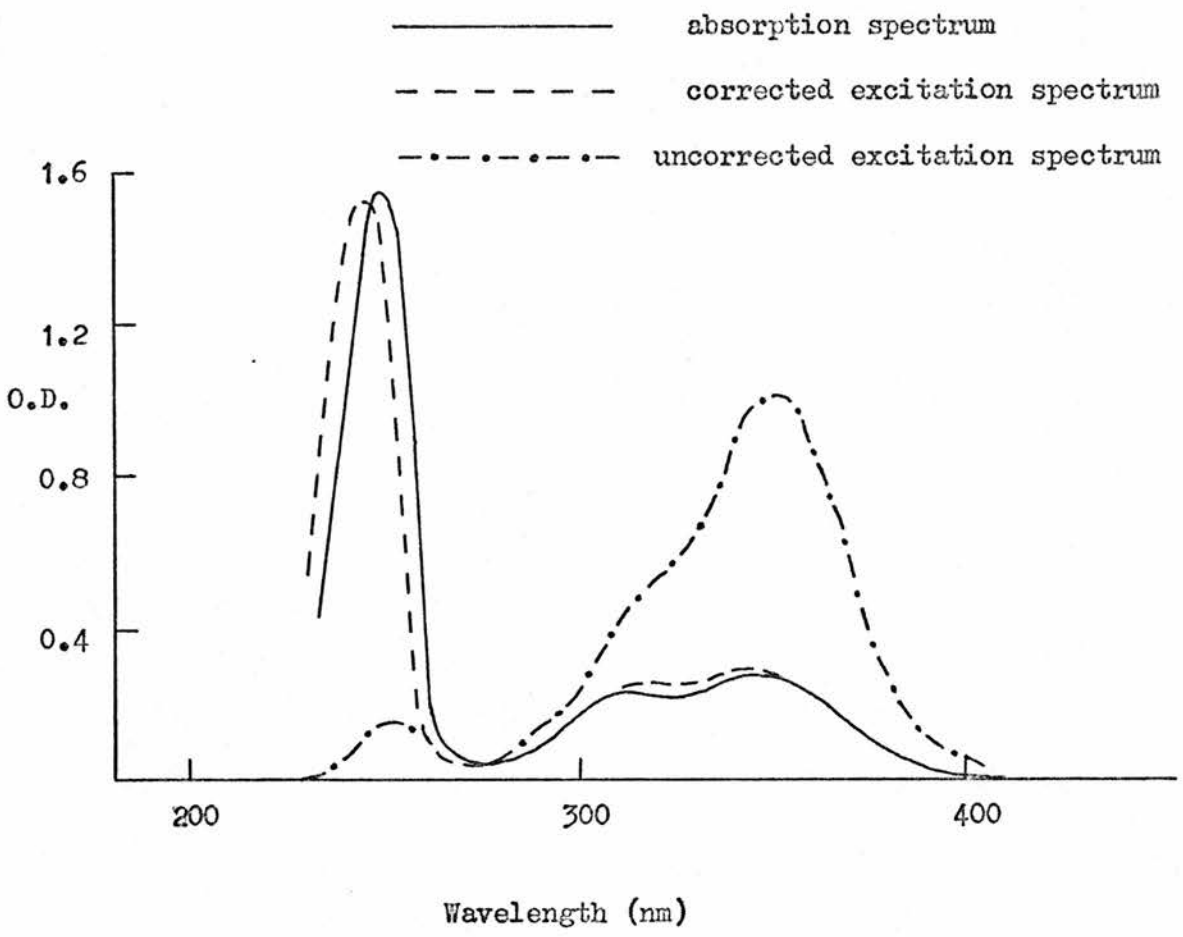

Figure 3.8 Absorption and Excitation Spectra of Quinine Sulphate in 0.5 M H_2SO_4

(iii) Automatic Digitalisation and Correction of Emission and Excitation Spectra

Manual correction of emission and excitation spectra is a tedious exercise, particularly with complicated spectra, and it is therefore necessary to have automation in some form to accomplish this. Several directly correcting spectrofluorimeters have been described with an internally stored correction factor such as a mechanical cam or its electrical equivalent[172-174].

Computers are used extensively to correct spectra[175,176] but the

full potential of such methods depend on the convenience and speed with which the spectrofluorimeter output can be transferred to a computer readable form. The apparatus described below achieves this requirement using automatically punched paper tape and a schematic representation of this apparatus is given in Figure 3.9.

The output signal from the particular spectrofluorimeter - the MPF-2A or the high resolution spectrofluorimeter - is connected to a Solartron LM 1604 digital voltmeter (DVM), with an EX 3054 positive logic fan - out unit. The DVM is interlinked with a Solartron 3230 data transfer unit (DTU), with a Facit 4070 paper tape punch as the output device.

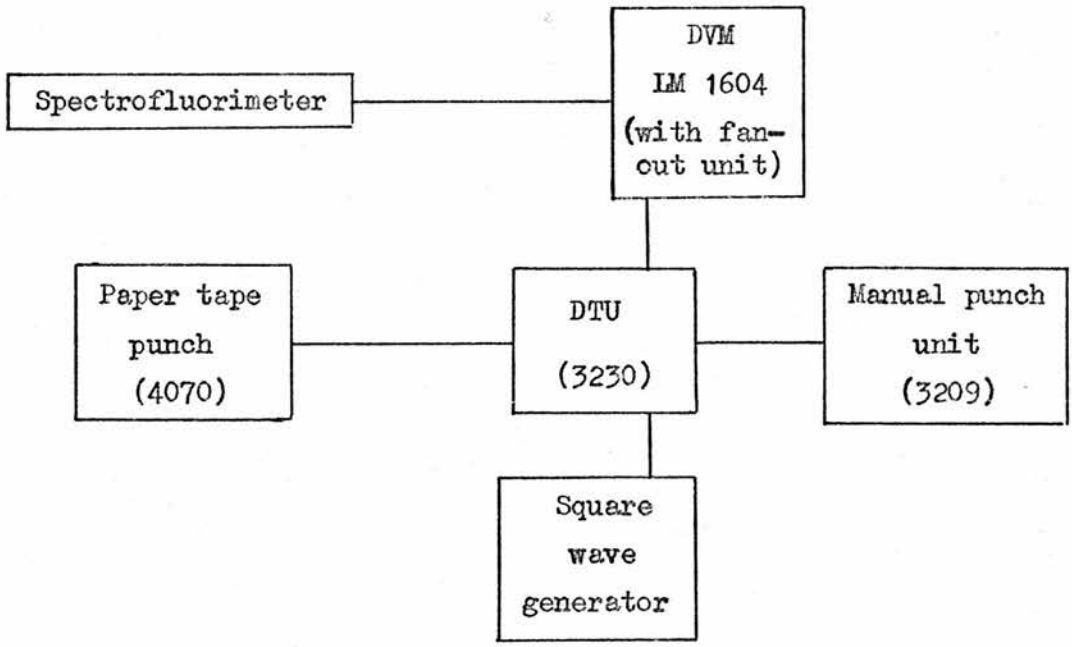

Figure 3.9 Schematic Representation of Automatic Digitalisation Apparatus

This arrangement allows for the photomultiplier detector voltage of the spectrofluorimeter to be sampled and recorded at variable rates. The normal sampling rate used is 4 per second, but slower

rates are obtained by initiating the sample cycle from a variable square wave generator. A Solartron 3209 manual punch unit is incorporated to allow inclusion of control numbers and symbols.

Operation

The following procedure was employed to record a spectrum over the wavelength range λ_1 to λ_2. The wavelengths λ_1 and λ_2, and a spectrum identification code were manually punched onto the paper tape. The spectrofluorimeter was scanned and the tape punch started at λ_1. Scanning and sampling were continued at a suitable rate until wavelength λ_2 was reached, when tape punch and spectrofluorimeter were stopped. An end of data set symbol was then manually punched on the paper tape.

Since the wavelength scan of the spectrofluorimeter was linear with time, the wavelength of the n^{th} record on the tape can be computed from the equation

$$\lambda_n = \lambda_1 + (n-1)(\lambda_2-1) / (N-1) \qquad 3.5$$

where N is the total number of records on a data set. The number N is computed in the program used to correct the spectrum. This method has been found to be convenient and accurate. The tape obtained was processed using a computer program which contained the predetermined response function, $S(\bar{\nu})$ or $S'(\lambda)$, associated with the appropriate spectrofluorimeter to give the corrected spectrum.

An IBM 360/44 computer with a Honeywell 3691 paper tape reader was used. Paper tapes were read and the data transferred directly to the computer core storage. The program used was written in Fortran IV language, with the exception of a short translation program in PL360. The program was written by Dr. C.R.S. Dean in conjunction with Dr. T.M. Shepherd.

(e) EXCITED STATE LIFETIME DETERMINATION

There are three fundamental methods which have been used to obtain excited state lifetimes directly. These are the (i) phase - shift[184-194], (ii) pulsed[195-202] and (iii) single photon counting[203-206] methods.

In the phase - shift method, introduced by Gaviola[177,178], the sample is irradiated with an intensity modulated light beam. The emitted fluorescence is phase shifted relative to the exciting light and the lifetime may be calculated from the phase shift between excitation and fluorescence.

Provided the quantum efficiency of luminescence is sufficiently high, the lifetime of the sample may be determined by pulse fluorometry. A short, intense light pulse is used for excitation and the induced fluorescence is detected by a fast photomultiplier during the intervals between the excitation pulses. The first accurate method of this type in the nanosecond region was described by Brody[179].

Time correlated single photon counting perhaps offers the highest sensitivity and accuracy of any method currently available for measuring fast fluorescence decay functions. In this technique, two photomultipliers are used, one of which observes the excitation source directly while the other detects the arrival of single photons emitted by the sample. The signal from the first photomultiplier provides the zero time reference and is used to gate the output from the second photomultiplier. Repetitive lamp pulsing and photon collection provide the fluorescence decay function which may be displayed on a multi - channel analyser. Early descriptions of this method were reported by Bollinger et al.[180] and Koechlin[181].

Several modifications of these techniques have been described for

direct measurement of fluorescence lifetimes. Ware[182] and Birks[37] have summarised methods employing phase and modulation and pulse sampling techniques, while applications of single photon counting techniques have also been reported[183].

The advantages and disadvantages of the phase - shift, pulsed and single photon counting techniques are summarised in Table 3.3.

Table 3.3 Comparison of Fluorescence Lifetime Techniques

Technique / Characteristic	Phase-Shift	Pulse Sampling	Single Photon Counting
Time resolution	50 ps	2-3 ns	0.5-1 ns
Sensitivity of absorbance at excitation wavelength x ϕ	10^{-6}	10^{-3}	10^{-7}
Direct display of decay	no	yes	yes
Number of half-lives followed	not applicable	1-2	1-7
Ease of analysis of multicomponent decays	very difficult	difficult	easy
Ease of operation	difficult	easy	difficult
Time resolved spectra	not possible	possible	possible
Scattered light	serious	tolerable	tolerable
Sensitivity to lamp intensity drift	not applicable	serious	not applicable

(i) Millisecond Lifetime Determination

A schematic representation of the apparatus used to obtain phosphorescence lifetimes of solid and liquid samples over the temperature range 77 to 300K is shown in Figure 3.10. This apparatus is capable of measuring lifetimes greater than 10μs and includes the Monospek 1000 monochromator previously described for the recording of emission spectra (Section (b)(ii)).

A single, short, intense flash is produced by an E.G. and G. type FX-6A tube and this is used for excitation. The tube is fired by a trigger pulse generated by the signal averager (Data Laboratories 200, DLI02, point averager) and the duration and intensity of the flash controlled by varying the voltage across a 16μF capacitor. The maximum potential available is 800 V. The emission is detected, after passing through the monochromator, by an EMI 9526 photomultiplier.

Figure 3.11 shows the timing sequence in a typical signal averaging procedure. After a predetermined delay, chosen to eliminate any signal from the flash, the photomultiplier output is sampled for a specified period of time and the resultant emission / time function monitored on a sampling oscilloscope. The sample cycle can be repeated for 2^n sweeps, where n = 0 to 8, and the data averaged to give an acceptable signal to noise ratio. The information stored in the signal averager memory can then be transferred onto paper tape by the data transfer unit previously described in Section (b)(ii).

Information concerning the number of averages, the sample temperature, the signal averaging settings and the run identification code is punched onto the paper tape before the data stored on the averager memory is transferred. The rate of output from the averager and the sampling rate of the paper tape unit are synchronised to give 50 values during

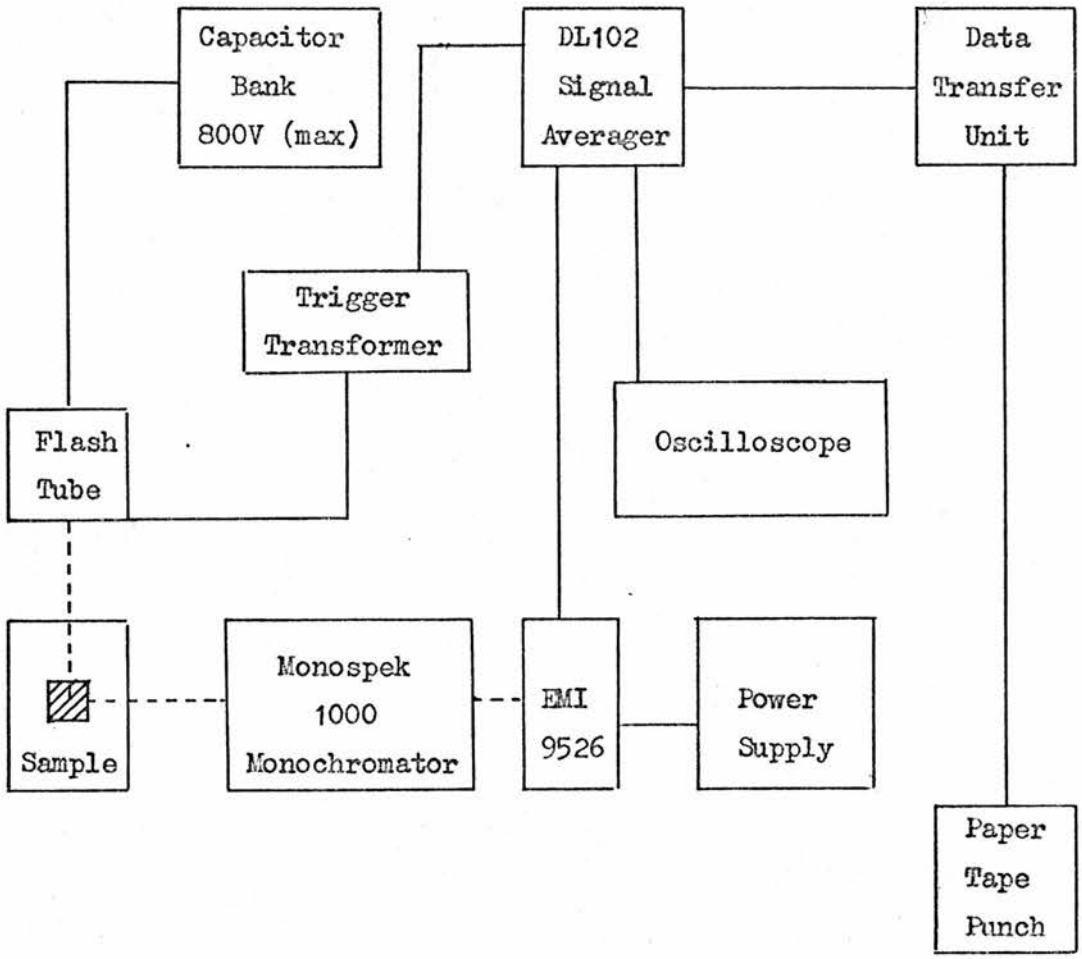

Figure 3.10 Schematic Representation of the Millisecond Lifetime Apparatus

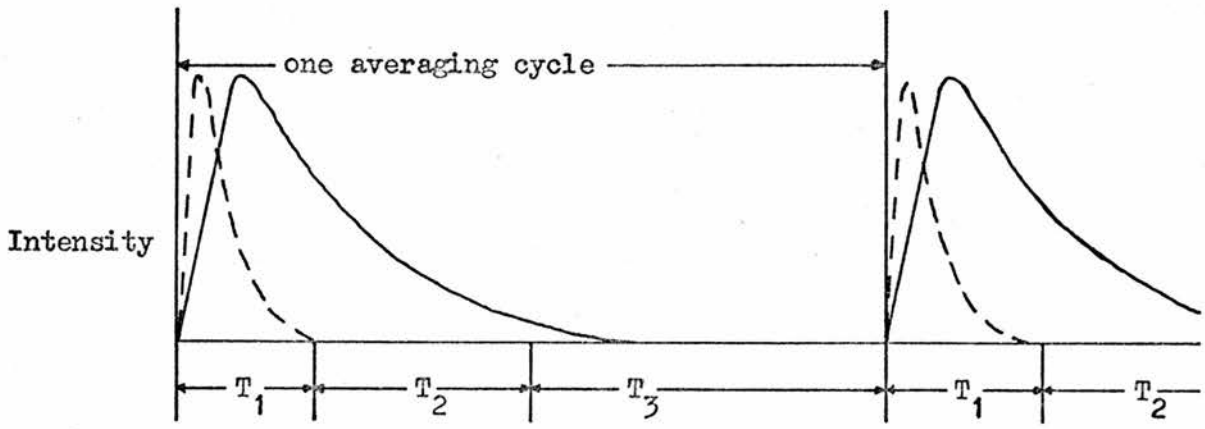

Figure 3.11 Typical Averaging Cycle

T_1 = delay before ; T_2 = sweep time ; T_3 = delay after .

the transfer procedure.

The paper tape output was processed using a computer program which performed a least squares regression to obtain a best straight line relationship between the natural logarithm of the phosphorescence intensity and time. From the gradient of this line, the program allowed calculation of the half- and exponential lifetimes and the difference and percentage difference between calculated and experimental lifetimes, from which the percentage standard deviation from a true exponential was determined.

The program was written by Dr. T.M. Shepherd.

Lifetimes obtained by this method were reproducible to better than 5%.

(ii) Nanosecond Lifetime Determination

The optical and electronic systems of the nanosecond spectrometer are shown in Figure 3.12. All optical components are mounted on a rectangular baseplate provided with locating holes for different configurations and the electronic modules are stacked in a standard 19" rack. This apparatus is capable of measuring lifetimes greater than 5 ns without deconvolution.

Optical System

The excitation source is a low pressure gated lamp with variable tungsten electrodes to optimise pulse duration and light intensity, contained in a shielded housing designed to reduce radiofrequency noise. Nitrogen at 0.5 atmosphere was used for the lamp filling and the electrode gap usually maintained at 2-4 nm. The control unit for the lamp, shown schematically in Figure 3.13, supplies a 2-5 kV discharge between the electrodes controlled by a hydrogen thyratron driven by a

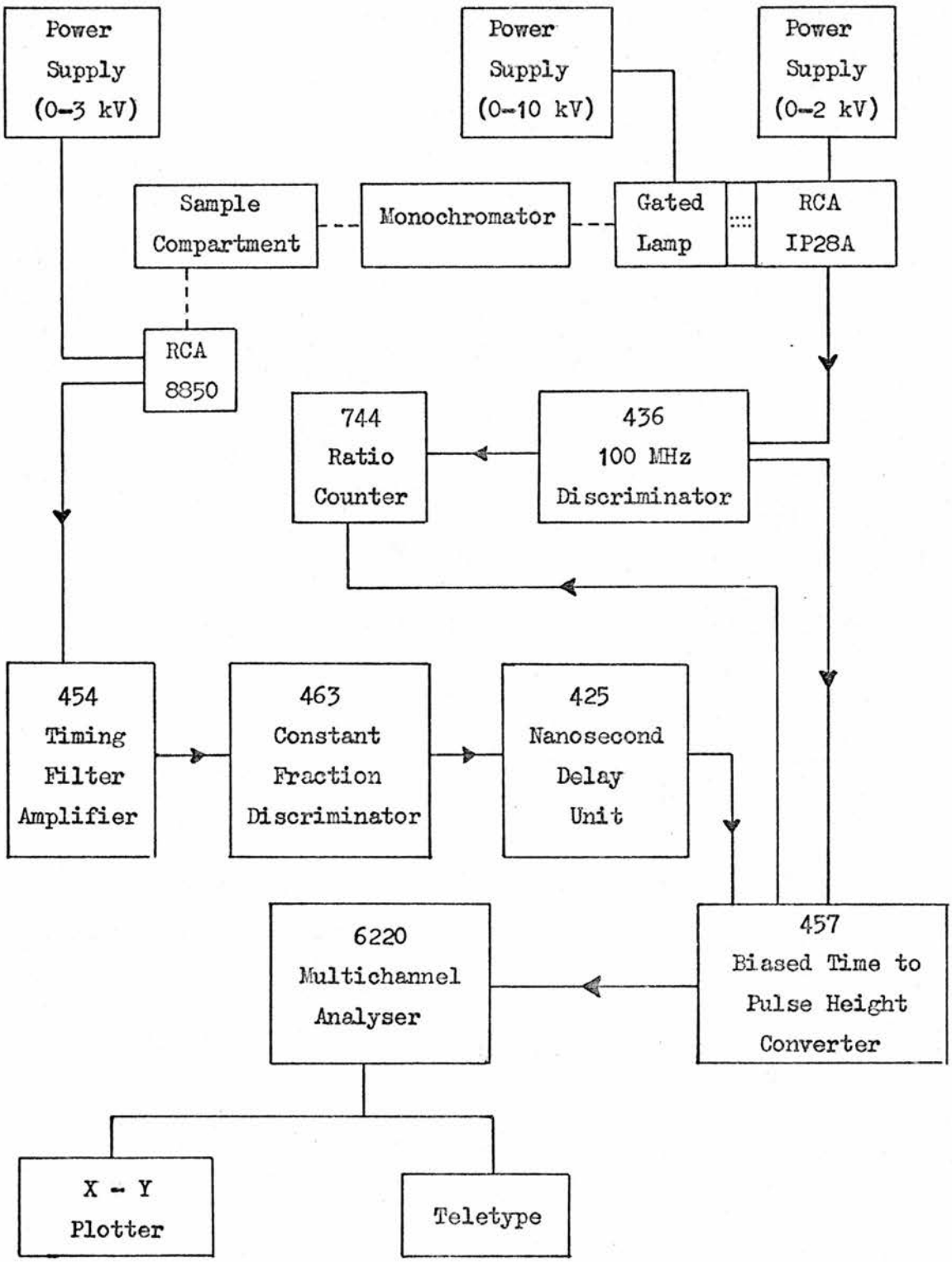

Figure 3.12 Schematic Representation of the Nanosecond Lifetime Apparatus

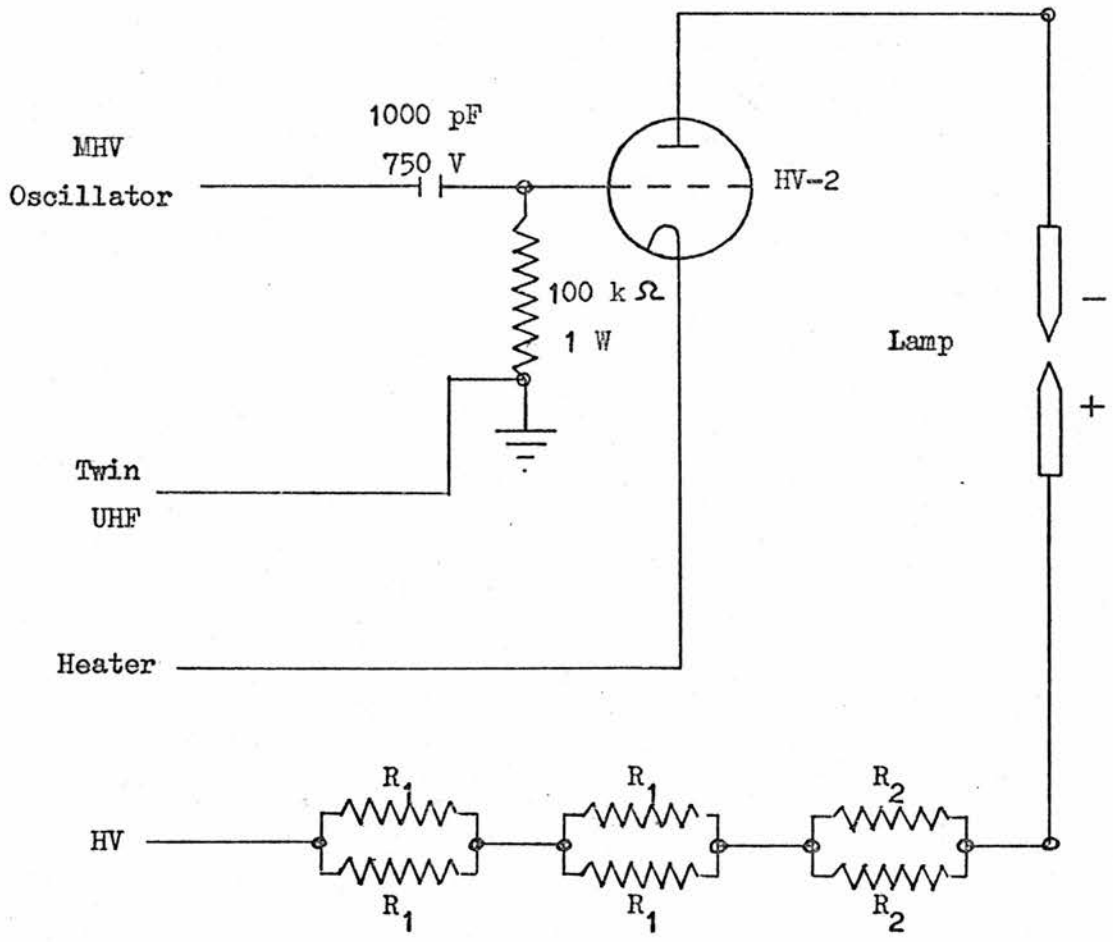

Figure 3.13 Lamp Assembly Circuit Diagram

R_1 = 1 MΩ, Fosters HVR 10B.5W.25kV

R_2 = 220 kΩ.2W

blocking oscillator. The discharge frequency was variable between 5 and 25 kHz. Typical output from the nitrogen filled lamp consists of a line spectrum with strong emission at 296, 316, 337, 358 and 381 nm and the width at half height of the lamp pulse was 2-3 ns.

Light from the gated lamp is passed through a high radiance monochromator which employs a Czerny - Turner optical configuration with a 1200 line/nm diffraction grating and of f/4 aperture. The light intensity could be varied by five fixed slits allowing band passes of 1-20 nm.

The monochromated light is focused onto the sample and fluorescence detected at right angles by means of a sensitive photomultiplier. The sample housing contains an externally adjustable iris for attenuating the light level and holders are provided on both excitation and emission sides of the sample to hold filters and supplementary lenses.

An RCA IP28A photomultiplier is used to monitor the excitation flash and is contained in the same compartment as the gated lamp. The single photon counting photomultiplier, held in a specially designed housing, is an RCA 8850 which has maximum sensitivity in the blue and a typical pulse half - life of 4 ns.

Electronic System

The electronic system used for signal processing consists of standard Nuclear Instrument Modules (NIM), each performing one particular function, and can be divided into two distinct channels - the start and stop channels.

The start signal is produced by a photomultiplier tube which looks directly at the lamp and pulses are produced every time the lamp fires. A 100 MHz discriminator (Ortec 436) generates a pulse of constant amplitude and width for each pulse from the photomultiplier above a preset threshold and this triggers the time base of the 457 Time to Pulse Height Converter (TPHC).

The stop signal, generated by the sensitive photomultiplier tube, is amplified by a 454 Timing Filter Amplifier (TFA) and passed to a 463 Constant Fraction Discriminator (CFD). These instruments shape the output pulse waveform from the photomultiplier and precisely identify the time of occurrence. The output from the CFD passes through a precision nanosecond delay unit (425) which retards its exit for a controlled, adjustable length of time. The 425 is also used for

accurate calibration of the time base. The output from the delay unit enters the stop input of the biased TPHC and stops measuring the time elapsed since the excitation light fired.

The sensitivity of the instrument is monitored using a digital counter to record the ratio of stop to start signals, ideally less than 1%. Experimentally, a rate of 2000 counts per second was found to give satisfactory results.

When the TPHC receives a start signal, a linearly increasing ramp voltage is generated internally which ceases immediately a stop pulse is received from the nanosecond delay module or when the range time of the TPHC is exceeded without receiving a stop pulse. When a stop pulse is detected, the final ramp voltage is proportional to the start - stop interval. This information is passed to the input of a 6220 Multichannel Analyser (MCA) for sorting and storage.

The MCA contains 1024 memory channels and can be used for 512 channel (half) and 256 channel (quarter) data acquisition. The MCA measures each input pulse amplitude, selects a channel number proportional to that amplitude, addresses that channel and adds one count each time it is addressed.

Repeated excitation therefore builds up in the MCA memory a representation of the fluorescence response function of the sample. The count levels and channel numbers are available in digital form and this information generally extracted using a teletype fitted with paper tape facilities. Paper tape output from the MCA was processed using a computer program, a brief description of which follows.

The spectrometer was normally operated using 256 channels to acquire data and output consists of 256 words of 6 characters corresponding to the number of counts in each channel. The first channel (channel zero) times the duration of the run in seconds and

the program totals all counts to compute an average count rate. The program performs a least squares regression to obtain a best straight line relationship between the natural logarithm of the fluorescence count and time. This gives the exponential lifetime of the sample and the percentage deviation from a true exponential. Two variable parameters are available - (a) the lifetime can be determined between any two channels, particularly useful if non - exponential behaviour is suspected and (b) background counts can be subtracted from each channel to negate problems due to spurious signals.

This program was written by Dr. T.M. Shepherd.

Lifetimes determined by this method are reproducible to within 5%.

(f) MOLECULAR WEIGHT DETERMINATIONS

Molecular weight determinations were obtained using a Mechrolab Vapour Pressure Osmometer model 301A. The 301A consists of two principal units - (i) the sample chamber assembly (Figure 3.14) and (ii) the control unit containing a Wheatstone bridge, a null detector and a heater control circuit.

Drops of pure solvent and solute were suspended on the two adjacent thermistors contained in the thermostated chamber which was saturated with solvent vapour. Due to the difference in vapour pressure of the two drops, net condensation occurs on the solution drop. This differential mass transfer causes a temperature difference between two drops which is proportional to the lowering of the vapour pressure and hence also to the solute concentration.

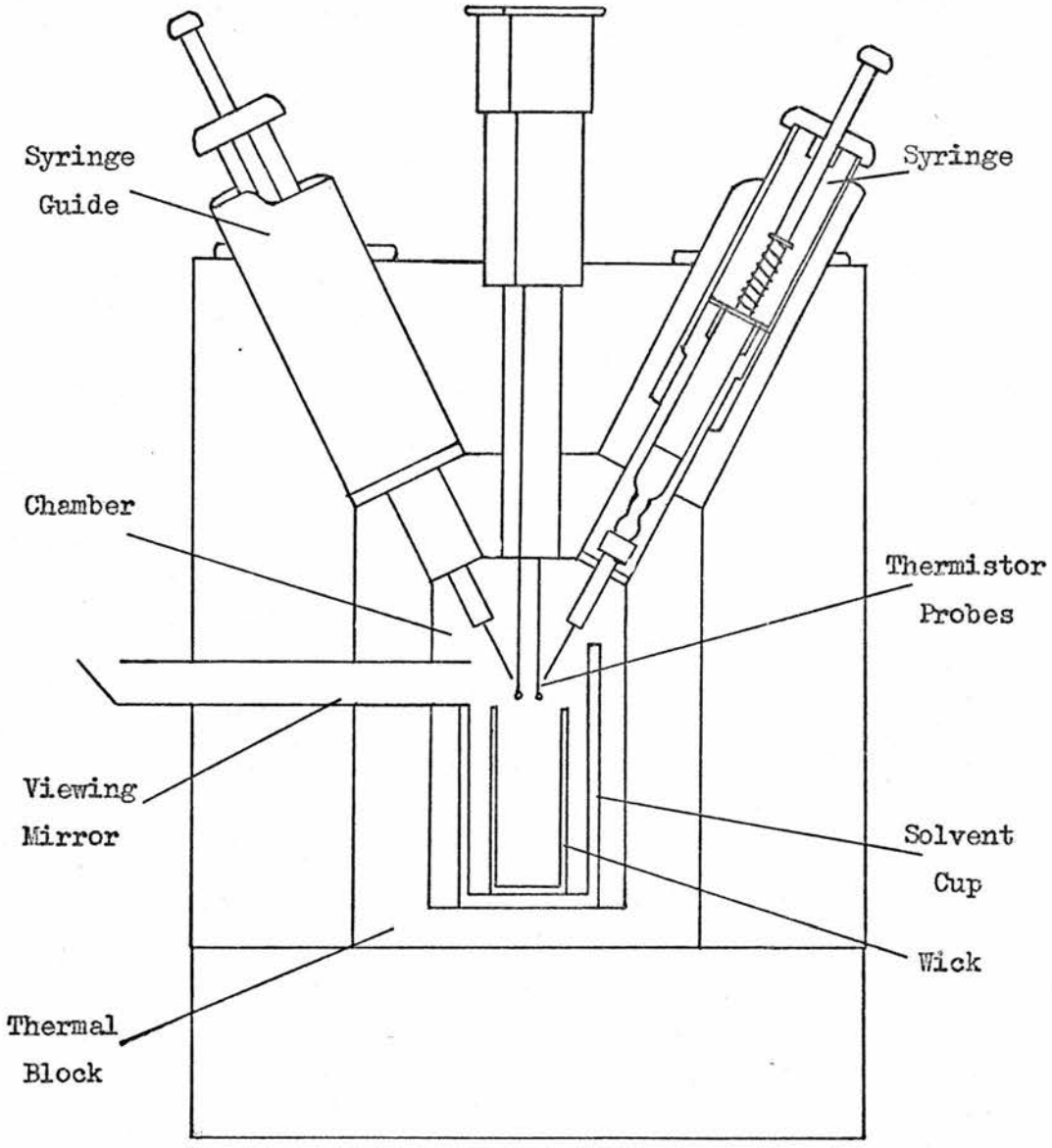

Figure 3.14 Sample Chamber Assembly of the Mechrolab 301A Osmometer

Since this temperature difference is a colligative property, the instrument may be calibrated with a series of solutions of known concentrations. The concentrations of unknown solutes in the same solvent may then be calculated directly from a calibration curve.

The 301A osmometer was calibrated at a temperature of 310K using

benzil (molecular weight = 210) and the experimental accuracy determined using 1,3,5 - trinitrobenzene (molecular weight = 213). For determinations in polar solvents the accuracy was found to be better than ± 10% , whereas in non - polar solvents the accuracy was found to be better than ± 5% .

Molecular weight measurements in similar quasi - isopiestic conditions have been discussed in the literature[207,208].

(g) NMR SPECTROSCOPY

Nmr spectra were recorded on a Varian HA-100 spectrometer (100 MHz) and a Varian EM-360 spectrometer (60 MHz). The HA-100 spectrometer was normally operated at 304K, but a variable temperature probe allowed spectra to be recorded in the temperature range 213 to 383K. The EM-360 spectrometer was operated at ambient temperature and was used for preliminary investigations.

All solutions for analysis were freshly prepared and care was taken throughout to maintain these solutions under anhydrous conditions since some of the observed shifts were very susceptible to traces of moisture. The nmr solvents $CDCl_3$, C_6D_6, DMSO - D_6 and acetone - D_6 (Fluorochem) were stored over molecular sieves. A.R. grade CCl_4 and pyridine (Fisons) were fractionally distilled and stored over molecular sieves.

The 220 MHz spectrum described in Chapter 7 was run by the Physical Chemistry Measurement Unit, Harwell.

CHAPTER 4

SPECTRAL INVESTIGATIONS OF DIAMAGNETIC METAL ACETYLACETONATES IN SOLUTION

I ABSORPTION SPECTRA

(a) INTRODUCTION

The most comprehensive study to date of the absorption spectra of metal acetylacetonates was made in 1958 by Holm and Cotton[209]. They reported the ultraviolet spectra of thirty one $M(AA)_n$ complexes in chloroform and/or ethanol and assigned the most intense absorption in the 240 - 400 nm region (λ_{max}) to a ligand $\pi^* \longleftarrow \pi$ transition. The results were compared with other reported data and discrepancies in the λ_{max} and extinction coefficient (ε_{max}) values for a number of complexes were observed. Three distinct types of complex were classified according to the spectral information, namely those complexes with

(i) a near symmetrical, single peak (e.g. Na(AA)),

(ii) a single peak with a shoulder on the long wavelength side (e.g. $Al(AA)_3$),

and (iii) more complex spectra with additional bands at higher energy due to the metal (e.g. $Cu(AA)_2$).

The shoulder observed with class (ii) and (iii) complexes was assigned to a $\pi^* \longleftarrow$ n transition. Holm and Cotton concluded that several factors, which could not be easily separated, contributed to the

position and intensity of the S_{π,π^*} and S_{n,π^*} bands for each complex[209].

The absorption spectra of a series of $M(AA)_3$ complexes have also been interpreted by Barnum[210] in terms of a molecular orbital model, with the splitting of three degenerate $\pi^* \leftarrow \pi$ transitions, calculated by the Hückel method. Yamasaki and Sone[211], taking the red shift of λ_{max} relative to that of acetylacetone as a measure of stability, concluded that the order of stability for a series of divalent transition metal complexes was Cu > Ni > Co > Zn > Fe, Mn and this trend was borne out by experimentally determined β_2 values. Holm and Cotton[209] reported that there was no comparable correlation between β_3 and λ_{max} for tris- acetylacetonates.

(b) LIGAND ABSORPTION OF METAL ACETYLACETONATES

The absorption spectra of a series of diamagnetic metal acetylacetonates in ethanol solution at various concentrations ranging from $< 10^{-5}$M to $> 10^{-3}$M have been determined. The main feature of these spectra is the single, intense absorption band which occurs in the 270 - 300 nm region and which is assigned to the $\pi^* \leftarrow \pi$ transition of the acetylacetonate ligand[209]. A distinct shoulder occurs on the low energy side of this absorption band in all the complexes examined (Table 4.1), with the exception of the Group Ia complexes. A number of the spectra showing this shoulder have been satisfactorily resolved into two Gaussian components using a Du Pont 310 Curve Resolver and the shoulder is consistent with the presence of a second, weaker absorption band with λ_{max} in the range 300 - 315 nm and $\varepsilon_{max} \leqslant 5000$ $cm^{-1}mol^{-1}dm^3$. This second band is assigned as a

$\pi^* \longleftarrow$ n transition of the acetylacetonate ligand[209]. Table 4.1 lists the found values of λ_{max} and ε_{max} for the main $\pi^* \longleftarrow \pi$ transitions for all the complexes at or near the highest concentration possible using 1 mm quartz cells.

Table 4.1 Absorption Data for Metal Acetylacetonates in Ethanol Solution

$M(AA)_n$ Complex	Concentration[a] mol dm^{-3} ($x10^4$)	λ_{max} nm	λ_{max} cm^{-1}	ε_{max} $cm^{-1}mol^{-1}dm^3$	$\log \varepsilon_{max}$
M= H^+	21.6	274	36500	8500	3.93
b H^+	19.2	274	36500	8700	3.94
Li^+	4.0	293	34100	20100	4.30
Na^+	8.2	294	34000	13500	4.13
K^+	8.7	294	34000	16900	4.23
Rb^+	6.5	294	34000	17700	4.25
Cs^+	5.2	294	34000	20300	4.31
Mg^{2+}	5.6	285	35100	32800	4.51
Ca^{2+}	5.5	291	34400	29000	4.46
Sr^{2+}	5.3	292	34300	24100	4.38
Ba^{2+}	6.2	295	33900	26250	4.42
Al^{3+}	3.6	287	34800	39100	4.59
Ga^{3+}	3.6	287	34800	36100	4.56
In^{3+}	3.2	287	34800	35300	4.55
Sc^{3+}	3.2	299	33400	32000	4.51
Y^{3+}	4.3	287	34800	32800	4.52
La^{3+}	4.7	291	34400	36100	4.56
c Gd^{3+}	4.1	289	34600	34900	4.54
Lu^{3+}	4.6	287	34800	38600	4.59
Zn^{2+}	4.7	285	35100	33000	4.52
Th^{4+}	3.6	285	35100	29400	4.47

(a) Spectra recorded in 1 mm cells.

(b) Comparable data in aqueous solution.

(c) $Gd(AA)_3.3H_2O$ was the only paramagnetic metal complex studied.

It was evident from measurements made over a range of concentrations that the spectral profiles of the absorption band and the extinction coefficients of many of the complexes were markedly concentration dependent, i.e. Beer's Law was not obeyed. These observations raise doubts about the validity of some previously reported data where the conditions were not stated[209,210].

A pronounced red shift in λ_{max} and a significant increase in ε_{max} were observed on increasing the concentration of ethanolic solutions of the Group Ia, Group IIa (with the exception of magnesium), lanthanum and thorium complexes. Specific examples of this effect are given in Table 4.2. It may be seen that, in these particular cases, λ_{max} at or near 10^{-5}M concentration is ca. 275 nm and that increasing the concentration causes the band to shift to a value of λ_{max} = 293 ± 2 nm ($Th(AA)_4$ is an exception) at ca. 5×10^{-4}M.

Table 4.2 Concentration Dependence of Certain Metal Complexes in Ethanol Solution

Metal Complex	"Dilute" Solution (10 mm cells)			"Conc." Solution (1 mm cells)		
	conc. mol dm^{-3}	λ_{max} nm	ε_{max} $cm^{-1}mol^{-1}dm^3$	conc. mol dm^3	λ_{max} nm	ε_{max} $cm^{-1}mol^{-1}dm^3$
Na(AA)	1×10^{-4}	275	8800	8×10^{-4}	295	13500
K(AA)	1×10^{-4}	275	8000	8×10^{-4}	295	16900
Rb(AA)	6×10^{-5}	275	7050	6×10^{-4}	293	18000
Cs(AA)	5×10^{-5}	275	10000	5×10^{-4}	295	21100
$Ca(AA)_2$	1×10^{-5}	277	19800	5×10^{-4}	291	29000
$Sr(AA)_2$	1×10^{-5}	276	17300	5×10^{-4}	292	26300
$Ba(AA)_2$	1×10^{-5}	277	16000	6×10^{-4}	295	26000
$La(AA)_3\cdot 3H_2O$	1×10^{-5}	276	25600	5×10^{-4}	292	36000
$Th(AA)_4$	1×10^{-5}	275	33400	3×10^{-4}	286	29400

The chelates of gallium, indium, yttrium and gadolinium showed a similar type of behaviour but the shifts were much less pronounced. Only in the cases of the aluminium and zinc acetylacetonates could the observed deviations be attributed to experimental error. In all other cases examined, significant deviations from Beer's Law were observed. One other feature of this concentration dependence was the development of the previously mentioned shoulder with increasing concentration in many of the spectra. Figure 4.1 illustrates the concentration dependence of the absorption spectrum of $Ba(AA)_2$.

An important feature of ethanolic solutions of the acetylacetonates of the Group Ia and lanthanide metals, which has only been reported previously for certain lanthanide complexes[212], is the temperature and/or time dependence of the absorption spectra. For example, ethanolic solutions of Na(AA), at all concentrations examined, showed pronounced blue shifts in λ_{max} with time under the conditions which occur in an unthermostated sample compartment of a spectrophotometer (Figure 4.2). The spectrum of the stock solution, thermostated at room temperature over the same time period as that of the example in Figure 4.2, showed only a very slight blue shift. Further experiments confirmed that this kinetic interaction was irreversible and that there was no photochemical explanation for this phenomenon. Similar results were obtained for methanolic solutions of Na(AA) but, in contrast, aqueous solutions showed no appreciable change in either λ_{max} (294 nm) or ε_{max} (14600 $cm^{-1}mol^{-1}dm^3$) under identical conditions. In dilute ethanolic solutions (ca. 10^{-5}M) the spectral profiles of all the Group Ia complexes changed to give limiting values for λ_{max} (275 nm) and ε_{max} (ca. 9000 $cm^{-1}mol^{-1}dm^3$) near identical to that of acetylacetone in ethanol.

The importance of this particular phenomenon is discussed in more detail later.

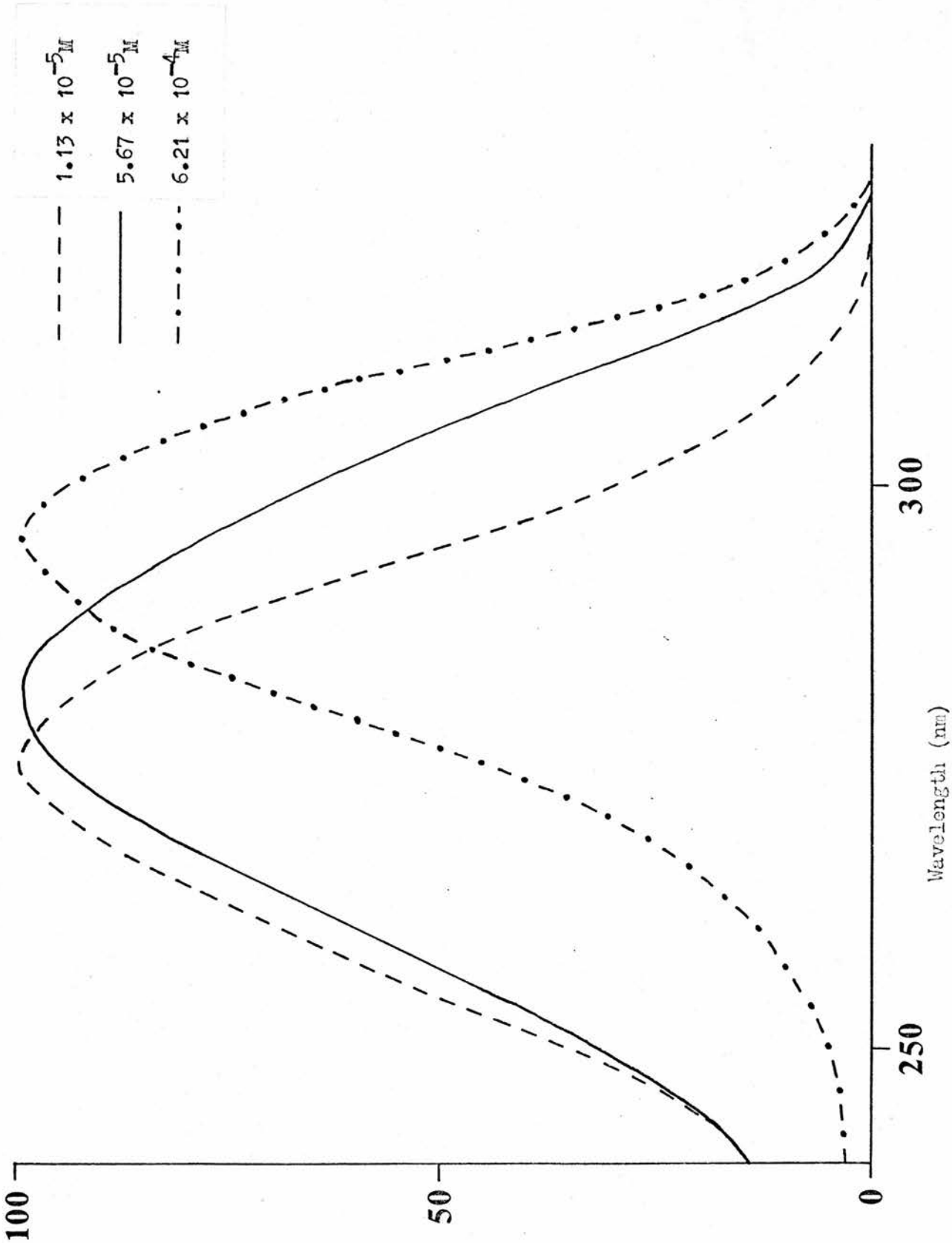

Figure 4.1 Absorption Spectra of $Ba(AA)_2$ in Ethanol Solutions at 300K, λ_{max} Normalised to 100 Units

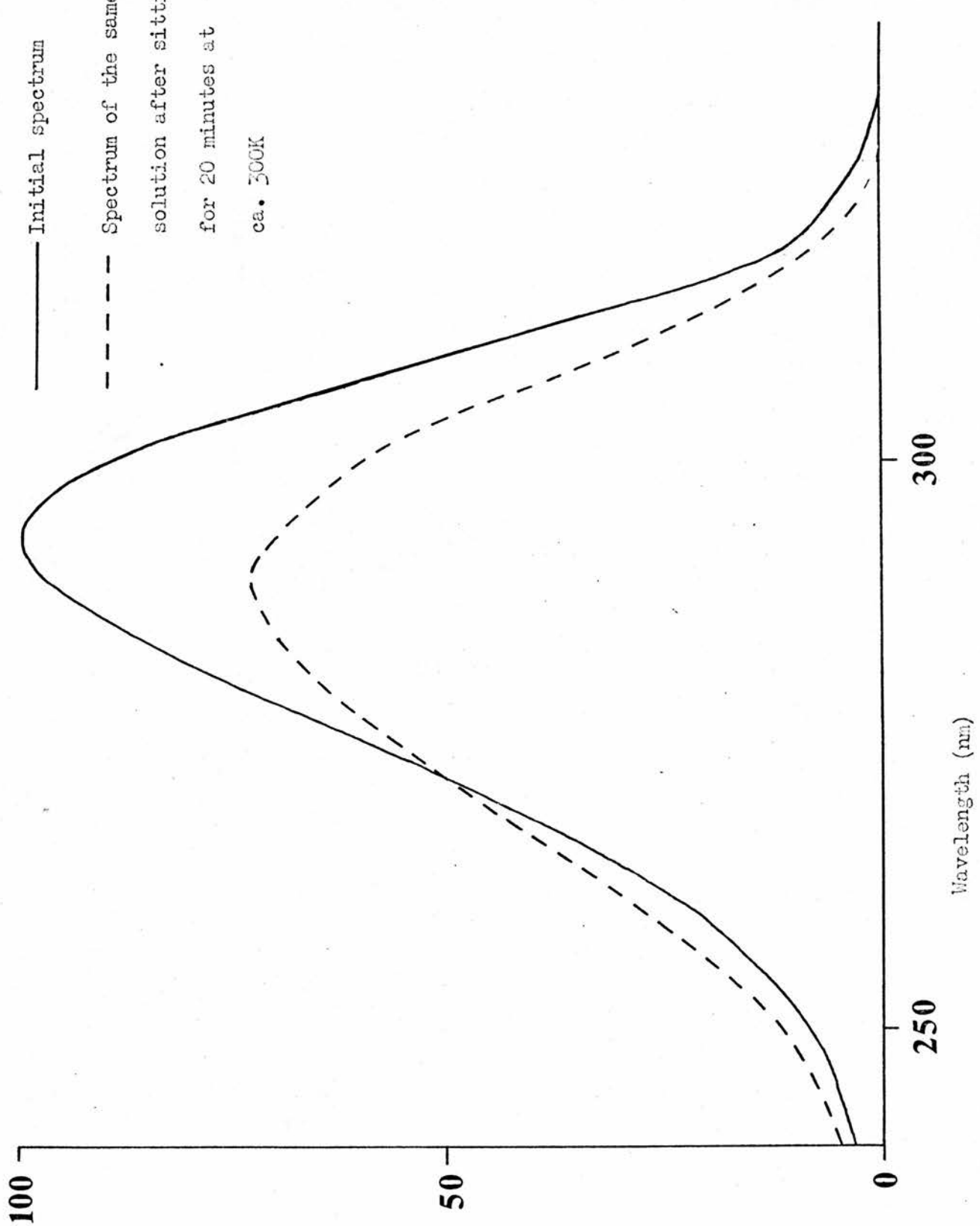

Figure 4.2 Absorption Spectrum of Na(AA) in Ethanol at ca. 7×10^{-4} mol dm^3

(c) MOLECULAR DISSOCIATION OF $M(AA)_n$ COMPLEXES

Perhaps the simplest explanation for the deviations from Beer's Law which were outlined above would be in terms of varying degrees of dissociation of the complexes. Any complex of the type $M(AA)_n$ may dissociate with the loss of one or more ligand groups to give ionic species according to the general scheme,

$$M(AA)_n \rightleftharpoons \left[M(AA)_{n-1}\right]^+ + AA^- \ ,$$

$$\left[M(AA)_{n-1}\right]^+ \rightleftharpoons \left[M(AA)_{n-2}\right]^{2+} + AA^- \ ,$$

through to

$$\left[M(AA)\right]^{(n-1)+} \rightleftharpoons M^{n+} + AA^- \qquad 4.1$$

Formation constants (K) for the equilibria have been reported for most of the metal acetylacetonates in aqueous solution, but in the case of Group Ia metal chelates the only reported values of K have been determined in ethanol or methanol solution[145]. The reported log K values for some of the Group Ia metal acetylacetonates in ethanol at 298K are given in Table 4.3. Since the formation constant for any of these complexes is given by

$$K = \frac{\left[M(AA)\right]}{\left[M^+\right]\left[(AA)^-\right]} \qquad 4.2$$

the concentration of free acetylacetonate ligand anion may be readily calculated and the percentage of dissociated ligand at various total concentrations are also presented in Table 4.3. These calculations assume that there are no equilibria other than

$$M(AA) \rightleftharpoons M^+ + (AA)^- \qquad 4.3$$

The calculated values indicate that near complete dissociation

Table 4.3 % Free Anion at Specific Concentrations of M(AA) in Ethanol at 298K

M(AA) Complex	log K [a]	% Free Anion at Concentration				
		10^{-1} M	10^{-2} M	10^{-3} M	10^{-4} M	10^{-5} M
H^+	11.81	<0.01	<0.01	<0.01	0.01	0.04
Li^+	4.6	1.6	4.9	14.6	39.2	76.6
Na^+	2.8	11.8	32.7	69.5	94.4	99.4
K^+	2.1	24.5	57.8	89.8	98.8	99.9

(a) Values obtained from reference 213.

will occur in ethanolic solutions of all the alkali metal acetylacetonates with the exception of lithium at concentrations below ca. 10^{-3} M.

The marked change observed in the absorption spectrum of, for example K(AA) over the concentration range 10^{-4} to 8×10^{-4} M (Table 4.2), cannot therefore be simply explained in terms of varying degrees of dissociation since the above calculations indicate that the complex is ca. 90% dissociated within this concentration range.

Formation equilibrium constants have not been reported for the other metal acetylacetonates in ethanol solution. These have, however, been determined in aqueous solution[145]. The stepwise formation constants (K) for the aqueous reactions

$$\left[M(AA)_{n-1}\right]^+ + (AA)^- \rightleftharpoons M(AA)_n \qquad 4.4$$

are given in Table 4.4. It is expected that the corresponding formation constants in ethanol will be considerably higher than the aqueous values.

The values of log K for the equilibrium

$$H^+ + (AA)^- \rightleftharpoons H(AA) \qquad 4.5$$

Table 4.4 Formation Constant Data for Metal Acetylacetonates in Water at 303K

$M(AA)_n$ Complex	log K	Reference
Mg^{2+}	2.54	214
Al^{3+}	5.8	215
Ga^{3+}	5.7	215
Y^{3+}	3.25	216
La^{3+}	2.50	216
Gd^{3+}	3.41	216
Lu^{3+}	3.63	216
Zn^{2+}	3.9	215
Th^{4+}	4.2	215

have been determined for ethanolic and aqueous solutions as 11.81[213] and 8.98[217] respectively and it is reasonable to suppose that the corresponding log K values in ethanol solution will be some 2 to 3 units higher than those shown in Table 4.4. It is also likely that the order of stability will be the same, i.e.

$$Al^{3+} > Ga^{3+} \gg Th^{4+} > Zn^{2+} > Lu^{3+} > Gd^{3+} > Y^{3+} > La^{3+} \approx Mg^{2+} ,$$

with respect to the loss of one ligand from the neutral complex.

This order does not, however, correspond with the varying extent of the deviations from Beer's Law described in Section (b) of this chapter. Therefore, the variations in absorption spectra cannot be directly attributed to varying degrees of dissociation with these complexes, and the absorption in the 275 nm region cannot be attributed to the acetylacetonate ligand. It is therefore necessary to consider the possibility of other reactions in these solutions.

(d) SOLVOLYSIS OF THE ACETYLACETONATE LIGAND

In the model presented above, it was assumed that the free acetylacetonate ligand, formed by dissociation of $M(AA)_n$ complexes, did not interact with the solvent. It is, however, possible that this anion may abstract a proton from a hydroxylic solvent,

$$(AA)^- + ROH \rightleftharpoons HAA + (OR)^- \qquad 4.6$$

to give acetylacetone and a hydroxide ion (R = H) or an alkoxide ion (R = alkyl group). The OR^- anion may in turn react with any available free metal ion or partially dissociated complex, $\left[M(AA)_{n-m}\right]^{m+}$ (where $n \geq m \geq 1$), leading to a further set of equilibria,

$$\left[M(AA)_{n-m}\right]^{m+} + (OR)^- \rightleftharpoons \left[M(AA)_{n-m}(OR)\right]^{(m-1)+} \qquad 4.7$$

A further complication with alcoholic solutions which are not completely dry is the presence of the equilibrium,

$$(OR)^- + H_2O \rightleftharpoons ROH + (OH)^- \qquad 4.8$$

With the present limited data, it has not been possible to usefully examine the validity of this complicated series of interdependent equilibria in quantitative terms. It is, however, possible to make a qualitative assessment.

Dissociation followed by solvolysis must lead to the formation of free acetylacetone in solution. The absorption spectra of acetylacetone in aqueous and ethanolic solutions have been determined over the experimentally attainable range (Table 4.1). The λ_{max} of acetylacetone in both solvents is concentration independent and identical at 274 nm with $\varepsilon_{max} = 8500\ cm^{-1}mol^{-1}dm^3$. This result

suggests that, in the " dilute " ethanolic solutions of Table 4.2, the predominant species is not free acetylacetonate ligand anion but is acetylacetone. The red shift on increasing concentration is thus likely to be due to an increase in the relative proportion of metal complex or, particularly in the case of M(AA) complexes, free acetylacetonate anion. It is improbable that there are any significant concentrations of undissociated complex in the concentration range in which absorption spectra were obtained, since the formation constants of M(AA) are low (Table 4.3).

Further support for this proposal was obtained from investigations of the absorption spectra of Na(AA) in aqueous solution. In this case, a consistant absorption profile (λ_{max} = 292 nm, ε_{max} = 12000 cm^{-1} $mol^{-1}dm^3$) was found over the concentration range 10^{-5} to 10^{-3} M. Similar results were obtained for the other M(AA) complexes, in agreement with the results of Holm and Cotton[209]. This contrast in the behaviour of ethanolic and aqueous solutions is consistent with equilibrium 4.7 being largely to the left when R = H, i.e.

$$Na^+ + OH^- \longrightarrow NaOH \qquad 4.9$$

and less so when the weaker base sodium ethoxide is present ($R = OEt^-$). The results in Table 4.2 indicate that the free ligand may have a considerably higher extinction coefficient than the associated complex, as shown by the trend in ε_{max} with the " concentrated " solutions Cs > Rb > K > Na.

The deviations in Beer's Law shown by metal complexes other than those of Group Ia can also be rationalised within this scheme. It can be seen that, of the three distinct equilibria proposed (4.1, 4.6 and 4.7), only the equilibrium shown by 4.6 is independent of the metal ion. As a general but not inviolate guide, it may be argued that those complexes which are least likely to dissociate are also

most likely, in dissociated form, to form stable ion - pairs or complexes with ethoxide or hydroxide ions. The counterbalance of these two effects makes it improbable that any direct relationship between K values and, for example, the extent of hydrolysis at low concentration should exist.

In the situation where one or more of the species $\left[M(AA)_{n-m}(OR)\right]^{(m-1)+}$ (equation 4.7) is insoluble, then the complex $M(AA)_n$ will ultimately be destroyed. It has been found in the case of lanthanide acetyl - acetonates in ethanol solution at concentrations of ca. 10^{-3}M that a slow spectral change occurs over a period of hours. The final spectrum corresponds to that of acetylacetone (λ_{max} = 275 nm) and a white precipitate is observed which is largely $In(OH)_3$[212]. It is known that alkali metal alkoxides in alcohol solutions readily form ion - pairs[218,219], presumably due to the lower dielectric constants of the alcohols relative to water[220]. It is therefore probable that stable ion - pairs of some of the metal ions with ethoxide ion will be formed in preference to the metal hydroxide complex.

Although the equilibrium constants for each of the valid equilibria may be calculable by methods other than studying absorption spectra, the rate of attainment of a particular equilibrium is less easily found. Since the spectrum of Na(AA) in water is unchanged over a period of hours at ca. 300K, it is presumed that the dissociation of this complex is completed very rapidly. It is further proposed that the dissociation of the comparable $M(AA)_n$ complexes in ethanol similarly occur in minutes. Since equation 4.6 will occur for each system, it is probable that the rate determining step is that shown by equation 4.7. For example, the absorption spectra of Na(AA) show marked changes in profile which are stabilised in ca. 20 minutes (Figure 4.2). In contrast, the comparable absorption spectral changes for the lanthanide

acetylacetonates require a period of hours to reach equilibrium. It is probable that the most stable complex, in terms of the absorption spectral results, $Al(AA)_3$, may eventually decompose to $Al(OH)_3$, although this particular reaction may take weeks to reach an equilibrium.

(e) CONCLUSIONS

In the concentration range in which absorption spectra are readily measurable, i.e. 10^{-5} to ca. 10^{-3} M, it has been found that a large number of metal acetylacetonate complexes show marked deviations from Beer's Law. These deviations can be qualitatively explained in terms of a series of interdependent equilibria involving dissociation of the complex, solvolysis of the acetylacetonate anion and the formation of metal ethoxide ion - pairs or, as is more likely with metals other than those of Group Ia, sparingly soluble metal hydroxides if the ethanol is not absolutely dry.

The absorption spectrum of free acetylacetonate anion has an absorption maximum at ca. 294 nm which is close to that of the coordinated ligand. Absorption spectroscopy is thus a poor diagnostic for the dissociation and subsequent solvolysis of metal acetylacetonates. The results also indicate that considerable caution should be taken regarding any precise interpretation of the λ_{max} values since it is not possible to assess the value of the undissociated complex unequivocally.

The intense band which occurs in the region 290 $\pm$ 5 nm is attributed to a $\pi^* \leftarrow \pi$ transition of the acetylacetonate ligand, free or coordinated. The shoulder on the low energy side, which is

only apparent in situations where the ligand is likely to be coordinated to a metal ion, is assigned as an $\pi^* \leftarrow n$ transition of anomalously high intensity. It is significant that this shoulder is noticably absent in the absorption spectra of the Group Ia metal complexes.

The absence of significant deviations from Beer's Law for complexes which have sufficient solubility in aqueous media, e.g. the Group Ia complexes, results from the higher basicity of NaOH relative to NaOEt.

CHAPTER 5

SPECTRAL INVESTIGATIONS OF DIAMAGNETIC METAL ACETYLACETONATES IN SOLUTION

II LIGAND PHOSPHORESCENCE

(a) INTRODUCTION

The absence of any appreciable ligand fluorescence from metal β - diketoenolate complexes suggests that efficient intersystem crossing occurs from the first excited singlet state of the ligand (S_1) to a ligand triplet state[221]. The excited ligand triplet (T_1) may then deactivate to the ground state singlet (S_0) by radiative and/or non - radiative processes[222,223]. The emission shown by some lanthanide complexes on excitation of the ligand is the result of an intramolecular transfer process involving a $T_1 \longrightarrow M^{n+}$ transition[224]. It is probable that those transition metal acetylacetonate complexes which do not emit ligand phosphorescence have a similar $T_1 \longrightarrow M^{n+}$ transition, with the metal ion exciting level relaxing entirely or almost entirely non - radiatively[225,226].

Brinen et al.[227] have investigated the ligand phosphorescence of some lanthanide β- diketoenolates in a 3:1 ethanol/methanol glass at various temperatures. They obtained phosphorescence spectra and lifetimes for $La(DPM)_3$, $La(TFAA)_3$ and $La(HFAA)_3$ and found that phosphorescence from the corresponding europium chelates was " very much weaker than from the lanthanum complexes " due to ligand - metal interactions. Crosby et al.[222] have studied the phosphorescence of the

acetylacetonates of the trivalent metals aluminium, lanthanum, lutetium, rhodium, iridium and gadolinium. They concluded that the emission was a π,π^* triplet - singlet phosphorescence originating from a ligand localised state. The triplet nature of the emitting level was corroborated by the trend in measured lifetimes of the Al, La and Lu complexes which were found to decrease as the atomic number increased. They observed no ligand triplet emission from the corresponding Rh and Ir chelates, contrary to the reported observations of De Armond and Hillis[226].

While the present work was in progress, the phosphorescence properties of the closed shell metal chelates $Al(AA)_3$, $Al(TFAA)_3$, $Al(HFAA)_3$, $Ga(AA)_3$, $In(AA)_3$ and $Mg(AA)_2$ were reported by Clarke and Connors[223]. Their results indicate that although the metal ion does not affect the position and structure of the ligand phosphorescence, it is important in intersystem crossing and radiative coupling to S_0. The successive replacement of methyl groups by CF_3 groups alters the electron distibution of the ligand enough to induce a red shift in the position of the ligand phosphorescence.

(b) LIGAND PHOSPHORESCENCE OF $Al(AA)_3$

The excitation spectrum of $Al(AA)_3$ in ethanol solution at 77K is shown in Figure 5.1. The excitation spectrum is identical, within experimental error, to the absorption spectrum which has been discussed in Chapter 4. Using a Du Pont 310 Curve Resolver, the absorption spectrum was resolved into two Gaussian components with absorption maxima at 286 nm (ε_{max} = ca. 40000 $cm^{-1}mol^{-1}dm^3$) and 303 nm (ε_{max} = ca. 5000 $cm^{-1}mol^{-1}dm^3$). The intense absorption at 286 nm is assigned to a ligand $\pi^* \leftarrow \pi$ transition and the weak shoulder at 303 nm is assigned to a ligand $\pi^* \leftarrow$ n transition[209]. The estimated absorption

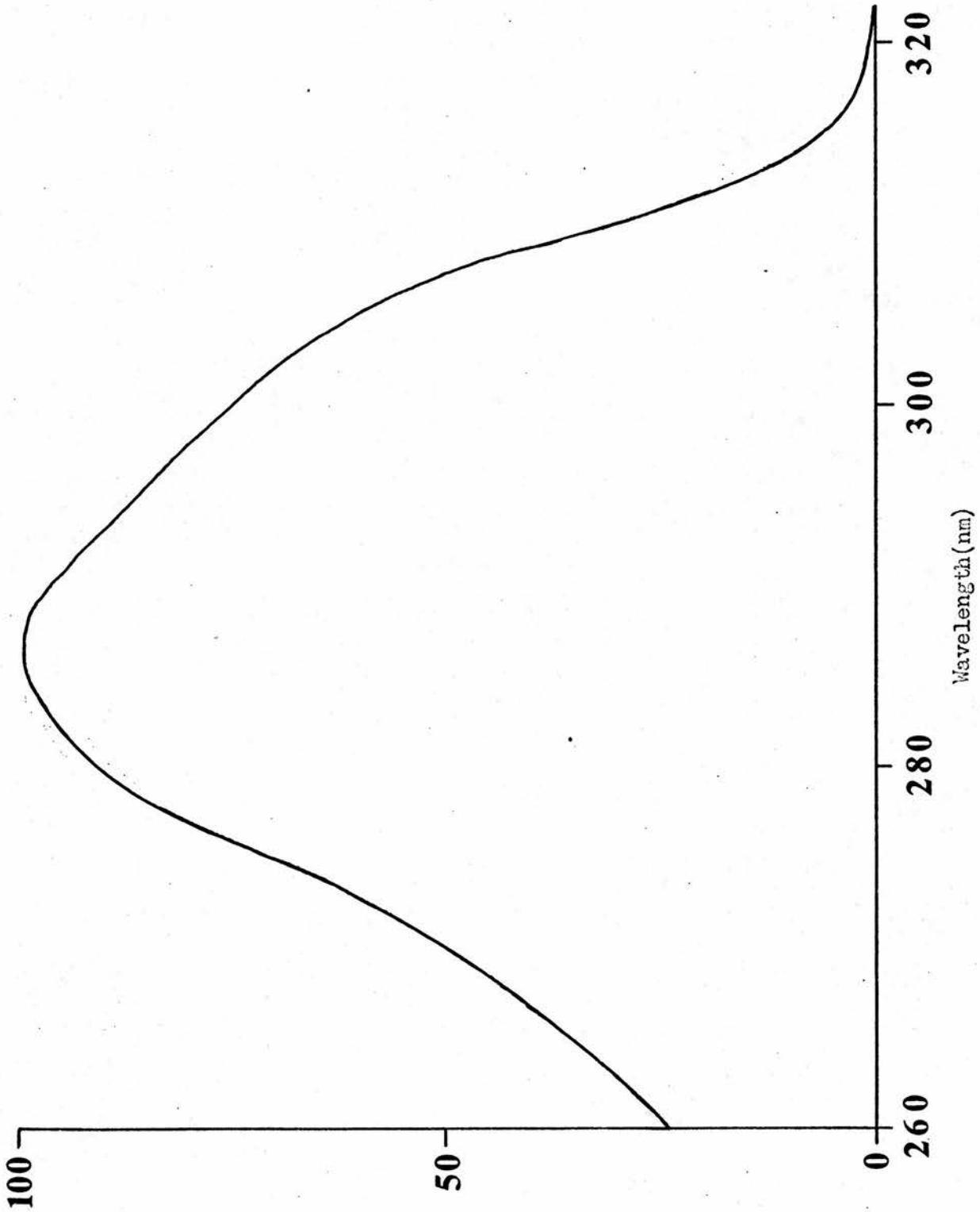

Figure 5.1 Corrected Excitation Spectrum of $Al(AA)_3$ in Ethanol Solution at 77K

coefficient of this state (ca. 5000 $cm^{-1}mol^{-1}dm^3$) is high relative to the values usually associated with uncoordinated ketones and it is reasonable to suggest that the Al^{3+} ion may affect the non - bonding molecular orbitals of the ligand oxygen atoms in such a way as to reduce the inherent symmetry forbidden character of the $\pi^* \leftarrow n$ transition and hence increase its absorption coefficient.

The corrected phosphorescence emission spectrum of $Al(AA)_3$ in ethanol solution at 77K is shown in Figure 5.2. It is a broad band with three ill - defined intensity maxima at ca. 395, 404 and 415 nm. If it is assumed that the 0-0 band is at 395 nm, the other band maxima may be vibrational components with spacings relative to the 0-0 band of ca. 600 and 1200 cm^{-1} [223]. Ligand vibrations in the region of 600 cm^{-1} have been assigned in the infrared spectra of several metal acetyl - acetonates[228], but the lack of resolution in the phosphorescence spectrum makes precise assignment of the apparent vibrational structure unreliable. It is clear, however, that the pronounced C=O frequency spacing expected from a T_{n,π^*} emitting level is absent. The energy difference between the S_{n,π^*} level and the emitting triplet level of the ligand is of the order of 10000 cm^{-1}. The phosphorescence decay is exponential with a lifetime of 0.336 ± 0.01 seconds. The absence of any pronounced vibrational structure, the relatively high singlet - triplet separation and the long phosphorescence lifetime indicate that the emitting level is a T_{π,π^*}, rather than a T_{n,π^*} state[9,222]. This is supported by the absence of any observable decomposition on prolonged exposure to ultraviolet radiation, since T_{n,π^*} states are known to be particularly reactive and may readily react with the solvent[229].

Since the spin - orbit coupling between singlets and triplets of different configurations is likely to be ca. 10^2 faster than that between states of the same configuration, the preferred intersystem

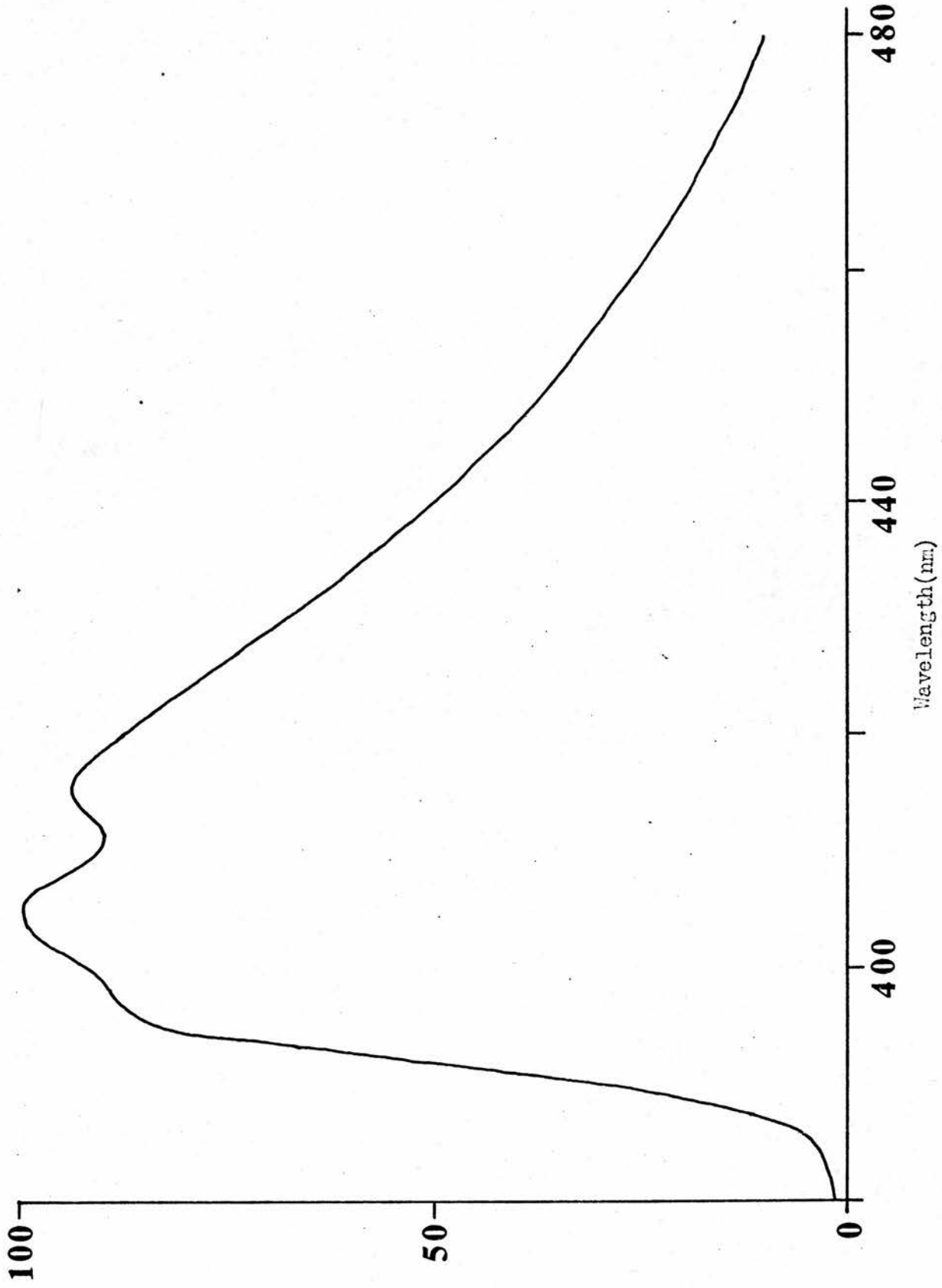

Figure 5.2 Corrected Emission Spectrum of $Al(AA)_3$ in Ethanol Solution at 77K

crossing route probably involves a direct $S_{n,\pi^*} \longrightarrow T_{\pi,\pi^*}$ step[229]. A schematic diagram of the lower energy electronic levels of the acetylacetonate ligand in $Al(AA)_3$ in ethanol solution at 77K is shown in Figure 5.3.

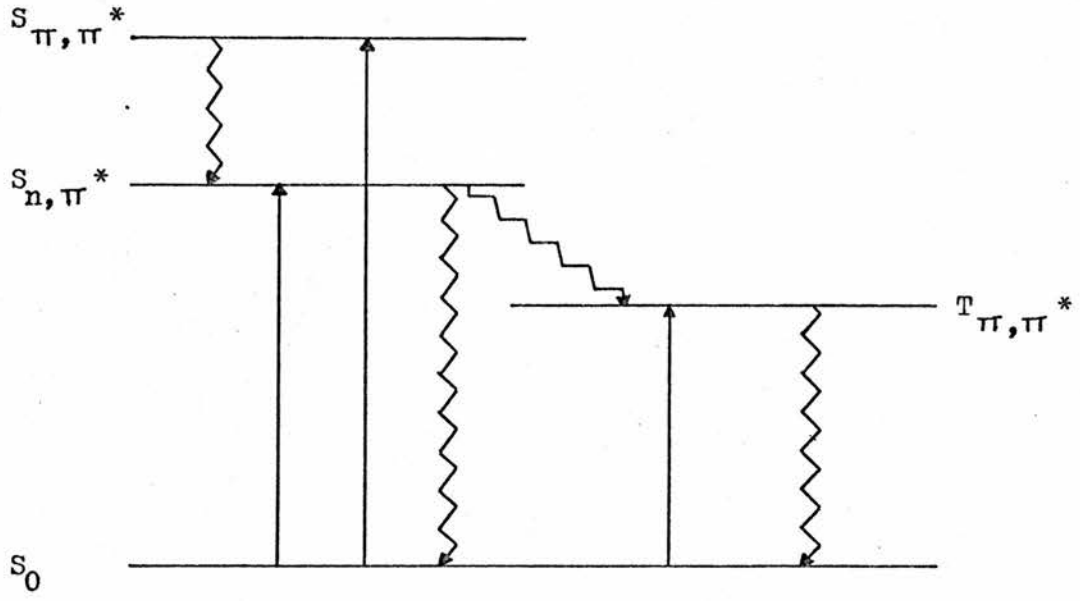

Figure 5.3 Schematic Representation of the Lower Energy Electronic Levels of the Acetylacetonate Ligand of $Al(AA)_3$

(c) METAL - LIGAND INTERACTIONS

Preliminary investigations of dilute ethanolic solutions ($\ll 10^{-2}$M) of diamagnetic metal acetylacetonates at 77K showed that phosphorescence occurred in all cases on excitation within the ligand absorption band. The emission spectral profiles were similar to that of $Al(AA)_3$ in terms of position and structure (Figure 5.2), and the absorption and excitation spectra were identical within experimental error in each case. However, the luminescence decay of many of the complexes showed

significant and, in some cases, very considerable deviations from exponential behaviour indicating that there was more than one phosphorescent species present. At concentrations $\geq 10^{-2}$M, the luminescence decay of the $M(AA)_3$ complexes, $Zn(AA)_2.H_2O$ and $Th(AA)_4$, were exponential within experimental error, whereas the Group Ia and IIa metal acetylacetonates showed markedly non - exponential decays.

A typical plot of photomultiplier output against time after the excitation flash was complete for a non - exponential curve is given in Figure 5.4. If it is assumed that the non - exponentiality is due to the presence of two luminescent species with different lifetimes, then the intensity, I(t), at any time, t, is given by

$$I(t) = A.\exp(-t/\tau_{short}) + B.\exp(-t/\tau_{long}) \qquad 5.1$$

From this expression, it can be seen that as $1/t \longrightarrow 0$,

$$I(t) \longrightarrow B.\exp(-t/\tau_{long}) \qquad 5.2$$

In order to resolve the experimental data in those cases where non - exponential behaviour was evident, a computer program was used. This is an iterative program which initially selects a portion of the output curve where t is high and calculates the apparent lifetime on the basis of the best least squares fit of

$$\ln I(t) = -B'.\ t/\tau'_{long} \qquad 5.3$$

The values of B' and τ'_{long} obtained in this way should be fairly good approximations to B and τ_{long} and are used as initial values in the subsequent fitting program. The value of τ'_{long} is then changed through a succession of values until the difference $I(t) - B.\exp(-t/\tau_{long})$ gives the best possible approximation to an exponential function, i.e. $A.\exp(-t/\tau_{short})$. It is obviously

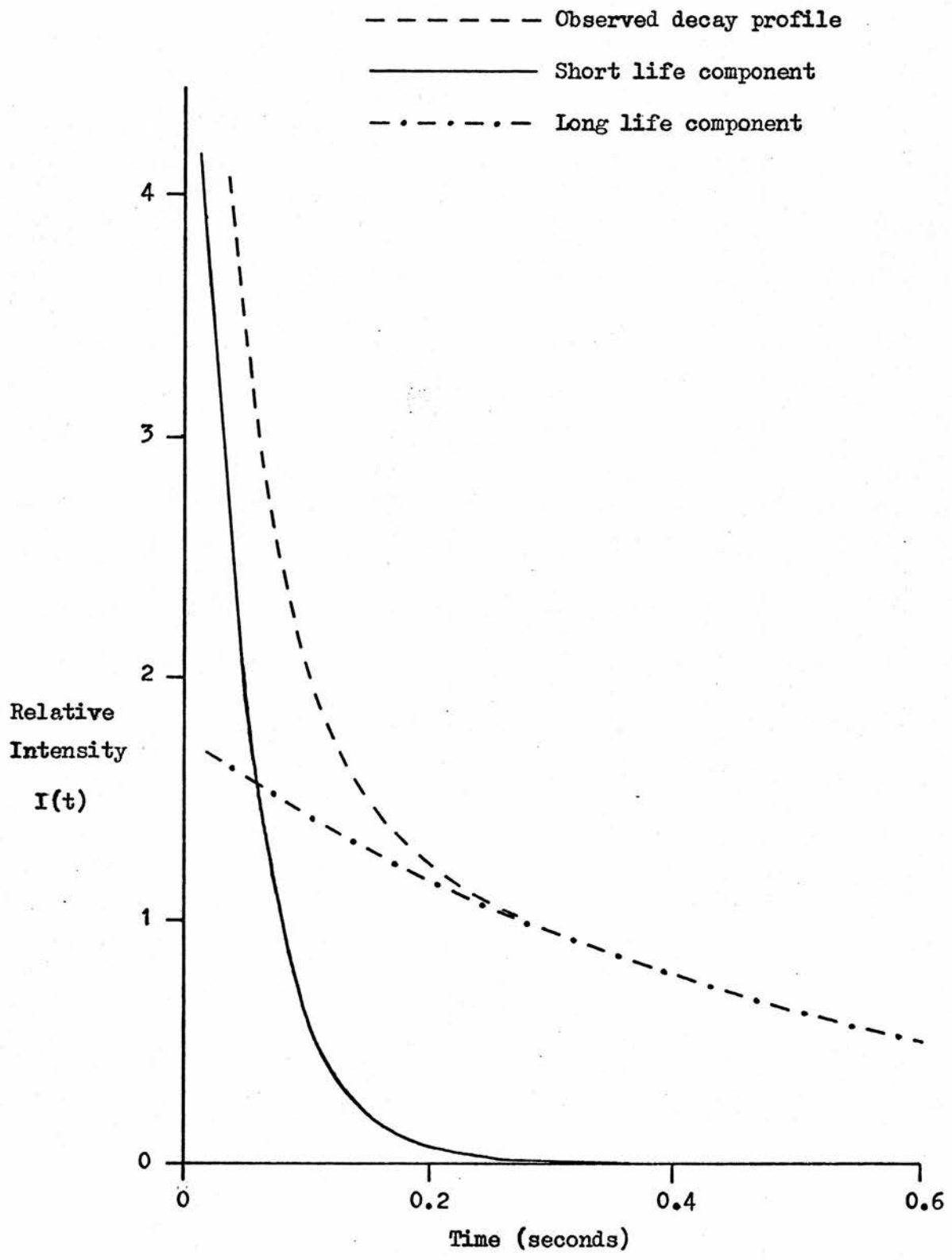

Figure 5.4 Non - Exponential Decay Profile of Cs(AA)

necessary to ignore any values of I(t) occurring in the duration of the excitation flash.

In all the cases examined, good fits of the experimental data I(t) to the function 5.1 were obtained for the Group Ia and IIa metal acetylacetonates at 77K and the results are given in Table 5.1. This treatment of the data presupposes the presence of only two emitting species, but the validity of this interpretation is supported by the presence of a near - constant value for τ_{long} of ca. 500 ms in all cases. The nature of the procedure does, however, result in the values τ_{short} being less reliable than those obtained from purely exponential photomultiplier curves as, for example, in the case of $Al(AA)_3$. The computed values of A,B, τ_{short} and τ_{long} also give some information on the relative quantum efficiencies of the two species, since

$$\frac{\Phi_{long}}{\Phi_{short}} = \frac{\int_0^\infty B.\exp(-t/\tau_{long})}{\int_0^\infty A.\exp(-t/\tau_{short})} \qquad 5.4$$

$$= \frac{B.\tau_{long}}{A.\tau_{short}} \qquad 5.5$$

Since the excitation pulse is not a theoretical δ function, the calculated values of A and B, and hence Φ_{long} and Φ_{short}, can only be regarded as a rough approximation, although the calculated values of τ will be unaffected. The luminescence decay curves of $5x10^{-2}$M ethanol glasses of the Group Ia and IIa metal acetylacetonates at 77K have been processed by the computer program described above and the results are presented in Table 5.1.

The results may therefore be interpreted in terms of an apparently constant long lived component of ca. 500 ms, due to some species

Table 5.1 Results Obtained by Computer Analysis of the Phosphorescence Decay Curves of M(AA) and $M(AA)_2$ Complexes

Metal Complex	Z	A	τ_{short} (s)	B	τ_{long} (s)	% Deviation	ϕ_{long}/ϕ_{short}
Li(AA)	3	3670	0.151	3962	0.500	0.2	3.57
Na(AA)	11	5702	0.076	3136	0.463	0.4	3.35
K(AA)	19	5105	0.058	1721	0.500	1.8	2.91
Rb(AA)	37	4838	0.063	1376	0.499	3.6	2.25
Cs(AA)	55	5723	0.045	1765	0.493	3.8	3.38
$Mg(AA)_2$	12	3088	0.183	4354	0.500	0.4	3.85
$Ca(AA)_2$	20	1583	0.130	5782	0.500	0.8	14.04
$Sr(AA)_2$	38	2816	0.069	3368	0.444	0.5	7.70
$Ba(AA)_2$	56	7059	0.063	1619	0.467	2.1	1.70

present in each of the solutions, and a short lived component which is dependent on the metal ion. Studies of the absorption spectra of metal acetylacetonates (Chapter 4) have shown that the M(AA) and $M(AA)_2$ complexes dissociate to a considerable extent in ethanol and that a 10^{-2} M solution of, for example, Na(AA) is ca. 30% dissociated at 303K[213]. These complexes will probably be dissociated to a considerable extent even at 77K and at relatively high concentrations, although the precise equilibrium concentration of each species is not known. As the temperature of the solution is lowered to 77K, ion association will be favoured, although the equilibrium rate for this process is known to be low (Chapter 4). The normal experimental procedure for good phosphor - escence glasses involves the slow immersion of the cell into liquid nitrogen and it is likely that an " equilibrium gradient " will result from this treatment. However, this procedure was adopted since the lifetimes of phosphorescent species are unaffected by concentration,

and only the A, B and quantum ratio of each complex (Table 5.1) will depend on the precise experimental technique used.

At equilibrium, the species likely to be in a solution of sodium acetylacetonate are Na(AA) , Na(OEt) ,HAA, Na^+, $(AA)^-$, $(OEt)^-$ and, of course, the solvent ethanol. Emission studies have shown that HAA and EtOH phosphoresce very weakly and that NaOEt phosphoresces in the blue region. However, the lifetimes of the analagous metal ethoxides will almost certainly show some dependence on the metal ion and consequently not give rise to the consistently long lifetime observed. It has been demonstrated in Chapter 4 that distinct similarities exist in the singlet energy levels, and hence electron distribution, of the $(AA)^-$ ion and of $M(AA)_n$ complexes. It is therefore probable that the triplet levels of the $(AA)^-$ ion and of the complexes are also similar and that, if a relation exists between the degree of dissociation and phosphor - escence decay for any complex, then the emitting species will be the metal complex (τ_{short}) and the acetylacetonate anion (τ_{long}). Experiments designed to alter the equilibrium between complex and anion by, for example, adding variable amounts of M(OH) or altering the concentration have proved inconclusive, mainly due to errors normally associated with low temperature phosphorescence measurements at high solution concentration.

The absorption and emission characteristics of all the metal acetylacetonates studied are summarised in Table 5.2. All the metal ions chosen have no excited state levels with energy less than the lowest triplet level of the acetylacetonate ligand and, with the exception of Gd^{3+}, all the metal ions are diamagnetic. It is obvious from Table 5.2 that, although there are minor differences in the S_{π,π^*} and T_{π,π^*} energy levels, the greatest variation occurs in the lifetime values. The very low lifetime for the gadolinium complex may

Table 5.2 Spectroscopic Data for Metal Acetylacetonates

Metal Complex	Z	$(S_{\pi,\pi^*})^a$ (cm^{-1})	$\log \varepsilon_{max}{}^a$ (S_{π,π^*})	$(T_{\pi,\pi^*})^{b,c}$ (cm^{-1})	$(S_{\pi,\pi^*})-(T_{\pi,\pi^*})$ (cm^{-1})	τ^c (s)
Li(AA)	3	34100	4.30	25400	8700	0.151 [d]
Na(AA)	11	34000	4.13	25400	8600	0.076 [d]
$Mg(AA)_2$	12	35100	4.51	25300	9800	0.183 [d]
$Al(AA)_3$	13	34800	4.59	25300	9500	0.336
K(AA)	19	34000	4.23	25400	8600	0.058 [d]
$Ca(AA)_2$	20	34400	4.46	25300	9100	0.130 [d]
$Sc(AA)_3$	21	33400	4.51	25300	8100	0.397
$Zn(AA)_2 \cdot H_2O$	30	35100	4.52	25200	9900	0.247
$Ga(AA)_3$	31	34800	4.56	25200	9600	0.375 [e]
Rb(AA)	37	34000	4.25	25300	8700	0.063 [d]
$Sr(AA)_2$	38	34300	4.38	25300	9000	0.069 [d]
$Y(AA)_3 \cdot 3H_2O$	39	34800	4.52	25300	9500	0.218
$In(AA)_3$	49	34800	4.55	25200	9600	0.150 [e]
Cs(AA)	55	34000	4.31	25300	8700	0.045 [d]
$Ba(AA)_2$	56	33900	4.42	25300	8600	0.063 [d]
$La(AA)_3 \cdot 3H_2O$	57	34400	4.56	25300	9100	0.070
$Gd(AA)_3 \cdot 3H_2O$	64	34600	4.54	25300	9300	0.002
$Lu(AA)_3 \cdot 2H_2O$	71	34800	4.59	25300	9500	0.077
$Th(AA)_4$	90	35100	4.47	25300	9800	0.006

(a) Maximum of observed absorption band in ca. 5×10^{-4} M ethanol solutions at 303K.

(b) Phosphorescence spectra were usually poorly resolved and the T_{π,π^*} transition is only estimated in some cases.

(c) 10^{-2} M glasses (ethanol) at 77K.

(d) Values of τ_{short} (Table 5.1).

(e) Values obtained from reference 223.

be attributed to the paramagnetism of this $4f^7$ ion, causing very effective spin - orbit coupling between the ligand triplet and ground state singlet. A simple monotonic relationship does not, however, exist between τ and the atomic number of the metal (Z), although for M^{n+} complexes of any given n, the general trend is for τ to decrease as Z increases (Figure 5.5).

This trend in measured lifetimes has been attributed to a " heavy atom effect " as, for example, in the case of $M(AA)_3$ complexes[222,223] and $M(DBM)_3$ complexes[230]. However, the lifetimes measured have almost invariably been of M^{3+} complexes and there have been discrepancies. For example, Yuster and Weissman[230] quote τ values for $Al(DBM)_3$,Z=13, and $Sc(DBM)_3$,Z=21, of 0.70 and 0.39 seconds respectively, whereas Clarke and Connors[223] report τ values for $Al(AA)_3$ and $Ga(AA)_3$,Z=31, of 0.335 and 0.397 seconds respectively. Clarke and Connors[223] further reported a lifetime for $Mg(AA)_2$,Z=12, of 0.325 seconds in EPA at 77K, although this value is probably high since the concentration used was ca. 10^{-4} M, at which concentration there is likely to be considerable dissociation in this solvent. The present work extends this range of τ values and questions the validity of ascribing the trend in measured lifetimes to a " heavy atom effect ".

The " heavy atom effect " is the result of an increase in the value of the spin - orbit Hamiltonian, caused by the presence of a heavy nucleus. The spin - orbit Hamiltonian in the x direction, H_{so} , may be expressed as

$$H_{so}(x) = \sum_{i}^{m} \sum_{j}^{n} c/r_{ij} \cdot dV_{(r_{ij})}/dr_{ij} \cdot (l_{xi}, s_{xi}) \qquad 5.6$$

where r_{ij} is the distance from the electron i to the nucleus j ; l_{xi} and s_{xi} are the orbital and spin operators in direction x of electron i ;

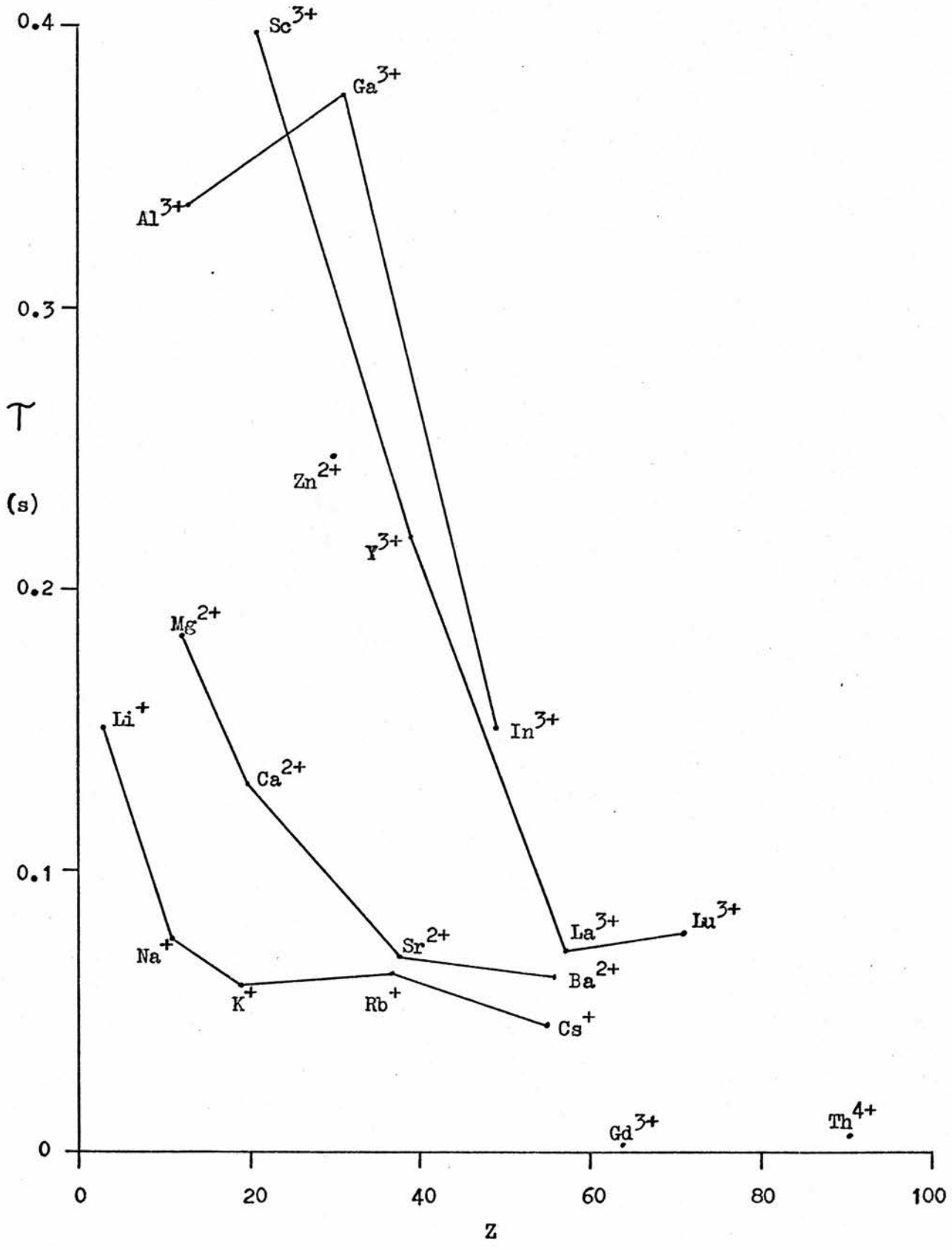

Figure 5.5 Relationship Between τ and Z for $M(AA)_n$ Complexes

m and n are the number of electrons and nuclei respectively and c is a constant. The magnitude of the spin - orbit interaction is therefore dependent on the average value of $(1/r_{ij})(dV/dr_{ij})$. Although the field gradient term near the nucleus will increase with Z, the singlet - triplet mixing also depends on the extent to which the relevant electrons penetrate the core of the heavy atom, i.e. the $1/r_{ij}$ term.

For example, the phosphorescence lifetimes of halo - substituted benzene and naphthalene have been studied in EPA at 77K[231-233] and, in these cases, the lifetimes of the substituted compounds fall in the order $\tau_{(H)} \gg \tau_{(Cl)} \gg \tau_{(Br)}$ and this has been attributed to the heavy atom effect. Ease of penetration of the ring electrons into the heavy atom core is consistent with the covalent nature of the C-Cl and C-Br bonds in these cases. However, in the case of the metal acetylacetonates, the degree of overlap of the delocalised ligand orbitals and the cation is likely to be rather limited, i.e. the M-O bond will have, at least, a substantial ionic character. Since there is not a monotonic relationship between τ and Z (as the dV/dr_{ij} term alone would predict for a heavy atom effect), then the variations from this should be capable of rationalisation in terms of varying degrees of electron penetration of the cations, if the heavy atom effect is responsible for the observed variations in τ. However, the very low value for the τ of Na(AA), compared with that for $Al(AA)_3$, implies a much greater degree of covalency in the Na-O bond according to this argument. In addition, although τ for $Al(AA)_3$ is low in comparison with $Sc(AA)_3$, the order is reversed for the corresponding dibenzoylmethide complexes[230,234]. It is therefore not possible to rationalise these variations in τ simply as a result of a heavy atom effect.

Since the metal acetylacetonates may have a substantial ionic character, the lifetimes may be considered in terms of a purely ionic

model, based on the charge to ionic radius ratio for each cation. The relevant data for each complex studied are presented in Table 5.3, and the relationship between τ and the charge to ionic radius ratio is shown in Figure 5.6. No special significance is implied in quoting the lifetimes as $\log_{10}\tau$, as this merely condenses the points in the y-axis in Figure 5.6.

Table 5.3 Data for Charge, Ionic Radius and τ for $M(AA)_n$ Complexes

Metal Ion	Ionic Charge	Ionic Radius[a] (Å)	Charge / Radius Ratio ($Å^{-1}$)	$\log_{10}\tau$[b]
Li^{+}	+1	0.68	1.47	2.18
Na^{+}	+1	0.97	1.03	1.88
Mg^{2+}	+2	0.66	3.03	2.26
Al^{3+}	+3	0.51	5.88	2.53
K^{+}	+1	1.33	0.75	1.76
Ca^{2+}	+2	0.99	2.02	2.11
Sc^{3+}	+3	0.73	4.11	2.60
Zn^{2+}	+2	0.74	2.70	2.39
Ga^{3+}	+3	0.62	4.84	2.57
Rb^{+}	+1	1.47	0.68	1.80
Sr^{2+}	+2	1.12	1.79	1.84
Y^{3+}	+3	0.89	3.37	2.34
In^{3+}	+3	0.81	3.70	2.18
Cs^{+}	+1	1.67	0.60	1.65
Ba^{2+}	+2	1.34	1.49	1.79
La^{3+}	+3	1.02	2.94	1.85
Gd^{3+}	+3	0.94	3.19	0.30
Lu^{3+}	+3	0.85	3.53	1.89
Th^{4+}	+4	1.02	3.92	0.78

(a) Values obtained from reference 235.

(b) $\log_{10}\tau$ values based on τ in milliseconds.

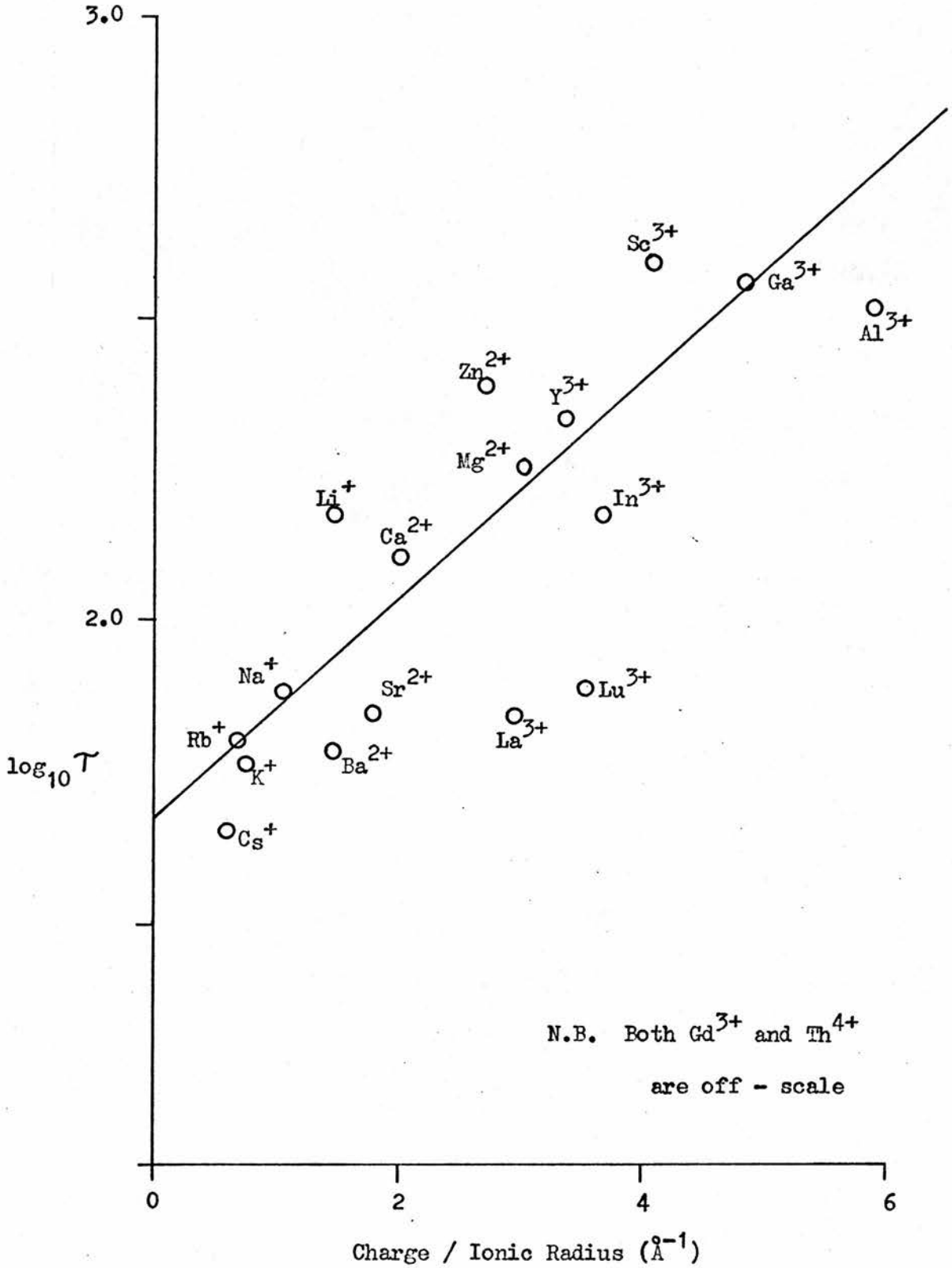

Figure 5.6 Relationship Between $\log_{10}\tau$ and Charge/Ionic Radius Ratio for $M(AA)_n$ Complexes

By inspection, a distinct relationship is shown to exist between τ and the charge to ionic radius ratio for each metal ion complex (Figure 5.6) with the notable exceptions of $Th(AA)_4$ and the lanthanide complexes. The low lifetime of the Gd^{3+} complex has already been discussed in terms of the paramagnetism of this ion, but the anomalous lifetimes of the other complexes can be explained in terms of a genuine " heavy atom effect ", found only with these very heavy ions.

(d) LIGAND PHOSPHORESCENCE OF 3-SUBSTITUTED $Al(AA)_3$ COMPLEXES

The absorption and emission characteristics of the 3 - substituted complexes $Al(R\text{-}AA)_3$, where R = Me, Et, Cl and Br, have also been investigated in ethanol solution and the results are summarised in Table 5.4. The corrected phosphorescence spectra of $Al(R\text{-}AA)_3$ complexes are red - shifted by more than 2000 cm^{-1} relative to the parent compound in all cases (Table 5.4). The profiles of the methyl- and ethyl-substituted complexes are similar to $Al(AA)_3$ in terms of structure, whereas in the case of the halo- substituted complexes, no structure is observed (Figure 5.7). The absorption spectra are similarly red - shifted[236] and the $S_{\pi,\pi^*} - T_{\pi,\pi^*}$ energy differences remain remarkably constant at 10000 $\pm$ 400 cm^{-1}.

Table 5.4 Spectroscopic Data for the $Al(R\text{-}AA)_3$ Complexes

R =	$(S_{\pi,\pi^*})^a$ (cm^{-1})	$\log \varepsilon_{max}{}^a$ (S_{π,π^*})	$(S_{n,\pi^*})^b$ (cm^{-1})	$(T_{\pi,\pi^*})^{c,d}$ (cm^{-1})	$(S_{\pi,\pi^*})-(T_{\pi,\pi^*})$ (cm^{-1})	τ^d (s)
H	35000	4.58	33000	25300	9700	0.336
Me	33300	4.50	31300	22900	10400	0.546
Et	33200	4.47	31200	23200	10000	0.548
Cl	32600	4.47	30800	22400	10200	0.169
Br	32400	4.40	30500	22400	10000	0.004

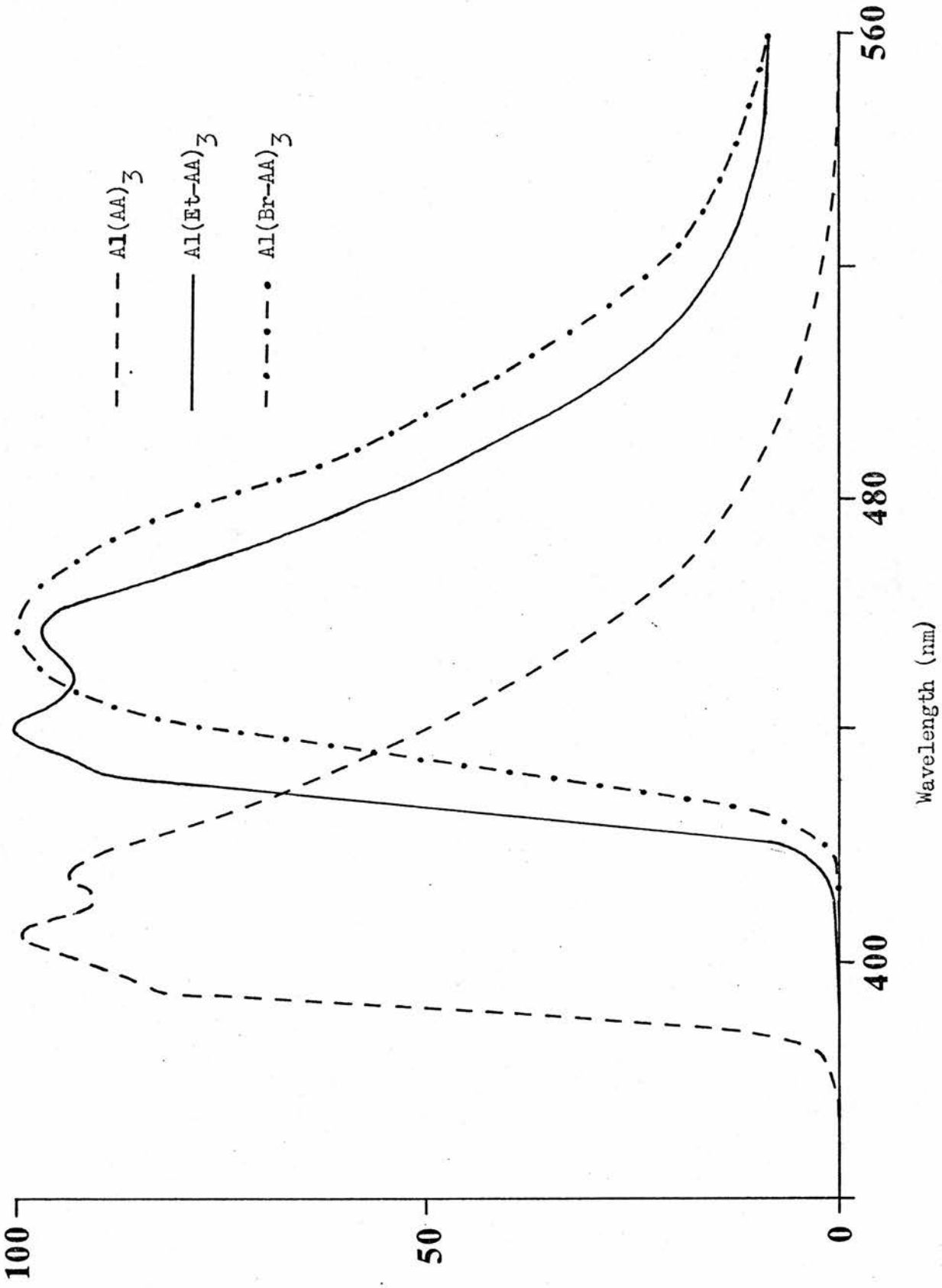

Figure 5.7 Corrected Emission Spectra of $Al(R\text{-}AA)_3$ Complexes in Ethanol at 77K

Key to Table 5.4 (p. 104)

(a) Maximum of observed absorption band in ca. 5 x 10^{-4} M ethanol solutions at 303K.

(b) Resolved from the absorption spectrum.

(c) Estimated 0-0 transition of the phosphorescence spectrum.

(d) 10^{-2} M ethanol glass at 77K.

Fackler and Cotton[237] have reported the absorption spectra of the corresponding $Cu(R\text{-}AA)_2$ complexes in chloroform and / or cyclohexane solution and have found the ligand absorption maxima at 33800 cm^{-1} (H), 32400 cm^{-1} (Me and Et), 31900 cm^{-1} (Cl) and 32400 cm^{-1} (Br). With the exception of the bromo- complex, there is therefore a similar ordering to that of the $Al(R\text{-}AA)_3$ complexes, but at lower energies. Fleming and Thornton[236] have investigated the electronic spectra of a series of 3 - substituted acetylacetonate complexes of trivalent metals. Their findings confirm that the gross effect of replacing the 3- proton by any substituent shifts the ligand and charge - transfer transitions to lower energies. They also report that replacing an electron - releasing substituent (e.g. Me) with an electron - withdrawing substituent (e.g. NO_2) induces a blue shift.

The corrected excitation spectra are identical to the absorption spectra in all the $Al(R\text{-}AA)_3$ complexes examined and there is therefore no evidence to suggest that the energy level pattern established for the parent compound (Figure 5.3) is altered by these substituents other than in terms of absolute energies.

The most striking effect of 3 - substitution is shown in the τ values(Table 5.4) where the chloro- and, in particular, the bromo- complexes have much lower lifetimes than the parent compound. The order of magnitude of this " heavy atom effect " may be compared with those previously reported for substituted benzenes and 1- and 2- substituted

naphthalenes (Table 5.5). Although the ordering $\tau_{(H)} > \tau_{(Cl)} > \tau_{(Br)}$ occurs in all cases, there are remarkable differences in the magnitude of this effect. For example, comparing $Al(R\text{-}AA)_3$ complexes with the corresponding benzene derivatives shows $\tau_{(Cl)} / \tau_{(Br)}$ to be ca. 40 in each case, whereas $\tau_{(H)} / \tau_{(Br)}$ is 1.99 for $Al(R\text{-}AA)_3$ and 1750 for benzene.

Table 5.5 Effects of Substituents on the Phosphorescence Lifetimes of Benzenoid Compounds

Parent Compound	$\tau_{(s)}$			
	R = Me	H	Cl	Br
$Al(R\text{-}AA)_3$	0.546	0.336	0.169	0.004
Benzene	8.8 [a]	7.0 [b]	0.004 [a]	0.0001 [a]
Naphthalene [c]	2.5 [a]	2.6 [a]	0.30 [a]	0.018 [a]
Naphthalene [d]	——	2.6 [a]	0.47 [a]	0.02 [a]

(a) Obtained in EPA at 77K - reference 231.

(b) Obtained in EPA at 77K - references 232, 233.

(c) 1 - substituted naphthalene.

(d) 2 - substituted naphthalene.

(e) DISCUSSION

Diamagnetic metal acetylacetonates phosphoresce in ethanol glasses at 77K when irradiated in the ligand absorption band[222,223]. The emission spectrum is identical in each case in terms of position and structure and the emitting level is assigned as T_{π,π^*}. There is evidence, however, that the metal centre is important in both inter -

system crossing and radiative and non - radiative coupling to the ground state. The phosphorescence lifetimes of the complexes are dependent on the nature of the metal ion but a simple monotonic relationship, indicative of a heavy atom effect, does not exist between τ and Z (Figure 5.5). However, for M^{n+} complexes of any given n, the observed trend is for τ to decrease as Z increases. Based on a purely ionic model for the complexes, a distinct relationship is shown to exist between τ and the charge to ionic radius ratio for each ion (Figure 5.6) with the notable exceptions of $Th(AA)_4$ and the lanthanide acetylacetonates. The low lifetime of the Gd^{3+} complex is attributed to the paramagnetism of this ion but the low τ of the other complexes is ascribed to a genuine heavy atom effect found only with very heavy ions.

Non - exponential luminescence decay is observed for those complexes which are known to dissociate even in concentrated ethanol solutions[213]. This has been attributed to the presence in solution of two luminescent species, namely the undissociated metal complex and the acetylacetonate anion. There is no apparent change in the phosphorescence spectra of these complexes due to the anion and it is therefore assumed that the anion has a T_{π,π^*} level similar to the metal complexes and a long lifetime (ca. 500 ms). No comparable ligand phosphorescence is observed in the parent molecule acetylacetone.

A marked alteration in the vibronic envelope of the ligand ring of $Al(R\text{-}AA)_3$ complexes is obtained by placing substituents in the 3 - position of the ligand. This results in the general lowering of the S_{π,π^*} and T_{π,π^*} energy levels, similar to the observations of Clarke and Connors for the $Al(TFAA)_3$ and $Al(HFAA)_3$ complexes[223]. 3 - substitution also results in the ordering of the τ values of the complexes as $\tau_{(H)} > \tau_{(Cl)} > \tau_{(Br)}$. It is interesting to compare the

relative effect of replacing a heavy atom into the ring of $M(AA)_n$ and $Al(R\text{-}AA)_3$ complexes. The $M(AA)_n$ complexes exhibit a definite non - monotonic relationship between τ and Z, indicative of a distinct dependence on ionic character. The $Al(R\text{-}AA)_3$ complexes show a monotonic relationship between τ and Z which may be attributed to the covalent C-Cl and C-Br bonds and hence to a genuine heavy atom effect. It is possible, however, that even in these cases, the heavy atom effect is only significant in the bromo- compound and that the smaller difference in τ between R = H and R = Cl is due to other causes.

CHAPTER 6

SPECTRAL INVESTIGATIONS OF DIAMAGNETIC METAL ACETYLACETONATES IN SOLUTION

III NUCLEAR MAGNETIC RESONANCE

(a) INTRODUCTION

The nuclear magnetic resonance (nmr) spectra of diamagnetic metal acetylacetonates have been described as " trivial ", with two distinct peaks attributed to the ligand methyl and 3 - carbon proton resonances in the ratio of 6:1 [209,238]. The chemical shifts of these resonances were reported to be largely insensitive both to the metal and to the solvent. One exception to this generalisation has been found, $Mg(AA)_2$ in $CDCl_3$, which has two methyl resonances at ca. 1.80 and 2.01 ppm relative to the internal standard tetramethyl-silane (TMS). Brittain[239] has attributed these resonances to non - equivalent methyl groups as a result of an equilibrium between planar and tetrahedral configurations of the complex. In support of this interpretation, Brittain reported comparable resonances of 2.01 and 2.00 ppm for the tetrahedral complexes $Be(AA)_2$ and $Zn(AA)_2.H_2O$. Resonances of 1.80 and 1.77 ppm were observed for the planar complexes $Ca(AA)_2$ and $Ba(AA)_2$. Carty et al.[240] have reported only one peak attributed to the methyl resonance of $Mg(AA)_2$ in DMSO.

The effect of solvent on the nmr spectra of various aluminium β - diketoenolates has been discussed by Linck and Sievers[241] on the basis of six interdependent factors. They reported ligand 3 - carbon

resonances for $Al(AA)_3$ of, for example, 5.50 ppm in acetone and 4.93 in benzene, corrected for " bulk susceptibility differences ". However, the solvent dependence on the nmr spectra of complexes with metals other than aluminium has largely been ignored in the literature. This is presumably due to the lack of solubility of complexes in a suitable range of solvents at the concentrations required to achieve a good signal to noise ratio. Similarly, systematic nmr studies of the metal dependence of a series of $M(AA)_n$ complexes in any specific solvent have been ignored.

The majority of recent nmr studies of metal acetylacetonates have been concerned with the intramolecular ligand exchange of complexes with unsymmetrical ligands[242-245], or with the intermolecular ligand exchange of complexes of general formula $M(A)_2(B)$ [246,247]. The kinetics of these rearrangements have been classified as fast or slow depending on the rate of interconversion at equilibrium[248]. The principal rearrangement mechanisms for these complexes have been defined as metal - ligand bond rupture[243] or twist processes[249], although the assignment of any mechanism to any particular complex is not unambiguous. However, the complete dissociation of metal complexes in solvents with low dielectric constants has been discounted as a possible mechanism[242].

(b) NMR SPECTRA OF $M(AA)_n$ COMPLEXES IN DMSO - D6

The nmr spectra of diamagnetic metal acetylacetonates have been recorded in a number of suitable solvents. In most instances, the low solubility of a complex in any particular solvent resulted in a poor signal to noise ratio. The most complete series of spectra of $M(AA)_n$ complexes was obtained using DMSO - D6 and the results are presented in Table 6.1 in order of increasing atomic number. For each complex, the ratio of the methyl and ring proton resonances was 6:1, within

Table 6.1 NMR Data for $M(AA)_n$ Complexes in DMSO - D6 at 310K

Metal Ion	Z	Ionic Radius[a] (Å)	Charge / Ionic Radius ($Å^{-1}$)	Methyl Proton[b] Resonances (ppm)	Ring Proton[b] Resonances (ppm)
Li^+	3	0.68	1.47	1.67	5.00
Na^+	11	0.97	1.03	1.66	4.86
Mg^{2+}	12	0.66	3.03	1.72	5.10
Al^{3+}	13	0.51	5.88	1.90	5.52
K^+	19	1.33	0.75	1.63	ca.4.70[c]
Ca^{2+}	20	0.99	2.02	1.70	5.10
Sc^{3+}	21	0.73	4.09	1.91	5.61
Co^{3+}	27	0.63	4.76	2.04	5.53
Zn^{2+}	30	0.74	2.70	1.83	5.26
Ga^{3+}	31	0.62	4.84	1.89	5.45
Rb^+	37	1.47	0.68	ca.1.73[c]	4.67
Sr^{2+}	38	1.12	1.79	ca.1.74[c]	----[d]
Y^{3+}	39	0.89	3.36	1.78	5.33
In^{3+}	49	0.81	3.70	1.93	5.46
Cs^+	55	1.67	0.60	ca.1.75[c]	4.65
Ba^{2+}	56	1.34	1.49	----[d]	----[d]
La^{3+}	57	1.02	2.95	1.73	5.13
Lu^{3+}	71	0.85	3.53	1.83	5.30
Pt^{2+}	78	0.80	2.50	1.85	5.62
Th^{4+}	90	1.02	3.92	1.74	5.33

(a) Values obtained from reference 235.

(b) ppm downfield from TMS.

(c) Broad resonances which were difficult to resolve accurately.

(d) Complexes were too insoluble in DMSO - D6 to give a good signal to noise ratio.

experimental error.

The relationship between the phosphorescence lifetimes of $M(AA)_n$ complexes and the charge / ionic radius ratio of the metal has been pointed out in Chapter 5. The results of the ^1H nmr spectral studies

in DMSO - D6 show that there is again an apparent relationship between the chemical shifts and the charge / ionic radius ratio. Figure 6.1 demonstrates the monotonic relationship found between the methyl and ring proton resonances and the charge / ionic radius ratio for each of the complexes.

The results indicate that the chemical shifts of the ring proton resonances, relative to TMS, are greater than the shifts attributed to the methyl proton resonances. The largest chemical shifts are observed with complexes such as $Al(AA)_3$, where the charge / radius ratio of the metal ion is large, whereas the smallest shifts are observed with complexes such as Cs(AA), where the charge / radius ratio of the metal ion is small. Considerable broadening of the methyl and ring proton resonances was observed with the complexes of the Group Ia metals in DMSO - D6, indicating that there is an equilibrium between two species, slower than the nmr time scale. It is probable that the equilibria result from dissociation of these ionic complexes in the polar solvent,

$$M(AA) \rightleftharpoons M^+ + (AA)^- \qquad 6.1$$

even at the relatively high concentrations necessary to achieve a good signal to noise ratio (ca. 10^{-1} M).

The trend in relative ionic character of metal acetylacetonates was corroborated by nmr spectral studies which were attempted using solvents other than DMSO - D6. The ionic M(AA) complexes were sparingly soluble in typically non - polar solvents such as CCl_4 and neither the methyl nor the ring proton resonances could be resolved from the background noise. The less ionic complexes, e.g. $Al(AA)_3$, were soluble in polar and non - polar solvents and the nmr spectra were well resolved in each case. The relative solvent effects on the spectra of $M(AA)_3$ complexes are shown in Table 6.2 , in order of incresing polarity of the solvent.

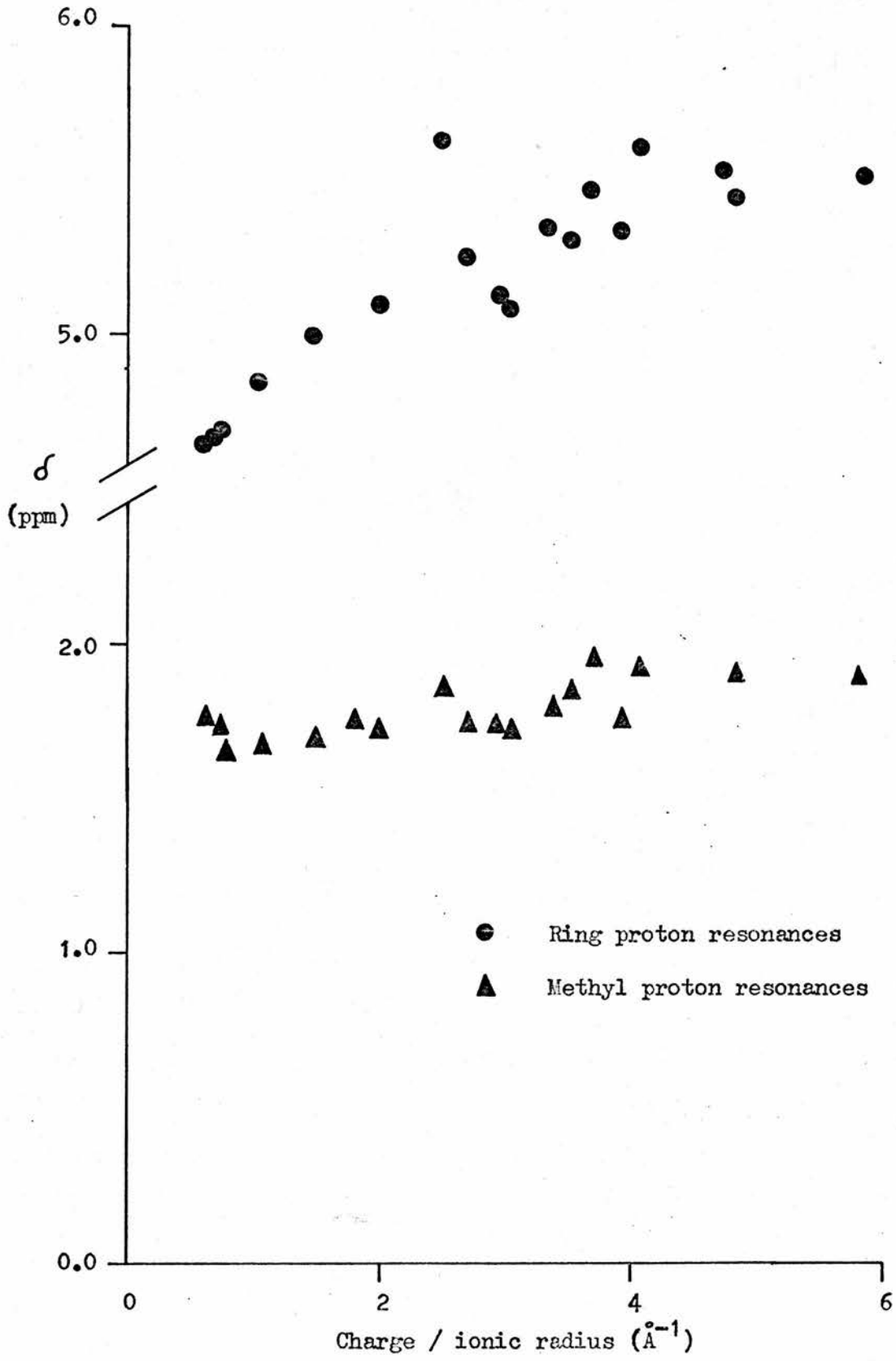

Figure 6.1 Plot of δ Values for CH_3- and Ring Protons Against Charge / Ionic Radius Ratio

Table 6.2 Solvent Effects on the NMR Spectra of $M(AA)_3$ Complexes at 310K

Solvent	$Al(AA)_3$		$Sc(AA)_3$	
	Methyl Proton Resonances (ppm)	Ring Proton Resonances (ppm)	Methyl Proton Resonances (ppm)	Ring Proton Resonances (ppm)
C_6D_6	1.80	5.25	1.77	5.30
CCl_4	1.85	5.33	1.86	5.47
$(CD_3)_2CO$	1.88	5.48	1.92	5.60
DMSO - D6	1.88	5.52	1.91	5.61
CD_3CN	1.95	5.53	1.90	5.56
Pyridine	1.92	5.52	1.95	5.63

(c) THE IONIC CHARACTER OF METAL ACETYLACETONATES IN SOLUTION - STATISTICAL ANALYSIS

The spectral investigations which have been reported in this thesis all indicate that metal acetylacetonates have considerable ionic character. Although it is difficult to compare directly the results obtained for the phosphorescence lifetimes in ethanol with, for example, methyl proton resonances in DMSO -D6, the trends for the series of $M(AA)_n$ complexes may be examined by applying statistical analysis. Spearman's Test[250] has been applied to each of the results obtained on the basis of the complexes being purely ionic, i.e. the charge / ionic radius ratio for the metal ion.

Each of the two sets of data to be compared was given its own set of rank values from smallest to largest. Spearman's Correlation Test initially assumes that there is no significant correlation between the two sets of measurements and then determines the probability of obtaining, purely by chance, a difference between the rank values as

small (or as large) as that which is observed. If the two sets of measurements are perfectly and directly correlated, there will be no difference between the ranking order of the two sets and there will be 0 probability of the ordering occurring by chance.

The data required for this test are, n = the number of pairs of measurements and / or ranked observations, plus all the individual measurements or rank values of the two characteristics to be compared. The mathematical procedure involved the following steps :-

(i) assessing the difference (d) between the rank values for each pair of observations,

(ii) squaring the difference (d^2) for each pair of observations,

(iii) summing the squares of the differences (D^2),

(iv) applying a correction factor ($T = \frac{1}{2} t_2$) for any tied observations, for which t_2 is the number of ties involving two observations,

and (v) adding $D^2 + T$.

The relationship $D^2 + T$ may then be referred to Spearman's Correlation Test tables and this gives the probability of any apparent correlation occurring by chance.

Spearman's Test has been applied to the results obtained from the nmr spectra in DMSO - D6 (Tables 6.3 and 6.4), Σ_{max} results in ethanol (Table 6.5) and phosphorescence lifetimes in ethanol (Table 6.6). In each case, the results were compared with the charge to ionic radius ratio for each metal ion. The $D^2 + T$ values obtained from Tables 6.3 , 6.4 , 6.5 and 6.6 were referred to Spearman's Correlation Test tables for the appropriate value of n. The probability of a direct correlation between charge to ionic radius ratio, proton resonances and Σ_{max} occurring purely by chance was thus found to be $\ll 1\%$. The probability of a direct correlation between the charge to ionic radius ratio and

Table 6.3 Spearman's Correlation Test

(i) Relationship Between Charge / Radius Ratio and Methyl Proton Resonances for $M(AA)_n$ Complexes

Metal Ion	Data Values		Rank Values		Difference (d)	d^2
	C/IR ($Å^{-1}$)	Me (H) (ppm)	C/IR	Me (H)		
Li^+	1.47	1.67	5	3	2	4
Na^+	1.03	1.66	4	2	2	4
Mg^{2+}	3.03	1.72	10	5	5	25
Al^{3+}	5.88	1.90	18	15	3	9
K^+	0.75	1.63	3	1	2	4
Ca^{2+}	2.02	1.70	6	4	2	4
Sc^{3+}	4.09	1.91	15	16	1	1
Co^{3+}	4.76	2.04	16	18	2	4
Zn^{2+}	2.70	1.83	8	11.5	3.5	12.25
Ga^{3+}	4.84	1.89	17	14	3	9
Rb^+	0.68	1.73	2	6.5	4.5	20.25
Y^{3+}	3.36	1.78	11	10	1	1
In^{3+}	3.70	1.93	13	17	4	16
Cs^+	0.60	1.75	1	9	8	64
La^{3+}	2.95	1.73	9	6.5	2.5	6.25
Lu^{3+}	3.53	1.83	12	11.5	0.5	0.25
Pt^{2+}	2.50	1.85	7	13	6	36
Th^{4+}	3.92	1.74	14	8	6	36

$n = 18$	$t_2 = 2$	$T = 1$	$D^2 = 256$

$D^2 + T = 257$

For n = 18, a value for $D^2 + T = 257$ gives <1% probability of the ordering occurring by chance.

Table 6.4 Spearman's Correlation Test

(ii) Relationship Between Charge / Radius Ratio and Ring Proton Resonances for $M(AA)_n$ Complexes

Metal Ion	Data Values		Rank Values		Difference (d)	d^2
	C/IR ($Å^{-1}$)	Me (H) (ppm)	C/IR	Me (H)		
Li^+	1.47	5.00	5	5	0	0
Na^+	1.03	4.86	4	4	0	0
Mg^{2+}	3.03	5.10	10	6.5	3.5	12.25
Al^{3+}	5.88	5.52	18	15	3	9
K^+	0.75	4.70	3	3	0	0
Ca^{2+}	2.02	5.10	6	6.5	0.5	0.25
Sc^{3+}	4.09	5.61	15	17	2	4
Co^{3+}	4.76	5.53	16	16	0	0
Zn^{2+}	2.70	5.26	8	9	1	1
Ga^{3+}	4.84	5.45	17	13	4	16
Rb^+	0.68	4.67	2	2	0	0
Y^{3+}	3.36	5.33	11	11.5	0.5	0.25
In^{3+}	3.70	5.46	13	14	1	1
Cs^+	0.60	4.65	1	1	0	0
La^{3+}	2.95	5.13	9	8	1	1
Lu^{3+}	3.53	5.30	12	10	2	4
Pt^{2+}	2.50	5.62	7	18	11	121
Th^{4+}	3.92	5.33	14	11.5	2.5	6.25

$n = 18$	$t_2 = 2$	$T = 1$	$D^2 = 176$

$D^2 + T = 177$

For n = 18, a value for $D^2 + T = 177$ gives <1% probability of the ordering occurring by chance.

Table 6.5 Spearman's Correlation Test

(iii) Relationship Between Charge / Radius Ratio and ε_{max} Values for $M(AA)_n$ Complexes

Metal Ion	Data Values		Rank Values		Difference (d)	d^2
	C/IR ($Å^{-1}$)	ε_{max} $cm^{-1}mol^{-1}dm^3$	C/IR	ε_{max}		
Li^+	1.47	20100	5	4	1	1
Na^+	1.03	13500	4	1	3	9
Mg^{2+}	3.03	32800	11	11.5	0.5	0.25
Al^{3+}	5.88	39100	19	19	0	0
K^+	0.75	16900	3	2	1	1
Ca^{2+}	2.02	29000	8	8	0	0
Sc^{3+}	4.09	32000	17	10	7	49
Zn^{2+}	2.70	33000	9	13	4	16
Ga^{3+}	4.84	36100	18	16.5	1.5	2.25
Rb^+	0.68	17700	2	3	1	1
Sr^{2+}	1.79	24100	7	6	1	1
Y^{3+}	3.36	32800	13	11.5	1.5	2.25
In^{3+}	3.70	35300	15	15	0	0
Cs^+	0.60	20300	1	5	4	16
Ba^{2+}	1.49	26250	6	7	1	1
La^{3+}	2.95	36100	10	16.5	6.5	42.25
Gd^{3+}	3.19	34900	12	14	2	4
Lu^{3+}	3.53	38600	14	18	4	16
Th^{4+}	3.92	29400	16	9	7	49

$n = 19$	$t_2 = 2$	$T = 1$	$D^2 = 211$

$D^2 + T = 212$

For n = 19, a value for $D^2 + T = 212$ gives <1% probability of the ordering occurring by chance.

Table 6.6 Spearman's Correlation Test

(iv) Relationship Between Charge / Radius Ratio and log τ Values for $M(AA)_n$ Complexes

Metal Ion	Data Values		Rank Values		Difference (d)	d^2
	C/IR ($Å^{-1}$)	log τ	C/IR	log τ		
Li^+	1.47	2.18	5	12.5	7.5	56.25
Na^+	1.03	1.88	4	9	5	25
Mg^{2+}	3.03	2.26	11	14	3	9
Al^{3+}	5.88	2.53	19	17	2	4
K^+	0.75	1.76	3	4	1	1
Ca^{2+}	2.02	2.11	8	11	3	9
Sc^{3+}	4.09	2.60	17	19	2	4
Zn^{2+}	2.70	2.39	9	16	7	49
Ga^{3+}	4.84	2.57	18	18	0	0
Rb^+	0.68	1.80	2	6	4	16
Sr^{2+}	1.79	1.84	7	7	0	0
Y^{3+}	3.36	2.34	13	15	2	4
In^{3+}	3.70	2.18	15	12.5	2.5	6.25
Cs^+	0.60	1.65	1	3	2	4
Ba^{2+}	1.49	1.79	6	5	1	1
La^{3+}	2.95	1.85	10	8	2	4
Gd^{3+}	3.19	0.30	12	1	11	121
Lu^{3+}	3.53	1.89	14	10	4	16
Th^{4+}	3.92	0.78	16	2	14	196

n = 19	t_2 = 1	T = 0.5	D^2 = 525.5

$D^2 + T = 526$

For n = 19, a value for $D^2 + T = 526$ gives 1 to 5% probability of the ordering occurring by chance.

τ occurring by chance was much greater (1 to 5%), mainly due to the anomalously high d^2 terms obtained for Th^{4+} and Gd^{3+}. This discrepancy is a result of the anomalously low τ values found with the very heavy metal ion Th^{4+} and paramagnetic Gd^{3+} complexes (Chapter 5).

Table 6.7 shows the rank values obtained with the 16 complexes for which complete data was available. Table 6.8 shows the calculated $D^2 + T$ terms for each combination of two sets of measurements and the probability of the relative ordering occurring purely by chance. It is evident that there is significant ordering within the complexes based on this purely ionic model and that the greatest deviation from this ordering is to be found with the results of the phosphorescence lifetime determinations.

Table 6.7 Rank Values for those Complexes for which Complete Data is Available

Metal Ion	Rank Values				
	Charge / Ionic Radius	Me (H) (nmr)	Ring (H) (nmr)	ε_{max}	log τ
Li^+	5	3	5	4	9.5
Na^+	4	2	4	1	6
Mg^{2+}	9	5	6.5	9.5	11
Al^{3+}	16	14	15	16	14
K^+	3	1	3	2	3
Ca^{2+}	6	4	6.5	6	8
Sc^{3+}	14	15	16	8	16
Zn^{2+}	7	11.5	9	11	13
Ga^{3+}	15	13	13	13.5	15
Rb^+	2	6.5	2	3	4
Y^{3+}	10	10	11.5	9.5	12
In^{3+}	12	16	14	12	9.5
Cs^+	1	9	1	5	2
La^{3+}	8	6.5	8	13.5	5
Lu^{3+}	11	11.5	10	15	7
Th^{4+}	13	8	11.5	7	1

Table 6.8 Calculated $D^2 + T$ Terms and Hence % Probability of a Relative Ordering Occurring by Chance for any Combination of Two Sets of Measurements

	Charge / Ionic Radius	Me (H)	Ring (H)	ε_{max}	log τ	
Charge / Ionic Radius		190	30	166	261	
Me (H)	<1		138	189.5	296	
Ring (H)	≪1	≪1		192	223	$D^2 + T$
ε_{max}	<1	<1	<1		333	
log τ	1-5	1-5	1	5		
	% Probability					

Friedman's Test[250] has been applied to four of the sets of measurements (log τ has been excluded) to ascertain the significance of the ordering. This test also uses ranked measurements and initially assumes that there is no significant difference between the various samples. The probability of obtaining the observed differences as a result of chance is then calculated. The data required are k = the number of samples being compared, n = the number of measurements in each sample, plus all the individual measurements (or ranks) in all the samples. The mathematical procedure involved the following steps :-

(i) summing the observed rank for each metal ion,

(ii) squaring the observed rank total,

(iii) summing the squares of each rank total (R) ,

(iv) calculating a value χ^2 from the formula

$$\chi^2 = \frac{12\ R}{nk(k+1)} - 3n(k+1) \qquad 6.2$$

The value of χ^2 for the results shown in Table 6.7 has been calculated using Friedman's Test, the relevant data being shown in Table 6.9.

Table 6.9 Friedman's Test Applied to the Ionic Nature of $M(AA)_n$ Complexes

Metal Ion	Rank Values				Rank Totals	Ranks Squared
	C/IR	Me (H)	Ring (H)	Σ_{max}		
Li^+	5	3	5	4	17	289
Na^+	4	2	4	1	11	121
Mg^{2+}	9	5	6.5	9.5	30	900
Al^{3+}	16	14	15	16	61	3721
K^+	3	1	3	2	9	81
Ca^{2+}	6	4	6.5	6	22.5	506.25
Sc^{3+}	14	15	16	8	53	2809
Zn^{2+}	7	11.5	9	11	38.5	1482.25
Ga^{3+}	15	13	13	13.5	54.5	2970.25
Rb^+	2	6.5	2	3	13.5	182.25
Y^{3+}	10	10	11.5	9.5	41	1681
In^{3+}	12	16	14	12	54	2916
Cs^+	1	9	1	5	16	256
La^{3+}	8	6.5	8	13.5	36	1296
Lu^{3+}	11	11.5	10	15	47.5	2256.25
Th^{4+}	13	8	11.5	7	39.5	1560.25
k = 16		n = 4		R = 23027.5		

$$\chi^2 = \frac{(12)(23027.5)}{(4)(16)(17)} - (3)(4)(17)$$

$$= (254) - (204)$$

$$= \underline{50}$$

The χ^2 value was referred to normal χ^2 tables using the row with (k - 1) degrees of freedom and the probability of the matched order

occurring by chance was assessed as 0.1 %. The order of ionic character indicated by this treatment of the data was

$$K^+ > Na^+ > Rb^+ > Cs^+ > Li^+ > Ca^{2+} > Mg^{2+} > La^{3+} >$$
$$Zn^{2+} > Th^{4+} > Y^{3+} > Lu^{3+} > Sc^{3+} > In^{3+} > Ga^{3+} > Al^{3+}.$$

CHAPTER 7

SELF - ASSOCIATION OF $M(AA)_n$ COMPLEXES IN SOLUTION

(a) INTRODUCTION

The recent development of lanthanide β - diketoenolates as nmr shift reagents has led to a greater understanding of the nature of the reacting species in solution[130]. It has been shown that, for example with $Ln(FOD)_3$ complexes[251], there are three competing reactions which may occur due to the Lewis acidity of these chelates, namely

(i) adduct formation with an organic substrate,

(ii) adduct formation with water which is present in nmr solvents which are not completely dry,

and (iii) oligomerisation.

The possible self - association of lanthanide tris - acetylacetonates in solution has been discussed by several workers. Blitz[252] reported some $Ln(AA)_3$ complexes to be dimeric in non - polar solvents. Freed et al.[253] later presented evidence that dimers occurred in benzene solutions of the europium complex and that a monomer - dimer equilibrium could exist. Moeller et al.[254], in conflict with the previous results, reported that the complexes were monomeric in carbon tetrachloride and benzene solutions. Pope et al.[149], who recognised the hydrated nature of these complexes, found that the trihydrates, $Ln(AA)_3.3H_2O$, in benzene gave apparent molecular weights between 500 and 700 which are inter - mediate between monomer and dimer.

More recently, Neilson and Shepherd[257] have reported that the intermolecular energy transfer quenching of the excited state Tb^{3+} ion, ($^5D_4$ level) in the complex $Tb(AA)_3.3H_2O$, by the lanthanide ions of other similar complexes in solution is markedly solvent dependent. It has been proposed that the $(Tb^{3+})^* \longrightarrow Ln^{3+}$ energy transfer step occurs very rapidly in mixed metal dimers where the distance between the lanthanide ions is relatively small[257]. Three main types of behaviour have been found and have been rationalised in terms of the presence of monomer and / or dimer in the various solvents. These types of solvent dependence may be summarised as :-

(i) in non - polar solvents, e.g. benzene, no dynamic quenching is observed only static quenching, consistent with the presence of kinetically stable dimers with a slow exchange rate,

(ii) in polar but not strongly coordinating solvents, e.g. acetone, dynamic quenching occurs and has been explained as a monomer - dimer equilibrium with a relatively rapid exchange rate,

and (iii) in strongly coordinating solvents, e.g. dimethyl - sulphoxide, neither dynamic nor static quenching has been observed indicating that only solvated monomers are present[257].

(b) MOLECULAR WEIGHT DETERMINATIONS

Molecular weight determinations of several lanthanide acetylacet - onate complexes, $Ln(AA)_3.3H_2O$, were made in benzene solution at 310K using vapour pressure osmometry. The results in terms of $\bar{n}$, the average number of monomers per solute molecule (Table 7.1),indicate that association occurs in all cases and suggest that the oligomeric species is a dimer. The decrease in $\bar{n}$ towards the end of the lanthanide series may be the result of incomplete dimerisation or the

Table 7.1 Molecular Weight Measurements of $Ln(AA)_3.3H_2O$ Complexes in Benzene Solution[a] at 310K

Ln^{3+} ion	$\bar{n}$ (± 0.15) [b]	Ln^{3+} ion	$\bar{n}$ (± 0.15) [b]
Pr	2.03	Dy	1.76
Nd	1.89	Ho	1.93
Sm	2.06	Er	1.87
Eu	2.03	Yb	1.67
Gd	2.12	Lu [c]	1.66
Tb	1.98		

(a) 0.01 M with respect to monomer.

(b) $\bar{n}$ = average number of monomers per solute molecule.

(c) The dihydrate complex.

loss of water from the dimeric species. In this respect, it is probably significant that a decreasing tendency for the smaller lanthanide ions to self - associate is observed in the crystalline state by the $Ln(FOD)_3.H_2O$ complexes. For example, the praesodymium complex is dimeric, containing octa - coordinate Pr^{3+} ions bridging across two β - diketoenolate oxygen atoms and one water oxygen atom[113]. The corresponding lutetium complex contains hepta - coordinate Lu^{3+} ions, with a single water oxygen bridge[255]. Similarly, the $Pr(DPM)_3$ complex is dimeric in the solid state, with two ligand oxygens bridging hepta - coordinate Pr^{3+} ions[112], while the corresponding $Er(DPM)_3$ complex is monomeric[94].

Molecular weight measurements of the acetylacetonate complexes of samarium, europium and terbium in the polar solvents acetone and acetonitrile at 0.01 M monomer concentration at 310K gave a mean value of $\bar{n} = 1.47 \pm 0.20$ in acetone and $\bar{n} = 1.67 \pm 0.20$ in acetonitrile. These results indicate that association also occurs in these solvents and

that a monomer - dimer equilibrium may exist. However, any quantitive interpretations from these results may be complicated by the possible loss of water from the complex to the solvent.

(c) PROTON NMR MEASUREMENTS OF $Lu(AA)_3.2H_2O$

(i) Non - Polar Solvents

The ^1H nmr spectra of the diamagnetic complex $Lu(AA)_3.2H_2O$ have been determined at ca. 10K intervals in toluene - D8 over the temper - ature range 213 - 343K , and in C_6D_6 solution over the temperature range 278 - 383K. Representative spectra are shown in Figure 7.1. At 278K, identical spectra are obtained in these solvents. The profiles of the spectra are temperature dependent. The resonance(s) in the region of 1.5 - 1.9 ppm (downfield from the internal reference TMS) may be assigned to the ligand methyl groups and the resonance(s) in the region 4.7 - 5.3 to the 3 - H ligand proton, and are in the expected 6:1 intensity ratio.

Two separate methyl and 3 - H resonances occur at temperatures below the coalescence temperature of ca. 343K (Figure 7.1(b)). The ratios of the low-field / high-field components of these resonances were found to be 2:1 at all temperatures and also to be independent of concentration. These results suggest that the resonances are due to a single species which, on the basis of the molecular weight measurements, is probably a dimer. As the temperature is decreased towards 213K, the low-field components of the resonances broaden (Figure 7.1(d)), but do not resolve. In view of this broadening, the spectrum was measured using a 220 MHz spectrometer at 203K. This spectrum shows a narrow high-field component at 1.51 ppm , but the low-field component is split into two equal - intensity broad resonances at ca. 1.82 and 1.89 ppm (Figure 7.2). The

Figure 7.1 Nmr Spectra of $Lu(AA)_3 \cdot 2H_2O$ in Toluene - D8

(See text)

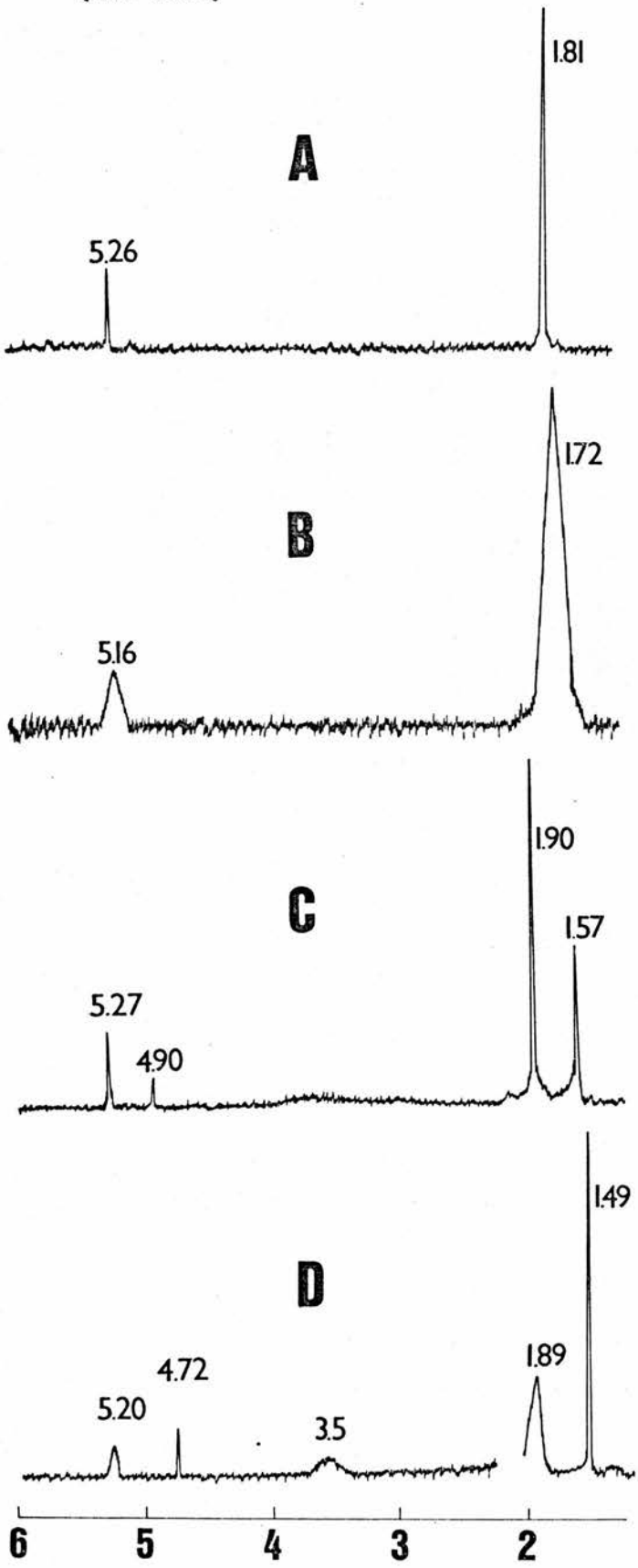

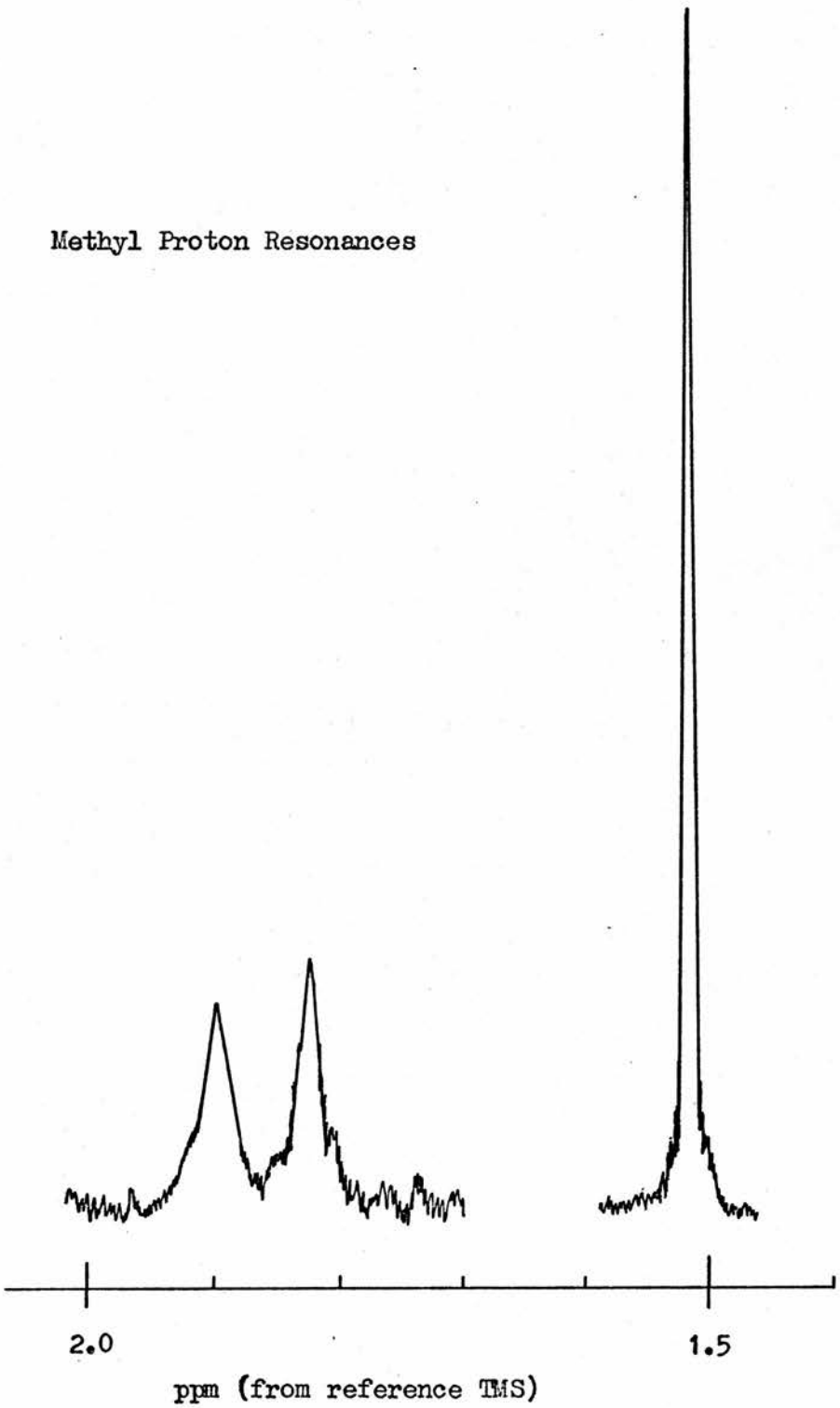

Figure 7.2 220 MHz Spectrum of $Lu(AA)_3.2H_2O$ in Toluene - D8 at 203K

temperature dependence of the spectral profiles indicate that two distinct types of intramolecular ligand exchange occur, one of which is relatively fast with a coalescence temperature below 213K and a much slower type with a coalescence temperature of ca. 340K, both relative to 100 MHz. Although the observed 2:1 and 1:1:1 ratios of the methyl resonances provide information about the inequivalences of the methyl groups, they do not allow any unambiguous assignment of structure to the complex, particularly since the water molecules may have a possible bridging role. A broad resonance at ca. 3.5 was observed in the lower temperature toluene - D8 solution spectra (Figure 7.1(d)), which is attributable to water on the basis of integration. The position of this resonance was temperature and concentration independent, suggesting that the water molecules are exchanging between similar sites on the complex. Increasing the temperature above 343K caused line - narrowing typical of a fast - exchange region (Figure 7.1(a)).

(ii) Polar, Non - Coordinating Solvents

The ^{1}H nmr spectra of the lutetium complex have also been determined in acetone - D6 solution over the temperature range 183 - 363K (Figure 7.3) At 183K single, narrow resonances corresponding to methyl and 3-H ligand protons occur at 1.79 and 5.38 respectively. With increasing temperature, additional resonances appear at 1.89 and ca. 5.40, which grow in intensity relative to the initial methyl and 3-H resonances and coalesce with them at ca. 303K. Further increase in temperature causes line narrowing. The temperature dependence of the relative areas of the methyl and 3-H components below 303K is different from the behaviour found in the non - polar solvents and suggests that these resonances are due to the presence of two discrete species. If the 1.89 and 1.79

Figure 7.3 Nmr Spectra of $Lu(AA)_3 \cdot 2H_2O$ in Acetone - D6

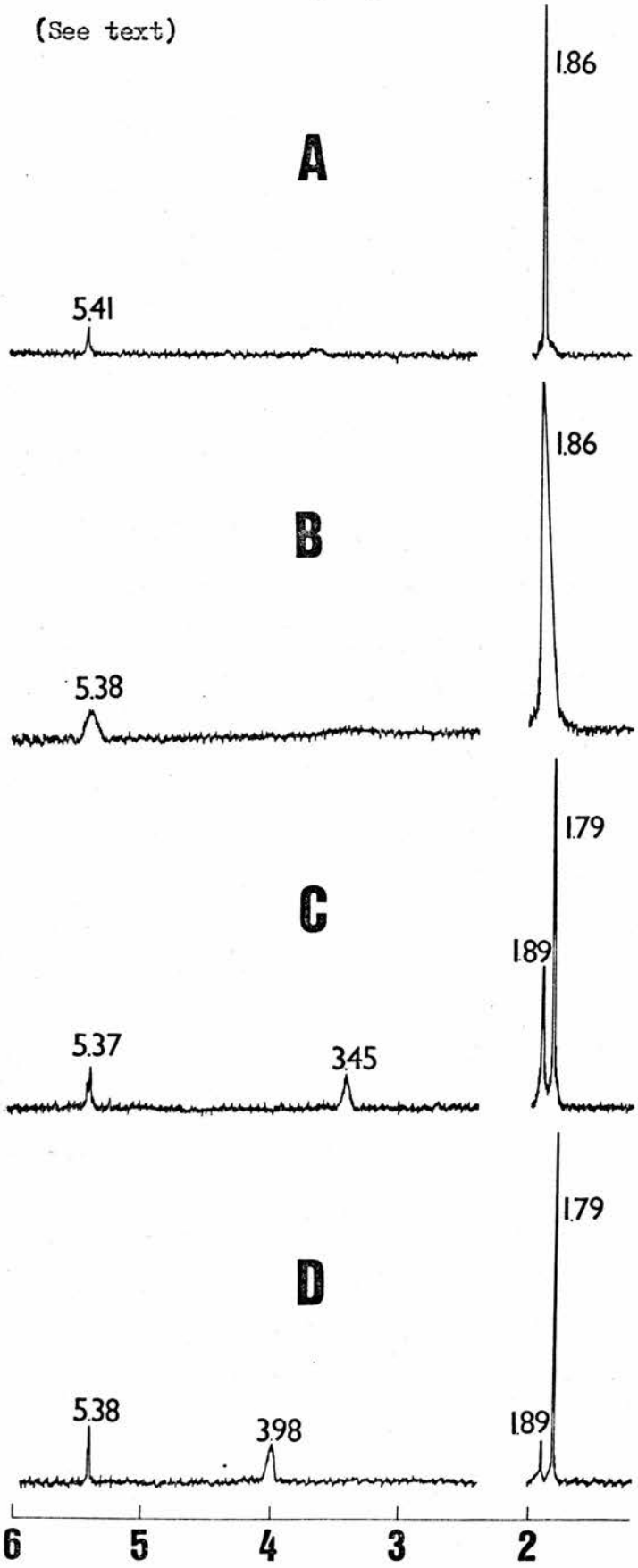

methyl resonances are attributable to monomeric and dimeric species respectively, then the dimer formation constant (K), where $K = [\text{Dimer}] / [\text{Monomer}]^2$, may be obtained in acetone solution at equilibrium using the spectral integrals. The integrals of the methyl resonances have been measured over the temperature range 233 - 293K (the 3-H peaks are not sufficiently resolved to be useful) and values of K have been determined on this basis. The linearity of the ln K against 1/T plot (Figure 7.4) supports the view that a monomer - dimer or stoichiometrically equivalent equilibrium is occurring. Further measurements at concentrations within the experimentally useful range of 0.04 - 0.14 M gave identical K values , within experimental error. The least - squares regression line of the ln K against 1/T plot gives values of

$$\Delta H^{o} = -28.2 \text{ kJ mol}^{-1} ,$$

and

$$\Delta S^{o} = -74.5 \text{ J K}^{-1}\text{mol}^{-1}$$

for the equilibrium. It is unlikely that the tetramethylsilane present as an internal reference (ca. 3%) in the acetone solution and the use of concentration rather than activity terms are likely to lead to large errors in the derived enthalpy and entropy values. The water molecules of the complex give a single resonance, the position of which is dependent on both concentration and temperature and shifts down-field with increasing temperature. This behaviour suggests that the water molecules are rapidly exchanging between solvent and complex sites with the latter probably predominant at the lower temperatures. The coalescence point at 303K (Figure 7.3(b)) can thus be assigned to an intermolecular exchange between monomers and dimers, in contrast to the intramolecular ligand exchange coalescences found with the non - polar solvents.

This difference implies that the ligand exchange rate is consider-

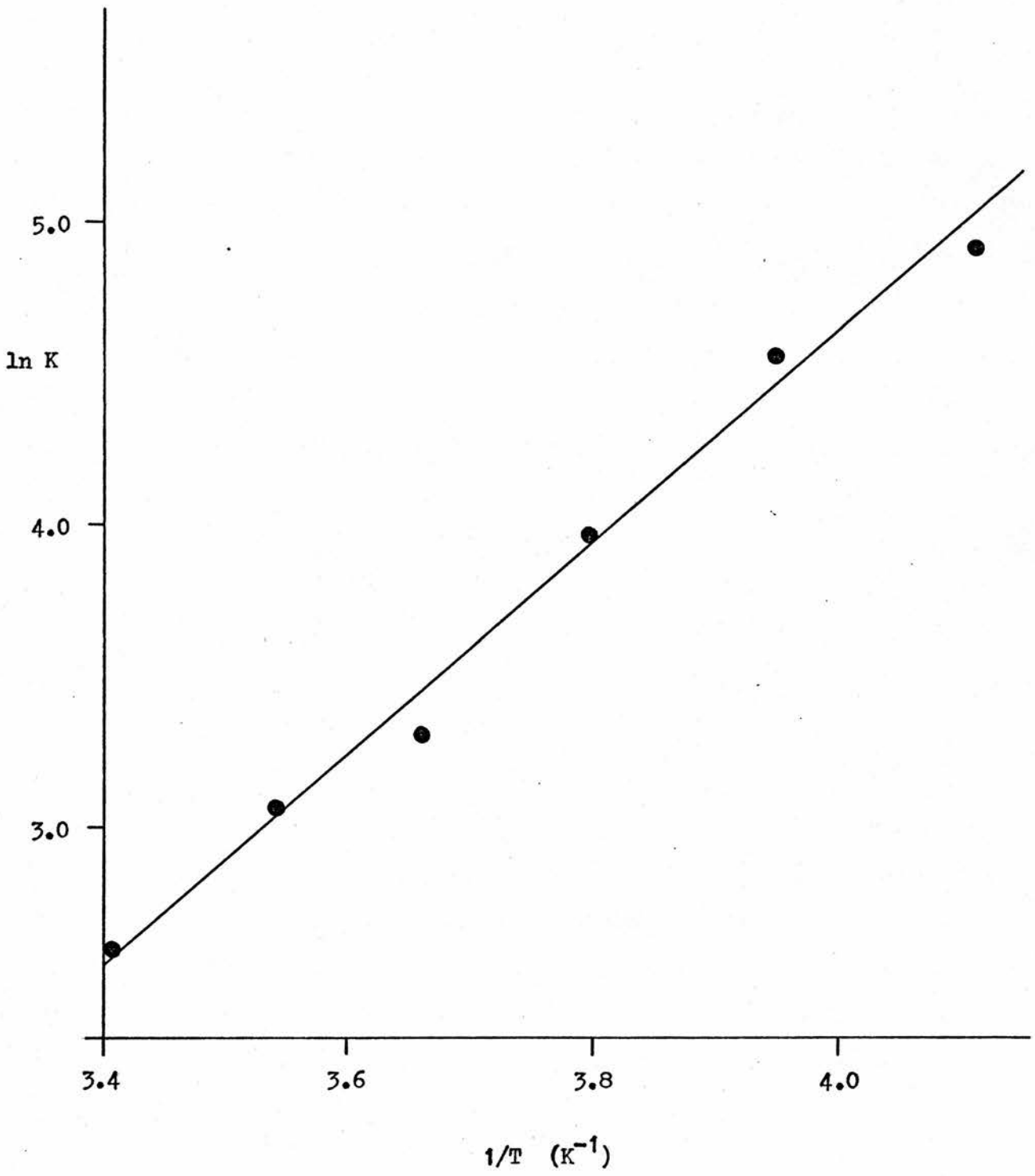

Figure 7.4 Plot of ln K against 1/T for $Lu(AA)_3 \cdot 2H_2O$ in Acetone - D6

ably faster in the dimeric species in acetone solution than in either benzene or toluene. It is therefore possible that the structures of the dimeric species in these solutions are not similar. The values of $\bar{n} = 1.47 \pm 0.20$ obtained for the molecular weight determinations for the Sm^{3+}, Eu^{3+} and Tb^{3+} acetylacetonates in acetone at 310K indicate a significantly higher degree of dimerisation in these complexes relative to the lutetium complex. This may reflect a decreasing tendency for self - association with complexes of the smaller Lu^{3+} ion, similar to that shown by the $\bar{n}$ values obtained in benzene solution (Table 7.1).

(iii) Polar, Coordinating Solvents

In both DMSO - D6 and pyridine solutions at 303K, single narrow resonances, corresponding to the methyl and 3-H ligand protons, occur at 1.78 and 5.33, and 1.84 and 5.41 ppm respectively. Addition of either of these solvents to acetone, benzene or toluene solutions of $Lu(AA)_3.2H_2O$ causes line narrowing and the appearance of these characteristic resonances. This behaviour indicates that, in these strongly coordinating solvents, the sole solution species is a solvated monomer.

(iv) Discussion

The nmr results are therefore consistent with previous proposals regarding the possible mechanisms of intermolecular energy transfer and its dependence on the nature of the solvent. They also show that it is necessary to obtain data over a wide range of temperatures with this type of system before it is possible to draw conclusions about the possible nature of the solution species, since any multiplicity of

resonances may arise from inter- and / or intramolecular exchange mechanisms. The other diamagnetic lanthanide acetylacetonate, $La(AA)_3 \cdot 3H_2O$, is not sufficiently soluble in benzene, toluene or acetone to allow determination of nmr spectra, but preliminary investigations with $Y(AA)_3 \cdot 3H_2O$ have shown the presence of more than one methyl resonance in these solvents.

(d) THE SELF - ASSOCIATION OF $Mg(AA)_2$ IN SOLUTION

Brittain has recently discussed the ^1H nmr spectra of some Group IIa metal acetylacetonates in various solvents and has proposed that the methyl resonances at 1.80 and 2.02 ppm, observed in $CDCl_3$ solutions of $Mg(AA)_2$ are due to square planar and tetrahedral isomers coexisting in the solution[239]. On the basis of the nmr data, it was also suggested that $Ca(AA)_2$ and $Ba(AA)_2$ are square planar in $CDCl_3$ solution whereas $Zn(AA)_2$ and $Be(AA)_2$ are tetrahedral. The implied stability of a D_{2h} configuration with Mg^{2+}, Ca^{2+} and Ba^{2+} ions is, however, questionable in that this would require a much higher degree of covalence in the metal - oxygen bonds than is probable with these electropositive ions. Without such covalence, the rotation of one acetylacetonate ligand about its C_2 axis will monotonically increase the energy of an $M(AA)_2$ system from a minimum at D_{2d} to a maximum at D_{4h} symmetry. Square planar acetylacetonate complexes are only known to occur with metal ions (e.g. Cu^{2+}, Pd^{2+}, Pt^{2+}) where there are specific energetic advantages over the sterically favoured tetrahedral configurations [73].

These considerations and the results obtained with lutetium acetylacetonate suggest that the nmr spectra of the Group IIa acetyl - acetonates may be more satisfactorily explained in terms of varying

degrees of oligomerisation. The self - association of several non - lanthanide metal acetylacetonates in the crystalline state and in solution is well established. For example, $Co(AA)_2$ and $Ni(AA)_2$ are tetrameric[108] and trimeric[109] in the solid state and also oligomerise in non - polar solvents[134]. Both complexes form six - coordinate solvated monomers in polar solvents[75]. Crystalline $Zn(AA)_2$ is trimeric[110] but molecular weight measurements have indicated that it is monomeric in non - polar solvents[128]. Considering the analagous Group IIa complexes, the small ionic radius of the Be^{2+} ion (4-coordinate radius = 0.27Å)[284] precludes oligomerisation which requires an increase in coordination number. The tetrahedral configuration found in the solid $Be(AA)_2$[77] is likely to be retained in solution in polar and non - polar solvents. The ionic radius of Mg^{2+} (0.72Å) is however similar to those of Co^{2+}(0.61Å), Ni^{2+}(0.60Å) and Zn^{2+}(0.75Å)[284]. In the case of Mg^{2+} and those of the larger Ca^{2+}(1.00Å) and Ba^{2+}(1.16Å) ions there is therefore the possibility that the corresponding acetylacetonates may oligomerise in non - polar solvents in order to increase the coordin - ation number of the metal ion.

The ligand methyl resonances reported by Brittain[239] are categor - ised in Table 7.2 in terms of monomeric and oligomeric species. It is proposed that all the complexes are monomeric in the polar solvents but that, in $CDCl_3$, only the beryllium complex is entirely monomeric, the magnesium complex exists in both monomeric and oligomeric forms and the calcium and barium complexes are predominantly oligomeric. Values for $Zn(AA)_2$ in DMSO - D6 and for the complex $Al(AA)_3$ are included in Table 7.2 to illustrate the downfield solvent shifts in chloroform and carbon tetrachloride. By making allowance for this solvent shift, it is possible to consider that the 2.02 ppm resonance of $Mg(AA)_2$ in $CDCl_3$ must be classified with the observed shifts in the polar solvents and

Table 7.2 Chemical Shifts of $M(AA)_2$ Complexes [239]

Complex \ Solvent	Methyl Resonance(s) ppm [a]			
	DMSO - D6 Monomer	CCl_4 Monomer	$CDCl_3$	
			Monomer	Oligomer
$Be(AA)_2$	N/A	1.93	2.02	— [b]
$Mg(AA)_2$	1.70	— [c]	2.02	1.80
$Ca(AA)_2$	1.72	— [c]	— [b]	1.78
$Ba(AA)_2$	1.70	— [c]	— [b]	1.77
$Zn(AA)_2.H_2O$	1.83 [d]	1.98	2.02	— [b]
$Al(AA)_3$ [e]	1.90 [d]	2.07 [d]	2.11 [d]	— [b]

(a) Resonances measured downfield from reference TMS.

(b) No detectable proton resonances.

(c) Samples insoluble in CCl_4. (d) Results from this laboratory.

(e) Results for $Al(AA)_3$ included for comparison.

can be attributed to monomer and that the anomalous resonance is that at 1.80 ppm. The latter resonance is attributed to the presence of oligomer.

This interpretation is supported by the resonance profiles and the temperature dependence of the $Mg(AA)_2$ spectrum in $CDCl_3$ solution. The 2.02 ppm resonance assigned here to monomer is narrow, in common with the linewidths observed in the polar solvents where the solution species is likely to be a solvated monomer. In contrast, the 1.80 ppm resonance is broad and suggests that exchange broadening is occurring. This can be explained as a tumbling effect in the oligomer in which sufficiently rapid exchange of terminal and bridging oxygens may occur to prevent observation of the inherent methyl inequivalences in such a structure. The ratio of the resonance areas (2.02 ppm/1.80 ppm) has been found to increase with temperature, consistent with the expected dissociation of

the oligomer. The apparent absence of complete reversibility in this respect suggests that the attainment of monomer--oligomer equilibrium is slow and it may be significant that the two resonances show no tendency to coalesce over the temperature range examined.

The occurrence of the $Ba(AA)_2$ and $Ca(AA)_2$ complexes as oligomers may only be explained in terms of the larger ionic radii of these ions relative to that of Mg^{2+}. It is probable that the 3-H resonance of the $Mg(AA)_2$ oligomer in $CDCl_3$, which is expected at ca. 5.0 ppm, is exchange - broadening to an extent where it becomes indistinguishable from the background noise in these necessarily dilute solutions. The nmr spectra of the benzoylacetone complexes of Be^{2+}, Mg^{2+} and Ca^{2+}, reported by Brittain[239], can be interpreted in a similar manner although the significance of the slight splittings reported for some of the methyl resonances is not clear.

CHAPTER 8

LUMINESCENCE QUENCHING BY INORGANIC IONS

(a) INTRODUCTION

The mechanisms of intermolecular quenching of fluorescence and phosphorescence have been extensively studied for various systems and details may be found in recent reviews [37,258]. A general classification of these mechanisms has been made on the basis of quenching due to

(a) heavy atom or paramagnetic molecules [259,260],

(b) electronic energy transfer [261-263],

(c) charge transfer [264,265],

or (d) enhanced radiationless decay through an excited complex (exciplex) [266,267].

The luminescence quenching by inorganic salts is characterised by the following properties :-

(i) a decrease in luminescence intensity, related to the quencher concentration,

(ii) a decrease in the luminescence lifetime as the concentration is increased,

(iii) the absorption spectrum of the emitting species is unchanged even at high quencher concentration, showing that quenching is not due to the formation of a ground state complex (i.e. static quenching),

and (iv) the rate constant of the quenching process decreases with increasing viscosity of the solvent.

It has been shown that for low concentrations of inorganic quenchers the Stern - Volmer equation

$$R - 1 = K[Q] \qquad 8.1$$

is valid, where R may be either the ratio of luminescence intensity (I_o/I) or of luminescence lifetime (τ_o/τ) and [Q] is the quencher concentration. I_o and τ_o are the intensity and lifetime respectively of the donor molecule. From the constant K and a value of τ_o, the absolute rate constant (k) for the process, in units of $dm^3\ mol^{-1}s^{-1}$, may be calculated from the expression

$$k = K/\tau_o \qquad 8.2$$

The constants K and k are independent of the donor concentration.

The quenching of organic singlet states by inorganic anions has been the subject of numerous investigations[264,265,285-287] and it was generally accepted until recently that charge - transfer was likely to be the predominant mechanism. Watkins[286] has however shown that radical species are not always formed in these reactions and has suggested that radiationless transitions from the excited singlet state, mainly to the triplet, are induced by the proximity of higher lying charge - transfer states.

Although the quenching of organic triplet states by metal ions and complexes have been widely studied[258,263,282] relatively little attention has been given to the quenching of organic singlet states by metal cations. Perhaps the most comprehensive study to date has been that of Varnes et al.[269] on the quenching of riboflavin fluorescence by metal ions. They concluded that electronic energy transfer was probably the most general quenching mechanism but did not reject the possibility of other mechanisms operating.

(b) FLUORESCENCE QUENCHING BY INORGANIC IONS

(i) Experimental Results

The fluorescence characteristics of the donor molecules used in the course of these investigations are shown in Table 8.1. The emission spectra were recorded on a Perkin - Elmer Hitachi MPF -2A Spectrofluorimeter and the fluorescence lifetimes and subsequent quenching studies were determined using the Single Photon Counting Technique.

Table 8.1 Fluorescence Characteristics of the Donor Molecules

Donor	Structure	Solvent	τ_o [a] (ms)	λ_{max} [a] (fluor.) (nm)
Quinine Sulphate	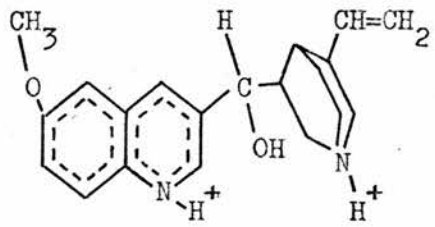	0.1 M HNO_3	20.89	460
		0.05 M H_2SO_4	19.45	
Acridine	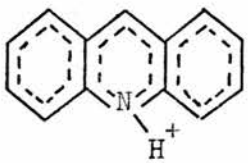	0.1 M HNO_3	31.15	475
		0.05 M H_2SO_4	37.23	
2 - Naphthamide	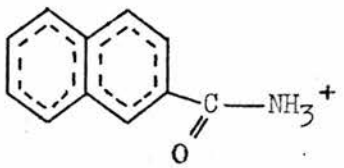	0.5 M HNO_3	14.70	430
		0.2 M H_2SO_4	17.20	
Xanthone	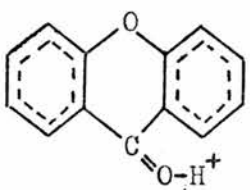	4 M HNO_3	18.91	460
		2 M H_2SO_4	26.61	

Table 8.1 (cont.)

Donor	Structure	Solvent	τ [a] (ms)	λ_{max} [a] (fluor.) (nm)
Acridone	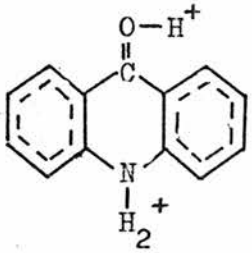	7 M HNO_3	21.84	459
		3.5 M H_2SO_4	23.20	

(a) The concentration of donor in each solvent was 10^{-5}M.

The donor molecules were recrystallised twice before use. Donor concentrations of ca. 10^{-5} mol dm^{-3} in acidic aqueous solutions were used in all cases. The acidities of the solutions were made sufficiently high to ensure that the donor molecules were protonated in both the ground and excited singlet states. With the exception of the Ag^+ ion, all the potential acceptor metal ions were added as metal sulphates to sulphuric acid solutions of the donor. The halide and pseudohalide ion quenchers were added as the appropriate A.R. grade potassium salt.

The corrected emission spectra of the donor molecules are shown in Figures 8.1 and 8.2 and it was found that there was no appreciable change in the emission spectral profiles of any of the donors in either HNO_3 or H_2SO_4. There were however significant differences in the measured lifetimes in these solvents. Ireland[163] has determined the rate constants for the fluorescence quenching of protonated xanthone by some inorganic anions and has reported that there was no appreciable quenching with NO_3^- or SO_4^{2-} except at very high acceptor concentrations. It is probable that the differences in measured lifetimes for each donor in NO_3^- and SO_4^{2-} (Table 8.1) reflect a trend in the relative quenching ability of these ions. However, the quenching rate constants for NO_3^-

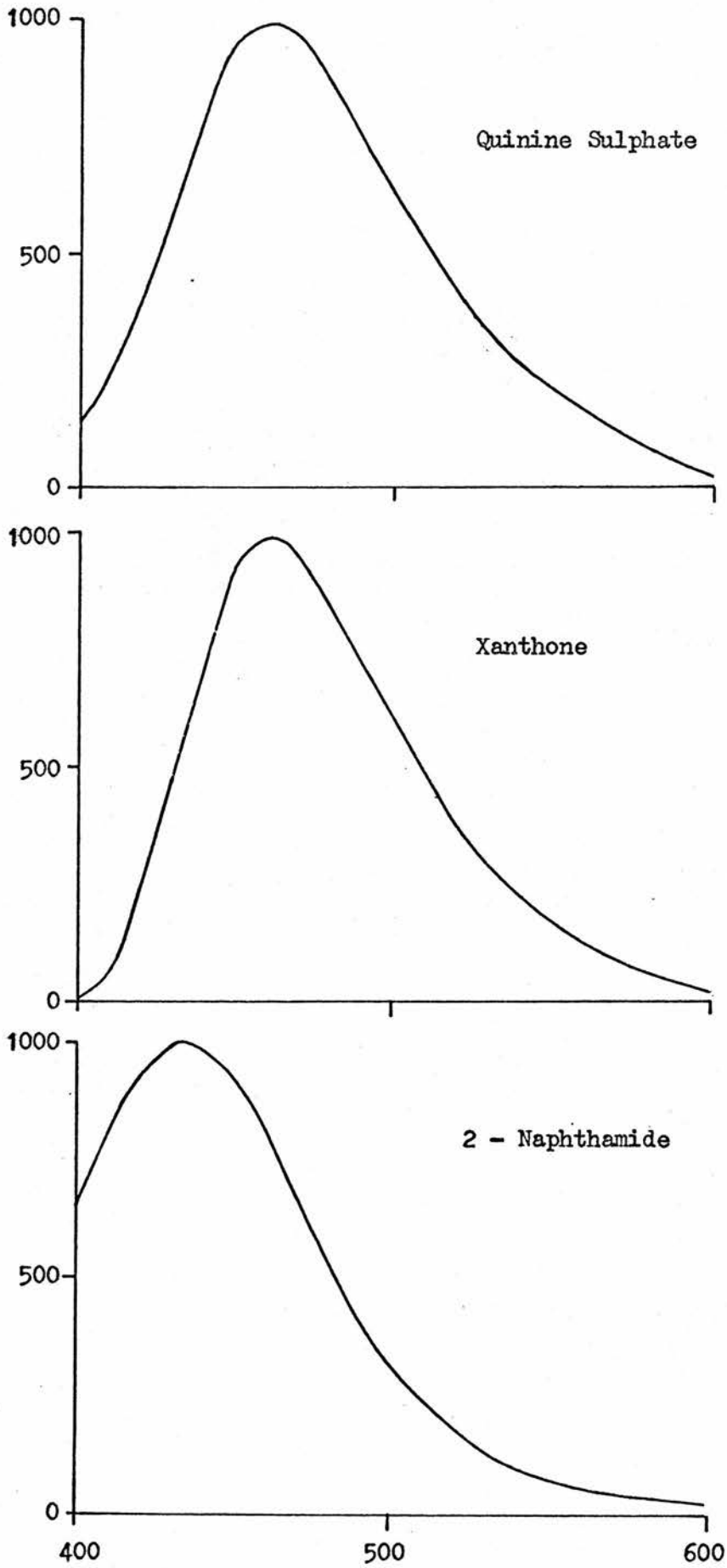

Figure 8.1

Corrected Emission Spectra of the Donor Molecules

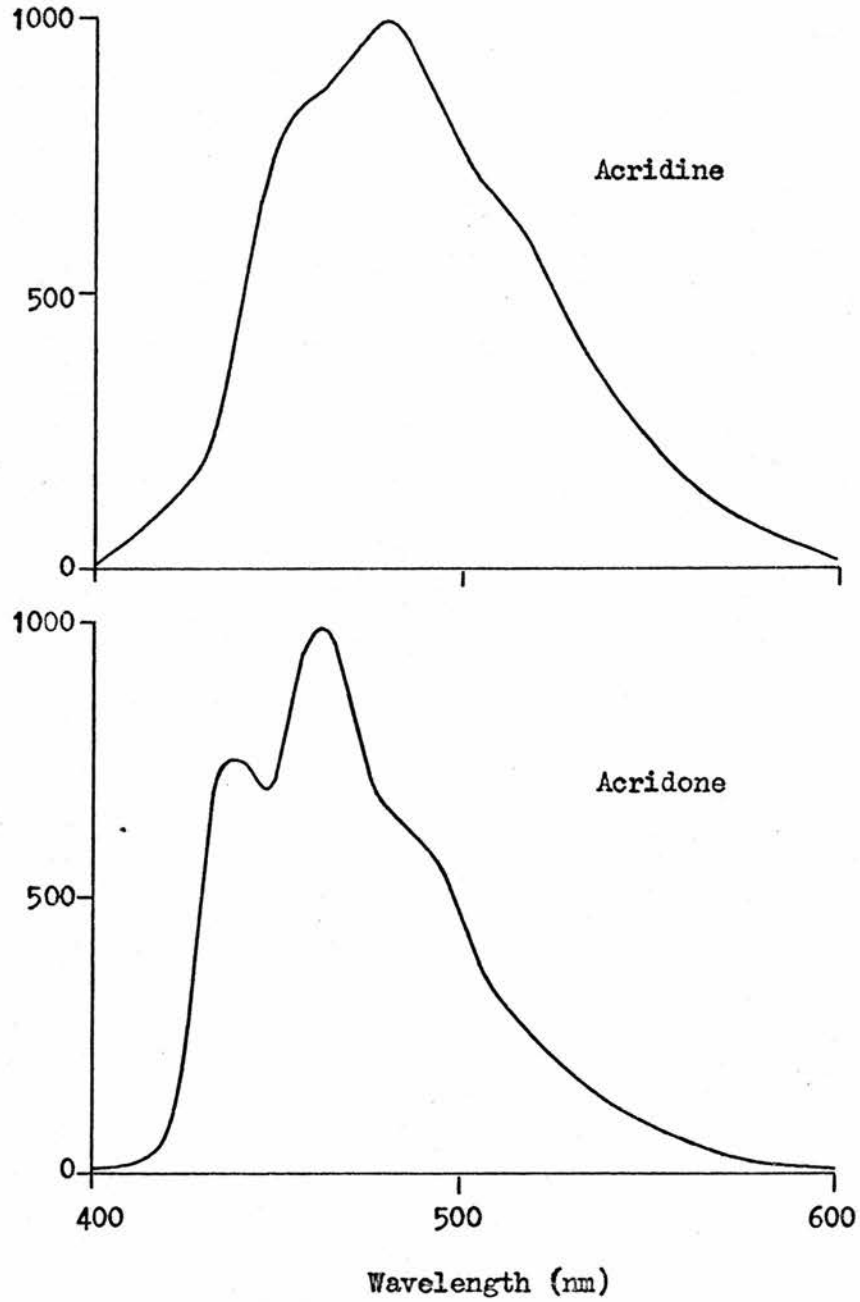

Figure 8.2 Corrected Emission Spectra of the Donor Molecules

and SO_4^{2-} ($<< 10^7$ dm^3 $mol^{-1}s^{-1}$) are small relative to the rates of the other quenching species reported in this thesis and, since the concentrations of these ions were essentially constant for the quenching studies, it is probable that errors due to these ions are minimal.

The fluorescence quenching of all the metal ions were studied using lifetime measurements of the donor fluorescence which successfully precluded possible interference from "inner - filter" effects[37]. For the anionic quenchers, both relative lifetime and quantum yield measurements were made and the rate constants derived from these results agreed in all cases within experimental error.

Measurements were made at 293 ± 2K . The solutions were not degassed and the only case in which this may have led to significant errors in the bimolecular quenching rates (k_q) is that of iodide quenching where some oxidation to iodine was observed after exposure to ultraviolet radiation. Measurements of the iodide system were only accurate using relative quantum yield measurements taken immediately after mixing. The values of τ_o remained unchanged after prolonged bubbling of O_2- free nitrogen through the solutions. At least four quencher concentrations were investigated to obtain the quoted values of k_q.

Table 8.2 shows some typical results for the relative intensity measurements for the addition of quencher at 293 K and Figure 8.3 shows the Stern - Volmer plot of these results.

Table 8.2 Relative Intensity Measurements for the Quenching of 2 - Naphthamide by Br^- and SCN^- at 293 K

Anion	Concentration (mol dm^{-3})x10^3	I_o	I	$(I_o / I) - 1$
Br^-	24.53	75	16.5	3.69
	9.81		30.5	1.46
	4.91		43.5	0.72
	2.45		54.0	0.39
SCN^-	23.23	77	14.0	4.50
	9.30		27.0	1.85
	4.65		41.0	0.88
	2.33		53.0	0.45

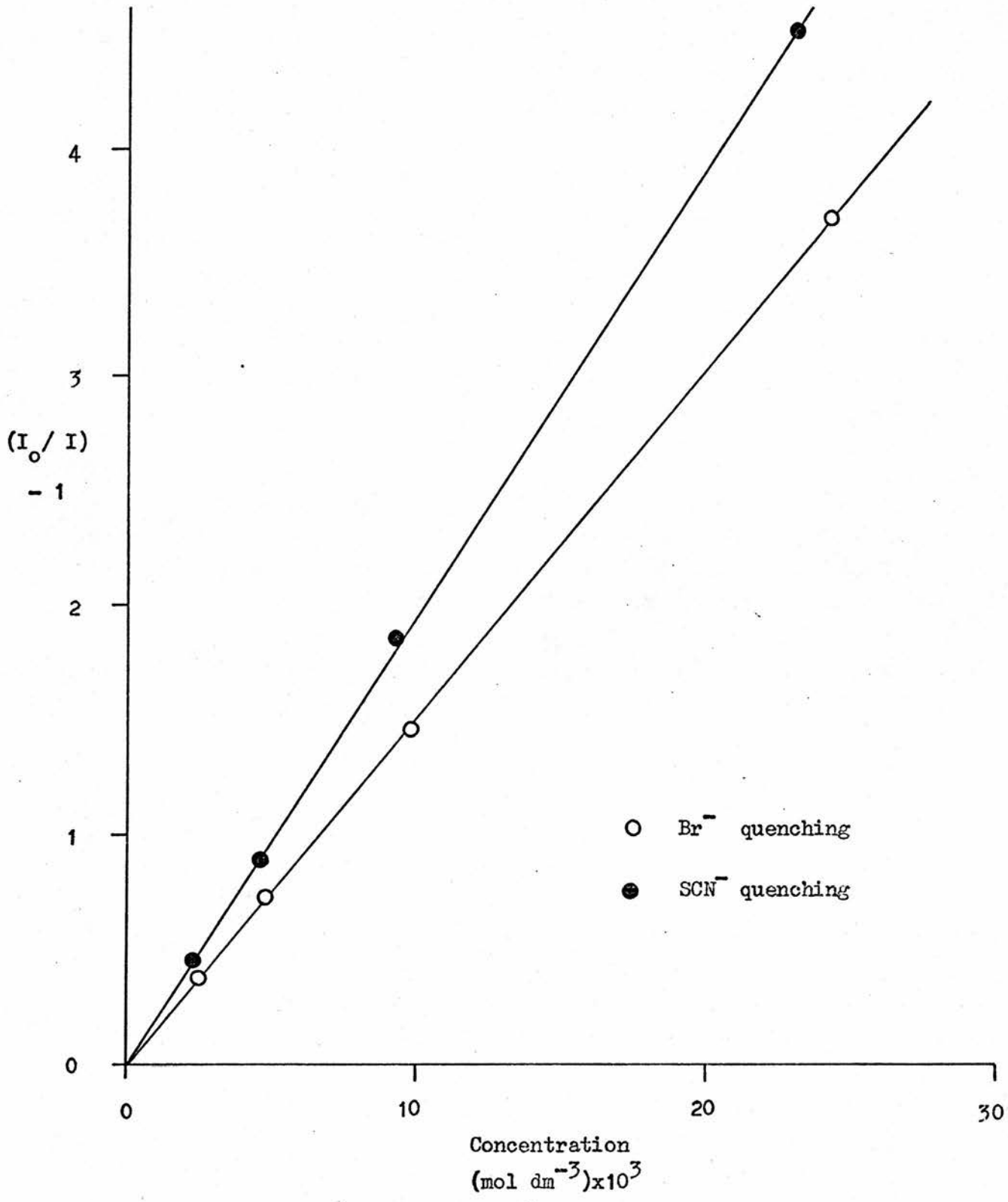

Figure 8.3 Stern - Volmer Plot for the Quenching of the Fluorescence of 2 - Naphthamide by Br^- and SCN^- at 293K

For each system studied a linear Stern - Volmer plot of $(\tau_o/\tau) - 1$ or of $(I_o/I) - 1$ against quencher concentration was obtained at low concentrations. At comparatively high concentrations , positive deviations from the Stern - Volmer plot were observed possibly due to non - stationary state effects since at these concentrations donor molecules will have acceptor ions within their reaction sphere and will deactivate immediately on excitation. The quenching rate constant was derived for each quencher from the slope of the Stern - Volmer plot and the absolute bimolecular rate constant (k_q) calculated using equation 8.2. For the example given in Table 8.3, the following values of K and k_q were obtained,

$$K_{(Br^-)} = 151 \text{ dm}^3 \text{ mol}^{-1} \; ; \quad k_{q\,(Br^-)} = 8.9 \times 10^9 \text{ dm}^3 \text{ mol}^{-1} \text{s}^{-1} \; :$$

$$K_{(SCN^-)} = 196 \text{ dm}^3 \text{ mol}^{-1} \; ; \quad k_{q\,(SCN^-)} = 11.5 \times 10^9 \text{ dm}^3 \text{ mol}^{-1} \text{s}^{-1} \; .$$

The absolute bimolecular rate constants obtained for the quenching by inorganic ions are shown in Table 8.3. The k_q values for the weak quenchers NO_3^-, SO_4^{2-} and Na^+ are included for comparison. Variations in k_q with temperature, due to viscosity changes, were expected to be very small in the temperature range found during the determinations[163]. Significant errors in k_q were however expected due to weighing errors, variations in the excitation energy (for the relative quantum yield measurements), the difficulty in measuring very short lifetimes close to the excitation flash and decomposition problems. Many of these problems were overcome by averaging the results from four independent runs and calculating k_q values solely on the basis of Stern - Volmer plots. The reproducibility was $\pm$ 5% and the total error for the k_q values was assessed as $\pm$ 10%.

Values for the bimolecular diffusion rate constants (k_d) have been calculated for the various concentrations of sulphuric acid solutions

Table 8.3 k_q Values for the Fluorescence Quenching of Donor Molecules (including the bimolecular diffusion rate constants for each of the sulphuric acid solutions)

Donor [a] / Acceptor	Quinine Sulphate 0.05 M H_2SO_4	Xanthone 2 M H_2SO_4	2 - Naphthamide 0.2 M H_2SO_4	Acridine 0.05 M H_2SO_4	Acridone 3.5 M H_2SO_4
I^-	1200 [b]	800	1060	1300	430
SCN^-	890	780	1120	1100	353
Br^-	760	580	880	1200	220
Cl^-	630	380	2	150	1
NO_3^-	1	1	1	1	1
SO_4^{2-}	1	1	1	1	1
Fe^{3+}	160	161	374	300	194
Cr^{3+}	170	122	141	94	131
Fe^{2+}	100	310	191	250	149
Co^{2+}	140	190	159	190	245
VO^{2+}	43	80	30	90	36
Nd^{3+}	30	48	8	100	34
Pr^{3+}	21	30	2	29	27
Cu^{2+}	21	14	54	25	36
Ni^{2+}	17	19	30	14	15
Mn^{2+}	6	13	3	1	1
Na^+	1	1	1	1	1
k_d [c]	730	490	690	730	360

(a) Protonated species.

(b) Units for k_q are $dm^3\ mol^{-1}s^{-1}$ $(x\ 10^{-7})$.

(c) Bimolecular diffusion rate constants (k_d) are calculated from $k_d = 8RT/3000\eta$. Units are $dm^3\ mol^{-1}s^{-1}$ $(x10^{-7})$.

used in these investigations from the approximation[11]

$$k_d = 8RT/3000\,\eta \qquad 8.3$$

where η = the solvent viscosity. Values of η were derived from previous

results[273].

(ii) Anionic Quenching

It may be seen that the experimentally determined k_q values for the anionic quenchers I^- and SCN^- exceed the relevant k_d values in each case (Table 8.3). Equation 8.3 is derived [288] from the Stokes-Einstein equation on the assumption that neutral molecules of equal molecular radii are involved. In the present systems the donor and acceptor species are not of equal size and are charged. Although differences in size of the interacting species need not necessarily lead to large errors in k_d values obtained from 8.3, allowance should be made for the relative charges. This may be done by using the modified Debye expression[288]

$$k'_d = (8RT/3000\eta)(\delta/\exp(\delta) - 1) \qquad 8.4$$

with $\delta = z_A z_B e^2/DkTl$; where z_A and z_B are the ionic charges, e = the electronic charge, D = the solvent dielectric constant and l = the distance of closest approach. Accepting the approximations inherent in equation 8.4 it is possible, at least in a qualitative manner, to rationalise the high k_q values found with I^- and SCN^- on the basis that these particular quenching reactions are operating at or very close to the diffusion limiting rate. For example, the values of k_q/k_d for I^- quenching of the donor molecules are 1.64, 1.63, 1.54, 1.78 and 1.36 indicating that the closest approach distances from equation 8.4 are 0.6 - 0.8 nm which are not unreasonable. The observed order of anionic quenching ability $I^- \approx SCN^- \geqslant Br^- \geqslant Cl^-$ is in agreement with previous results[287].

There was no evidence to support a quenching mechanism due to a heavy atom effect which predicts an order of $I^- > Br^- > Cl^- > SCN^-$ based on the spin - orbit coupling parameters[274]. In addition there was no

significant quenching for either NO_3^- or SO_4^{2-} contrary to the predictions of a heavy atom effect.

Since there is no overlap between the donor emission and acceptor absorption spectra for any system, it is unlikely that an electronic energy transfer mechanism operates for anionic quenching.

If quenching occurs due to a charge - transfer process between donor and acceptor molecules, then the following relationship should be found[275],

$$\log k_q \approx \text{a constant} + IP_A \qquad 8.5$$

where IP_A is the ionisation potential of the acceptor species. The ionisation potentials for each species are also related to the polarographic oxidation potentials[276] which have been determined for the anions I^-(-0.54 V), SCN^-(-0.77 V), Br^-(-1.07 V) and Cl^-(-1.36 V)[235]. In Figure 8.4, the log k_q values obtained with each of the systems are plotted against the oxidation potentials of the anions. Linear plots of log k_q against oxidation potentials are only found where the rate constants approach the diffusion-controlled rates for the appropriate solvents. This linear correlation supports, at least in part, a charge-transfer mechanism which operates through the formation of an intermediate complex

$$(D^+)^* + (A^-) \rightleftharpoons (D.....A)^* \qquad 8.6$$

However, there was no evidence to support complex formation in the excited state since there was no variation in the emission spectra of any of the molecules even at the highest quencher concentration used.

The recent investigations by Watkins[285-287] have shown that radical species are not always formed in reactions presumed to occur by charge - transfer processes. It has been suggested[286] that the excited singlet state energy is deactivated by radiationless transitions, mainly to the triplet, and that this quenching process is induced by

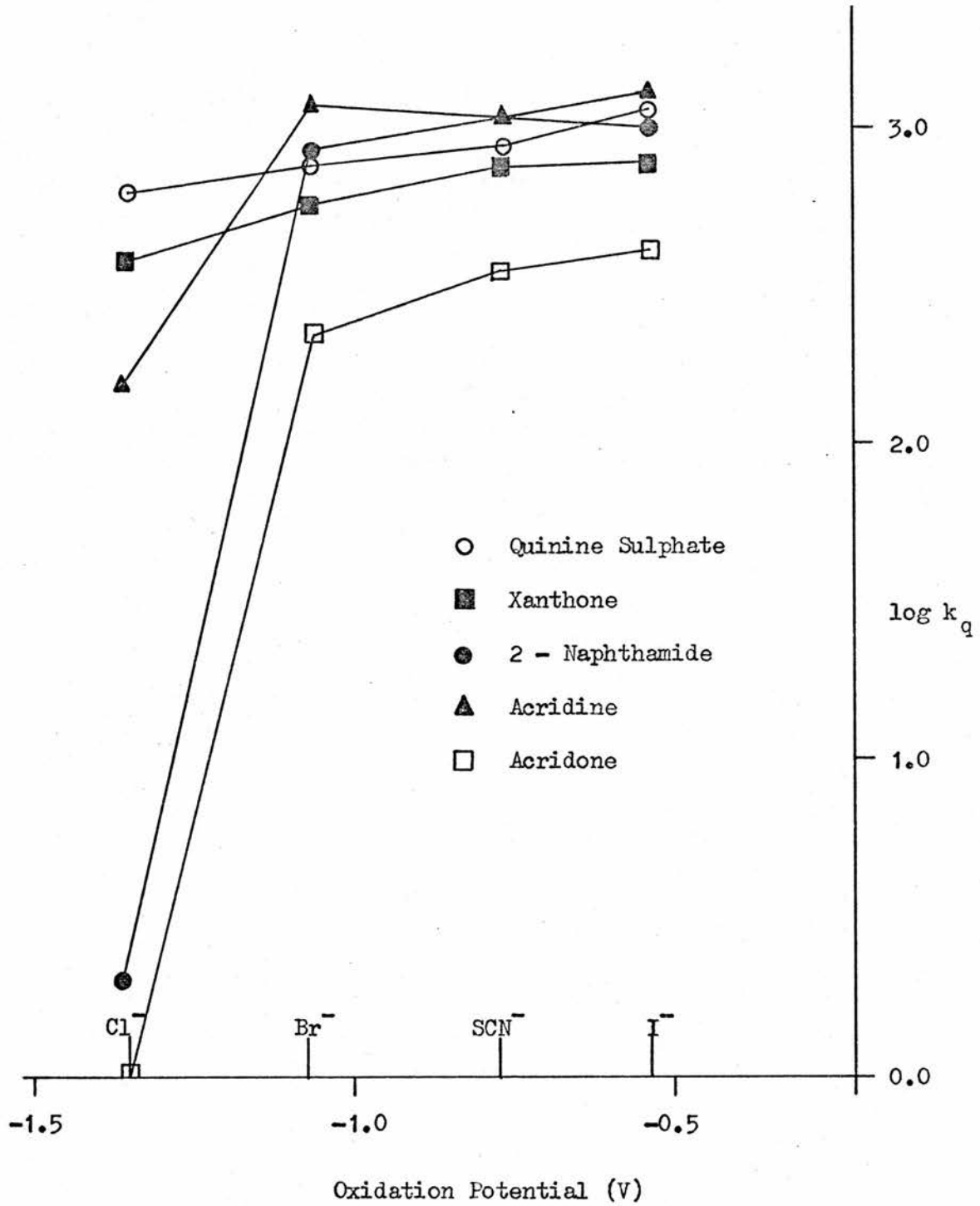

Figure 8.4 Relationship Between log k_q and Oxidation Potential for Donor / Anionic Quencher Systems

the proximity of higher energy charge - transfer states. It is therefore not unreasonable to suggest that a similar mechanism operates in the systems of anionic quenchers reported in this thesis. By this mechanism, deactivation will occur immediately on diffusional encounter between donor and acceptor. The non - monotonic behaviour of the Cl^- ion, in particular, may be explained by the large hydration "shell" of this ion which effectively prevents the donor and acceptor molecules interacting.

(iii) Cationic Quenchers

Possible mechanisms which may account for the quenching of singlet states by metal ions are (a) heavy atom or paramagnetically induced increases in spin - orbit coupling leading to increased intersystem crossing rates in the donor molecules, (b) ground and/or excited state complexation of the donor to the metal ion, (c) complete or partial charge - transfer between the donor and the metal ion - or an induced radiationless process of the type proposed by Watkins[286] and (d) electronic energy transfer from donor to acceptor.

Of these possibilities, (a) may be discounted as a significant mechanism since there was no observable quenching either with the diamagnetic La^{3+} ion (Z = 57) or with the heavier paramagnetic Gd^{3+} ion. The protonated nature of the donor molecules and the acidity of the solutions should also preclude complex formation between the donor and the metal ions as an important mechanism. In addition, the charge - transfer related mechanisms (c) alone cannot satisfactorily account for the appatent ordering of quenching ability, i.e. Fe^{3+}, Cr^{3+}, Fe^{2+}, $Co^{2+} > VO^{2+}$, Nd^{3+}, Pr^{3+}, Cu^{2+}, $Ni^{2+} > Mn^{2+}$, since this order does not show any obvious correlation with the redox potentials of the metal ions.

Electronic energy transfer, either by a Coulombic or an electron - exchange mechanism requires a finite overlap of the donor emission band and the absorption band(s) of the acceptor. Efficient transfer from an excited singlet state, $^1S_1^*$, to an acceptor with ground state ^mA

$$^1S_1^* + {}^mA \longrightarrow {}^1S_o + {}^nA^* \qquad 8.7$$

by either mechanism requires that m = n, i.e. that the acceptor transition is spin - allowed. Energy transfer from excited triplet states is less restricted in this respect. The fluorescence emission spectra of the donor molecules (Figures 8.1 and 8.2) show that, with the exception of the protonated 2 - Naphthamide, > 95% of the fluorescence yield occurs within the region 400 - 600 nm. A summary of the absorption characteristics of the metal ion acceptors is given in Table 8.4 and the absorption spectra of the metal ions (as the metal sulphate in dilute sulphuric acid) are shown in Figures 8.5 and 8.6.

Table 8.4 Summary of Spectroscopic Characteristics of the Quencher Metal ions

Metal Ion	Electronic Configuration	Ground State	Absorption Transitions
Fe^{3+}	$3d^5$	^6S	All d-d transitions spin-forbidden; intense charge-transfer absorption extends into the visible
Cr^{3+}	$3d^3$	^4F	$^4A_{2g} \longrightarrow {}^4T_{2g}$(575 nm), $^4T_{1g}$(F)(405 nm), $^4T_{1g}$(P)(270 nm)
Fe^{2+}	$3d^6$	^5D	$^5T_{2g} \longrightarrow {}^5E_g$ (ca. 1000 nm)
Co^{2+}	$3d^7$	^4F	$^4T_{1g}$(F) $\longrightarrow {}^4T_{1g}$(P)(ca. 530 nm), $^4T_{2g}$(1200 nm)
VO^{2+}	$3d^1$	^2D	λ_{max} = 800 nm. Assignment difficult due to strong VO π-bonding component

Table 8.4 (cont.)

Metal Ion	Electronic Configuration	Ground State	Absorption Transitions
Nd^{3+}	$4f^3$	^4I	$^4I \longrightarrow {}^4G$ transitions in 400-600 nm region
Pr^{3+}	$4f^2$	^3H	$^3H \longrightarrow {}^3P$ transitions in 400-600 nm region
Cu^{2+}	$3d^9$	^2D	$^2T_{2g} \longrightarrow {}^2E_g$ (ca. 800 nm)
Ni^{2+}	$3d^8$	^3F	$^3A_{2g} \longrightarrow {}^3T_{2g}$(1180 nm), $^3T_{1g}$(F)(685 nm), $^3T_{1g}$(P)(395 nm)
Mn^{2+}	$3d^5$	^6S	All d-d transitions spin-forbidden
Ag^+	$3d^{10}$	^1S	No d-d transitions; lowest energy transitions 4d $\longrightarrow$ 5s type (224, 211 193 nm)

The absorption spectra of those metal ions listed in Table 8.3 with k_q values greater than 10^7 dm^3 $mol^{-1}s^{-1}$ show that the overlap criterion for electronic energy transfer is met in all cases except possibly Fe^{2+}. It is also observable that the metal ions which do not quench significantly do not absorb in the donor fluorescence region. The relatively low values for the molar extinction coefficients (ϵ) of the Laporte forbidden transitions of the metal aquo complexes in the overlap region , in conjunction with the donor lifetimes of $<$ 40ns, favours electron exchange as an energy transfer mechanism since the Coulombic type is dependent on the magnitude of ϵ.

Although there are no a priori reasons for assuming that all metal ions quench excited singlet states by the same, or even a single, mechanism the considerations above suggest that energy transfer, probably electron exchange, may be the predominant mechanism in many cases. For example, the spectral overlaps between the absorption spectra

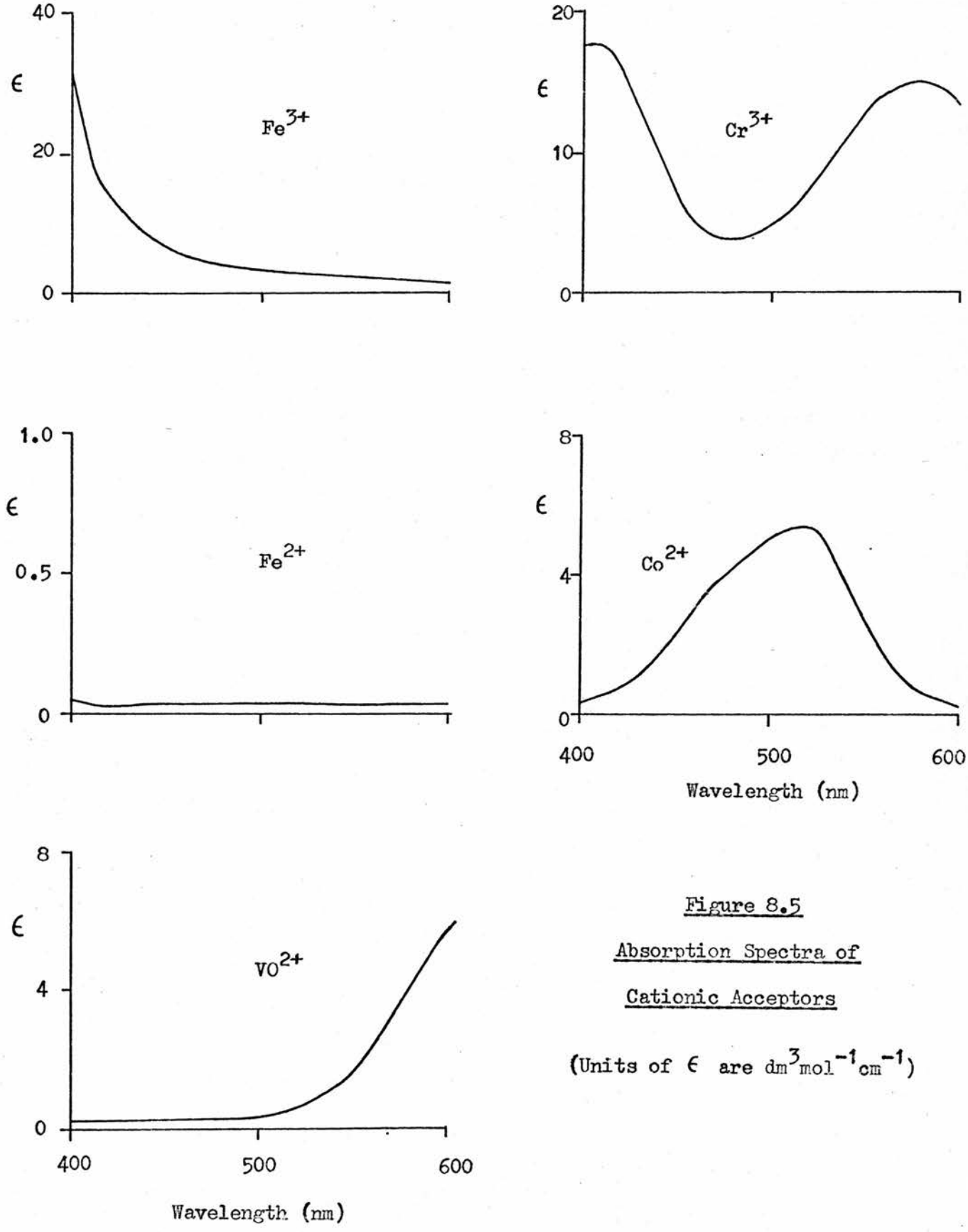

Figure 8.5

Absorption Spectra of

Cationic Acceptors

(Units of ϵ are $dm^3 mol^{-1} cm^{-1}$)

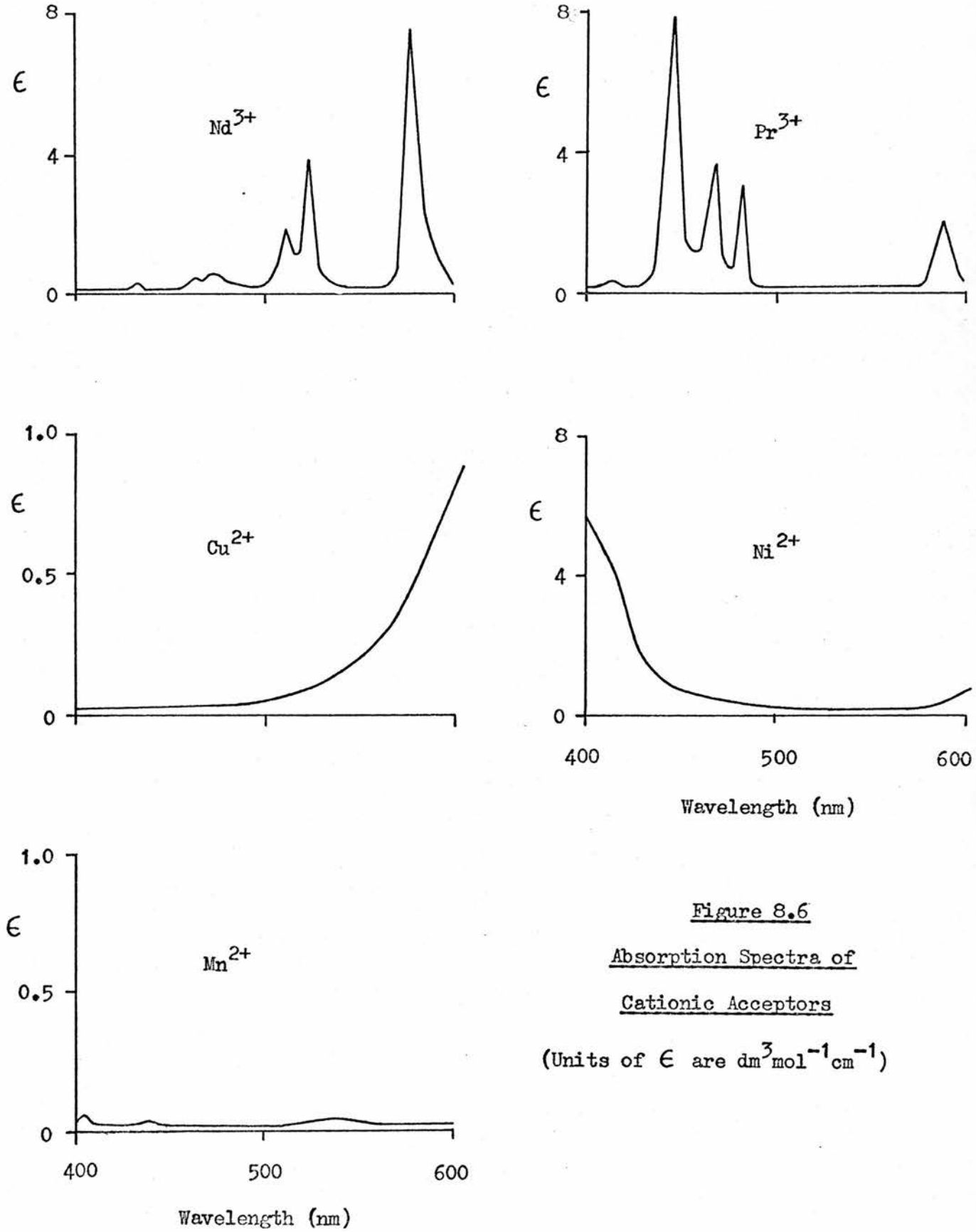

Figure 8.6

Absorption Spectra of

Cationic Acceptors

(Units of ϵ are $dm^3 mol^{-1} cm^{-1}$)

of the Co^{2+} and Cr^{3+} ions and the donor fluorescence spectra are significantly greater than those of the slower quenching VO^{2+}, Cu^{2+} and Ni^{2+} ions irrespective of whether they are calculated on the basis of a Coulombic transfer, i.e. $\oint D(\nu)\epsilon(\nu)d\nu / \nu^4$, or an electron exchange transfer, i.e. $\oint D(\nu)A(\nu)d\nu$, where $D(\nu)$ and $A(\nu)$ are normalised emission and absorption spectra respectively and $\epsilon(\nu)$ is the absorption coefficient. Although the spectral overlap is greater with the lanthanide ions Nd^{3+} and Pr^{3+} than with VO^{2+} and Cu^{2+}, the observed k_q values may reflect the decreased orbital overlap between the donors and the well shielded f-electron orbitals of the lanthanide ions in comparison with the more poorly shielded d-electron orbitals of the transition metal ions. The relatively low k_q values obtained with the Mn^{2+} ion are consistent with the absence of spin allowed d-d transitions from the ^6S ground state. It is thus possible to rationalise the quenching behaviour of all the metal ions in Table 8.3, except Fe^{2+} and possibly Fe^{3+} (see Table 8.4), in terms of electron exchange energy transfer.

The Fe^{2+} ion has a single d-d transition, $^5T_{2g} \longrightarrow {}^5E_g$ (λ_{max} ca. 1000 nm) which has considerably less overlap with the donor emission bands than, for example, Cu^{2+}. The Fe^{3+} ion has the same d^5 electronic configuration as Mn^{2+} but charge-transfer absorption does extend from the ultraviolet into the visible region and overlaps the donor fluorescence. It is therefore not possible to satisfactorily explain the high k_q values obtained with these ions in terms of overlap of d-d absorption and fluorescence spectral bands. They may, however, be associated with the relatively low Fe^{3+}/ Fe^{2+} reduction potential (0.77 V) and the consequent possibilities of charge-transfer related mechanisms. Since the Fe^{3+}/ Fe^{2+} reduction potential is almost identical to that of $Ag^+/$ Ag (0.80 V), the quenching ability of the Ag^+ ion was also examined. These measurements were made in nitric acid solutions (Table 8.5) and

linear Stern - Volmer plots of $\tau_o/\tau = 1 + K\,[Ag^+]$ were obtained in all cases. The Ag^+ ion quenches three of the donors at or close to the diffusion - controlled limit and the other two at slower but measurable rates. The lowest energy transitions of the d^{10} Ag^+ ion are Laporte allowed and lie at wavelengths of less than 250 nm.

Table 8.5 k_q Values for the Quenching by Ag^+ Ions

	Donor Molecule				
	Quinine Sulphate 0.1 M HNO_3	Xanthone 4 M HNO_3	2-Naphthamide 0.5 M HNO_3	Acridine 0.1 M HNO_3	Acridone 7 M HNO_3
k_q = ($dm^3 mol^{-1} s^{-1} x10^{-7}$)	38	270	280	430	1
τ_o (ns)	20.9	18.9	14.7	31.2	21.8

The results above suggest, at least in the absence of ground state complexation, that the ability of a metal ion (M^{n+}) to quench excited singlet states depends on two principal factors (a) the ease of oxidation or reduction of M^{n+} and (b) the degree of spectral overlap of the excited singlet emission and spin-allowed transitions of M^{n+}. Two conclusions, which are likely to have general validity are:-

(a) if M^{n+} is readily reduced or oxidised by a single electron process, efficient dynamic quenching (say $>10^8 dm^3 mol^{-1} s^{-1}$) may occur without spectral overlap, and

(b) if M^{n+} is not readily oxidised or reduced, then efficient quenching is only likely if there is appreciable overlap between the fluorescence spectrum and spin-allowed transitions of M^{n+}.

(c) PHOSPHORESCENCE QUENCHING BY METAL ACETYLACETONATE COMPLEXES

The triplet quenching of aluminium acetylacetonate by some metal acetylacetonates has been studied in ethanol glasses at 77K. It has been shown in Chapter 5 that most diamagnetic and some paramagnetic metal acetylacetonates have triplet energy levels of ca. 26000 cm^{-1} and measurable lifetimes in the millisecond region. The range of suitable $M(AA)_n$ quenchers was therefore restricted to transition metal or lanthanide complexes. Some quenching results were also obtained for the Gd^{3+} and Th^{4+} complexes which have measurable lifetimes of 2 and 6 milliseconds respectively, although these results were characterised by non - exponential lifetimes. For each donor - acceptor system, relative quenching rates were obtained only on the basis of phosphor - escence lifetimes which were measured on the High Resolution spectrofluorimeter.

Although it is not strictly correct to use a Stern - Volmer relationship to derive quenching rate constants for systems where there is no diffusion, e.g. in solid glasses, the variations in lifetime with quencher concentration were correlated by means of a Stern - Volmer plot. For each system, a linear plot of $\tau_o/\tau - 1$ against $[Q]$ was obtained and the slopes of these plots were used to assess the relative quenching abilities of the $M(AA)_n$ complexes (Table 8.7).

The quenching of triplet states by transition metal complexes has been the subject of many recent investigations [258,263,282] but definitive experimental evidence distinguishing between possible mechanisms is rare. In many cases, electronic energy transfer has been suggested as the most probable mechanism and it is likely that the quenching of the phosphorescence of $Al(AA)_3$ by $M(AA)_n$ complexes is also controlled by this process. Since the results of these investigations (Table 8.7)

Table 8.7 Stern - Volmer Results for the Phosphorescence Quenching of $Al(AA)_3$ by $M(AA)_n$ Complexes

$M(AA)_n$ Complex (Quencher)	Lifetime [a] (s)	$(\tau_o/\tau - 1)/Q$ [a] ($dm^3 mol^{-1}$)
Al^{3+}	0.336	—
Mn^{3+}	—	57
Co^{3+}	—	31
Cr^{3+}	— [b]	28
VO^{2+}	—	15
Tb^{3+}	—	0.5
Gd^{3+}	0.002	5 [c]
Th^{4+}	0.006	3 [c]

(a) Emission at 420 nm , wide slits.

(b) No detectable phosphorescence at 420 nm : cf. reference 225.

(c) Non - exponential lifetimes obtained for ethanolic glasses of $Al(AA)_3$ with these quenchers.

were obtained using lifetime measurements, static quenching is not considered as a possible quenching mechanism. The absence of appreciable quenching by the lanthanide complexes or $Th(AA)_4$ effectively eliminates a heavy atom or paramagnetic effect. The possibility of exciplexes being formed in a charge - transfer mechanism cannot be completely discounted but is considered unlikely.

A calculated value for the quenching rate constant of $Mn(AA)_3$ in glasses of $Al(AA)_3$ is ca. 171 $dm^3 mol^{-1} s^{-1}$ which is high for a system which is not diffusion - controlled. An electronic energy transfer mechanism is unlikely to proceed via a dipole - dipole interaction since the T_{π,π^*} ligand absorption for $M(AA)_n$ complexes is spin - forbidden and Wigner's spin rule[280] is not obeyed. However, similar

spin restrictions are not placed on electron - exchange interaction and, since the ligand T_{π,π^*} energy levels of all the $M(AA)_n$ complexes are at ca. 26000 cm^{-1} (Chapter 5), this mechanism is considered to be the most probable quenching process for these systems.

The ordering of the quenching abilities of the acetylacetonates,

$$Mn^{3+} > Co^{3+} > Cr^{3+} > VO^{2+} > Nd^{3+}$$

is dependent on certain properties of the metal complexes which have not been fully explained by the present results. A similar ordering of $Mn^{3+} > Co^{3+} > Cr^{3+}$ has been reported by Napier[283] for the phosphorescence quenching of the $Tb(AA)_3.3H_2O$ complex in n-butanol at 293K. The reported values are 3.59×10^6 , 1.63×10^6 and 1.11×10^6 $dm^3mol^{-1}s^{-1}$ respectively and are much larger than those derived from Table 8.7. However, the n-butanol results are from a system which is diffusion - controlled and it is not unreasonable to conclude that it is only the relative ordering of the metals that is important. Napier has also been unable to interpret the significance of the results although electron - exchange is not considered as a probable mechanism [283].

REFERENCES

1. R.P. Wayne, " Photochemistry ", Butterworths, 1970.
2. A. Jablonski, Nature, 1933, 131, 839.
3. A.N. Terenin, Acta Physicochem., 1943, 18, 210.
4. G.N. Lewis, M. Kasha, J. Amer. Chem. Soc., 1944, 66, 2100.
5. G.N. Lewis, M. Kasha, J. Amer. Chem. Soc., 1945, 67, 994.
6. M. Kasha, Discuss. Faraday Soc., 1950, 9, 14.
7. R.S. Mulliken, J. Chem. Phys., 1955, 23, 1997.
8. J.R. Platt, J. Opt. Soc. Amer., 1953, 43, 252.
9. R.S. Becker, " Theory and Interpretation of Fluorescence and Phosphorescence ", Interscience, 1969.
10. A. Einstein, Z. Phys., 1917, 18, 121.
11. C.A. Parker, " Photoluminescence of Solutions ", Elsevier, 1968.
12. P.A. Leermakers, " Techniques of Organic Chemistry ", Vol. 8, Interscience, 1969.
13. J.N. Demas, G.A. Crosby, J. Phys. Chem., 1971, 75, 991.
14. J.B. Birks, I.H. Munro, Progr. Reaction Kinetics, 1967, 4, 239.
15. W.A. Noyes, G.B. Porter, J.E. Jolly, Chem. Rev., 1956, 56, 49.
16. A.C. Day, Chem. Soc. Ann. Rev., 1967, 46B, 161.
17. S.K. Lower, M.A. El-Sayed, Chem. Rev., 1966, 66, 199.
18. P. Suppan, Chem. Brit., 1968, 4, 538.
19. N.J. Turro, J. Chem. Educ., 1969, 46, 2.
20. J.S. Swenton, J. Chem. Educ., 1969, 46, 7.
21. A. Jablonski, Z. Phys., 1935, 94, 38.
22. D.M. Hercules, " Fluorescence and Phosphorescence Analysis ", Wiley, 1966.

23. G. Binsch, E. Heilbronner, R. Jankow, D. Schmidt, Chem. Phys. Lett., 1967, 1, 135.

24. M. Beer, H.C. Longuet-Higgins, J. Chem. Phys., 1955, 23, 1390.

25. C.E. Easterly, L.G. Christophorau, R.P. Blaunstein, J.G. Carter, J. Chem. Soc. Faraday II, 1973, 69, 471.

26. W.R. Dawson, J.L. Kropp, J. Phys. Chem., 1969, 73, 1752.

27. G.I. Kobyshev, A.N. Terenin, Proc. Int. Conf. on Luminescence, Akaděmai Kaidŏ Budapest, 1968, 520.

28. L.S. Forster, D. Dadley, J. Phys. Chem., 1962, 66, 838.

29. H. Labhardt, Helv. Chim. Acta, 1964, 47, 2279.

30. J.D. Laposa, E.C. Lim, R.E. Kellogg, J. Chem. Phys., 1965, 42, 3025.

31. J.B. Birks, T.A. King, Phys. Lett., 1965, 18, 128.

32. R.G. Bennett, P.J. McCartin, J. Chem. Phys., 1966, 44, 1969.

33. A. Sklar, J. Chem. Phys., 1937, 5, 699.

34. S.P. McGlynn, T. Azumi, M. Kinoshita, " Molecular Spectroscopy of the Triplet State ", Prentice-Hall, 1969.

35. C.A. Parker, C.G. Hatchard, J. Phys. Chem., 1962, 66, 2506.

36. R.M. Noyes, Progr. Reaction Kinetics, 1961, 1, 129.

37. J.B. Birks, " Photophysics of Aromatic Molecules ", Wiley-Interscience, 1970.

38. A. Weller, Progr. Reaction Kinetics, 1961, 1, 187.

39. J.Q. Umberger, V.K. La Mer, J. Amer. Chem. Soc., 1945, 67, 1099.

40. B. Williamson, V.K. La Mer, J. Amer. Chem. Soc., 1948, 70, 717.

41. B. Stevens, J.T. Dubois, Trans. Faraday Soc., 1963, 59, 2813.

42. W.R. Ware, J. Phys. Chem., 1962, 66, 455.

43. J.L. Kropp, M. Burton, J. Chem. Phys., 1962, 37, 1752.

44. H.P. Kallmann, M. Furst, F. Brown, I.E.E.E. Trans. Nucl. Sci. NS-3, 1960, 6, 51.

45. Y.N. Kerr, F.N. Hayes, D.G. Ott, Int. J. Appl. Radiat. Isotopes, 1957, 1, 284.

46. V.L. Agranovitch, I.V. Konobeev, Opt. Spektrosk., 1959, 6, 155.

47. A. Budo, L. Szalay, Z. Naturforsch., 1963, 18A, 90.

48. M.D. Galanin, I.V. Konobeev, Z.A. Chizhikova, Opt. Spektrosk., 1962, 13, 214.

49. T.D.S. Hamilton, Proc. Phys. Soc., 1961, 78, 743.

50. S.F. Kilin, I.M. Rozman, Opt. Spektrosk., 1959, 6, 40.

51. A.M. Samson, Opt. Spektrosk., 1960, 8, 43.

52. V.L. Ermolaev, E.B. Sveshnikova, Izv. Akad. Nauk SSSR, Ser. Fiz., 1962, 26, 29.

53. R.G. Bennett, R.P. Schwenker, R.E. Kellogg, J. Chem. Phys., 1964, 41, 3040.

54. N. Mataga, H. Obashi, T. Okada, J. Chem. Phys., 1969, 73, 370.

55. A.N. Terenin, V.L. Ermolaev, Trans. Faraday Soc., 1956, 52, 1042.

56. V.L. Ermolaev, Opt. Spektrosk., 1959, 6, 417.

57. H.L.J. Bäckström, K. Sandros, Acta Chem. Scand., 1958, 12, 823.

58. G. Porter, G. Wilkinson, Proc. Roy. Soc., 1961, A264, 1.

59. J.B. Birks, J.M.D. Conte, G. Walker, I.E.E.E. Trans. Nucl. Sci., 1966, 13, 148.

60. T. Forster, K. Kasper, Z. Elektrochem., 1955, 59, 976.

61. J.B. Birks, L.G. Christophorau, Nature, 1962, 196, 33.

62. J.B. Birks, L.G. Christophorau, Nature, 1963, 197, 1064.

63. J.B. Birks, L.G. Christophorau, Proc. Roy. Soc., 1963, A274, 552.

64. J.B. Birks, L.G. Christophorau, Proc. Roy. Soc., 1964, A277, 571.

65. J.L. Burdett, M.T. Rogers, J. Amer. Chem. Soc., 1964, 86, 2105.

66. G.T. Morgan, H.D.K. Drew, J. Chem. Soc., 1925, 127, 2611.

67. A. Combes, Compt. Rend., 1887, 105, 869.

68. N.V. Sidgwick, F.M. Brewer, J. Chem. Soc., 1925, 127, 2379.

69. A.E. Martell, M. Calvin, " Chemistry of the Metal Chelate Compounds ", Prentice-Hall, 1952.

70. W.C. Fernelius, B.E. Bryant, Inorg. Synth., 1957, 5, 105.

71. C.M. Harris, S.E. Livingstone, " Chelating Agents and Metal Chelates ", Academic Press, 1964.

72. R.W. Moshier, R.E. Sievers, " Gas Chromatography of Metal Chelates ", Pergamon, 1965.

73. J.P. Fackler, Jr., Progr. Inorg. Chem., 1966, 7, 361.

74. J. Lewis, C. Oldham, J. Chem. Soc. A, 1966, 1456.

75. D.P. Graddon, Coord. Chem. Rev., 1969, 4, 1.

76. R.H. Holm, M.J. O'Connor, Progr. Inorg. Chem., 1971, 14, 241.

77. V. Amirthalingam, V.M. Padmanabhan, J. Shankar, Acta Cryst., 1960, 13, 201.

78. L. Dahl, Mol. Phys., 1962, 5, 169.

79. T.M. Shepherd, J. Chem. Soc., 1972, 813.

80. R.P. Dodge, D.H. Templeton, A. Zalkin, J. Chem. Phys., 1961, 35,55.

81. R.L. Carlin, F.A. Walker, J. Amer. Chem. Soc., 1965, 87, 2128.

82. J. Selbin, Chem. Rev., 1965, 65, 153.

83. D.H. Gerlach, R.H. Holm, Inorg. Chem., 1969, 8, 2292.

84. D.A. Buckingham, R.C. Gorges, G.T. Henry, Aust. J. Chem., 1967, 20, 281.

85. F.A. Cotton, J.S. Wood, Inorg. Chem., 1964, 3, 245.

86. F.A. Cotton, J.J. Wise, Inorg. Chem., 1966, 5, 1200.

87. M. Blackstone, J. van Thiujl, C. Romers, Rec. Trav. Chim., 1966, 85, 557.

88. E.A. Shugam, L.M. Shkol'nikova, Dokl. Akad. Nauk SSSR, 1960, 133, 386.

89. B. Morosin, J.R. Brathovde, Acta Cryst., 1964, 17, 705.

90. R.B. Roof, Acta Cryst., 1956, 9, 781.

91. G.J. Kruger, E.C. Reynhardt, Acta Cryst., 1974, 30B, 822.

92. K. Dymock, G.J. Palenick, Acta Cryst., 1974, 30B, 1364.

93. J.C. Morrow, E.B. Parker, Acta Cryst., 1973, 29B, 1145.

94. J.P.R. De Villiers, J.C.A. Boeyens, Acta Cryst., 1971, 27B, 2335.

95. J.V. Silverton, J.L. Hoard, Inorg. Chem., 1963, 2, 243.

96. T.J. Pinnavaia, B.L. Barnett, G. Podolsky, A. Tulinsky, J. Amer. Chem. Soc., 1975, 97, 2712.

97. B. Matkovic, D. Grdenic, Acta Cryst., 1963, 16, 456.

98. S. Ooi, Q. Fernando, Chem. Commun., 1967, 532.

99. G.J. Bullen, Acta Cryst., 1959, 12, 703.

100. R.C. Elder, Inorg. Chem., 1968, 7, 1117.

101. H. Montgomery, E.C. Lingafelter, Acta Cryst., 1964, 17, 1481.

102. J.T. Hashagan, J.P. Fackler, Jr., J. Amer. Chem. Soc., 1965, 87, 2821.

103. H. Montgomery, E.C. Lingafelter, Acta Cryst., 1963, 16, 748.

104. L.A. Aslanov, M.A. Porai-Koshits, M.O. Dekaprilevich, J. Struct. Chem. (USSR), 1971, 12, 470.

105. L.A. Aslanov, E.F. Korytnyi, M.A. Porai-Koshits, J. Struct. Chem. (USSR), 1971, 12, 661.

106. L.R. Nassimbeni, M.M. Thackeray, Acta Cryst., 1974, 30B, 1072.

107. F.A. Von Schroder, H.P. Weber, Acta Cryst., 1975, 31B, 1745.

108. F.A. Cotton, R.C. Elder, Inorg. Chem., 1965, 4, 1145.

109. G.J. Bullen, R. Mason, P. Pauling, Inorg. Chem., 1965, 4, 456.

110. M.J. Bennett, F.A. Cotton, R. Eiss, Acta Cryst., 1968, 24B, 904.

111. G.D. Smith, C.N. Caughlin, J.A. Campbell, Inorg. Chem., 1972, 11, 2989.

112. C.S. Erasmus, J.C.A. Boeyens, Acta Cryst., 1970, 26B, 1843.

113. J.P.R. De Villiers, J.C.A. Boeyens, Acta Cryst., 1971, 27B, 692.

114. M.J. Bennett, F.A. Cotton, P. Legzdins, S.J. Lippard, Inorg. Chem., 1968, 7, 1770.

115. J.H. Burns, M.D. Danford, Inorg. Chem., 1969, 8, 1780.

116. R.A. Lalancette, M. Cefola, W.C. Hamilton, S.J. La Placca, Inorg. Chem., 1967, 6, 2127.

117. G.T. Morgan, R.B. Tunstall, J. Chem. Soc., 1924, 125, 1963.

118. T. Moeller, " Lanthanides and Actinides ", Butterworths, 1972.

119. K.J. Eisentraut, R.E. Sievers, J. Amer. Chem. Soc., 1965, 87, 5254.

120. V.A. Mode, G.S. Smith, J. Inorg. Nucl. Chem., 1969, 31, 1857.

121. J.E. Sicre, J.T. Dubois, K.J. Eisentraut, R.E. Sievers, J. Amer. Chem. Soc., 1969, 91, 3476.

122. J.K.M. Sanders, S.W. Hanson, D.H. Williams, J. Amer. Chem. Soc., 1972, 94, 5325.

123. J.S. Ghotra, F.A. Hart, G.P. Moss, M.L. Staniforth, Chem. Commun., 1973, 113.

124. S.J. Lippard, B.J. Ross, Inorg. Chem., 1968, 7, 1686.

125. F.P. Dwyer, A.M. Sargeson, J. Proc. Roy. Soc. NSW, 1956, 90, 29.

126. G.T. Morgan, H.W. Moss, J. Chem. Soc., 1914, 105, 189.

127. E.J. Olszewski, D.F. Martin, J. Inorg. Nucl. Chem., 1965, 27, 1043.

128. D.P. Graddon, D.G. Weeden, Aust. J. Chem., 1963, 16, 980.

129. M.F. Richardson, W.F. Wagner, D.E. Sands, Inorg. Chem., 1968, 7, 2495.

130. R.E. Sievers, " Nuclear Magnetic Resonance Shift Reagents ", Academic Press, 1973.

131. R.E. Cramer, K. Seff, Chem. Commun., 1972, 400.

132. W.D. Horrocks, J.P. Sipe, J.R. Luber, J. Amer. Chem. Soc., 1971, 93, 5258.

133. J.F. Desreux, L.E. Fox, C.N. Reilley, Anal. Chem., 1972, 44, 2217.

134. D.P. Graddon, E.C. Watton, Nature, 1961, 190, 906.

135. S. Shibata, M. Kishita, M. Kudo, Nature, 1957, 179, 320.

136. E.W. Berg, J.T. Truemper, Anal. Chim. Acta, 1965, 32, 245.

137. E.L. Muetterties, C.M. Wright, J. Amer. Chem. Soc., 1965, 87, 21.

138. R.F. Riley, R. West, R. Barbarin, Inorg. Synth., 1963, 7, 30.

139. S.K. Dhar, V. Doron, S. Kirschner, J. Amer. Chem. Soc., 1959, 81, 6372.

140. G.T. Morgan, A.R. Bowen, J. Chem. Soc., 1924, 125, 1252.

141. E. White, J. Chem. Soc., 1928, 129, 1413.

142. S.J. Lyle, A.D. Witts, Inorg. Chim. Acta, 1971, 5, 481.

143. M.O. Workman, J.H. Burns, Inorg. Chem., 1969, 8, 1542.

144. H. Soling, Acta Chem. Scand., 1975, A29, 523.

145. A.E. Martell, " Stability Constants of Metal Ion Complexes ", Supplement No. 1, The Chemical Society, 1971.

146. J.K. Marsh, J. Chem. Soc., 1947, 1084.

147. J.G. Stites, C.N. McCarty, L.L. Quill, J. Amer. Chem. Soc., 1948, 70, 3142.

148. F.P. Dwyer, A.M. Sargeson, J. Amer. Chem. Soc., 1953, 75, 984.

149. G.W. Pope, J.F. Steinbach, W.F. Wagner, J. Inorg. Nucl. Chem., 1961, 20, 304.

150. A. Job, P. Goissedet, Compt. Rend., 1913, 157, 50.

151. L.F. Hatch, G. Sutherland, J. Org. Chem., 1948, 13, 249.

152. R.C. Young, Inorg. Synth., 1946, 2, 25.

153. B.E. Bryant, W.C. Fernelius, Inorg. Synth., 1957, 5, 115.

154. W.C. Fernelius, J.E. Blanch, Inorg. Synth., 1957, 5, 130.

155. R.G. Charles, Inorg. Synth., 1963, 7, 183.

156. B.E. Bryant, W.C. Fernelius, Inorg. Synth., 1957, 5, 188.

157. G. Rudolph, M.C. Henry, Inorg. Chem., 1964, 3, 1317.

158. R.C. Young, J. Kovitz, Inorg. Synth., 1946, 2, 123.

159. A. Lodzinska, A. Rozploch, Rocz. Chem., 1970, 44, 1363.

160. T.M. Shepherd, Chem. Ind. (London), 1970, 567.

161. M. Suzuki, M. Nagawa, J. Pharm. Soc. Japan, 1953, 73, 394.

162. C.E. White, R.J. Argauer, " Fluorescence Analysis ", Dekker, 1970.

163. J.F. Ireland, Ph.D. Thesis, (St. Andrews), 1972.

164. R. Lippert, W. Nagele, I. Siebold-Blankenstein, W. Staiger, W. Voss, Z. Anal. Chem., 1959, 170, 1.

165. W.H. Melhuish, J. Phys. Chem., 1960, 64, 792.

166. C.A. Parker, W.T. Rees, Analyst, 1960, 85, 587.

167. R. Rusakowicz, A.C. Testa, J. Phys. Chem., 1968, 72, 2680.

168. R.J. Argauer, C.E. White, Anal. Chem., 1964, 36, 2141.

169. C.G. Hatchard, C.A. Parker, Proc. Roy. Soc., 1956, A235, 518.

170. R.F. Chen, Anal. Biochem., 1967, 20, 339.

171. C.E. White, Anal. Chem., 1960, 32, 438.

172. F.R. Lipsett, J. Opt. Soc. Amer., 1962, 49, 673.

173. C.A. Parker, Anal. Chem., 1962, 34, 302.

174. G.M. Edelman, Rev. Sci. Instrum., 1965, 39, 809.

175. H.V. Drushel, A.L. Sommers, R.C. Cox, Anal. Chem., 1963, 35, 2166.

176. P. Byron, J.B. Hudson, Talanta, 1968, 15, 714.

177. E. Gaviola, Z. Physik., 1926, 35, 748.

178. E. Gaviola, Ann. Physik., 1926, 81, 681.

179. S.S. Brody, Rev. Sci. Instrum., 1957, 31, 1021.

180. L.M. Bollinger, G.E. Thomas, Rev. Sci. Instrum., 1961, 32, 1044.

181. Y. Koechlin, Thesis, (Paris), 1961.

182. W.R. Ware, " Creation and Detection of the Excited State ", Dekker, 1971.

183. M.A. West, G.S. Beddard, Int. Lab., 1975, May/June, 61.

184. A. Muller, R. Lumry, H. Kokubun, Rev. Sci. Instrum., 1965, 36, 1214.

185. W.R. Ware, J. Amer. Chem. Soc., 1961, 83, 4374.

186. L. Brewer, C.G. James, R.G. Brewer, F.E. Stafford, R.A. Berg, G.M. Rosenblatt, Rev. Sci. Instrum., 1962, 33, 1450.

187. W.S. Metcalf, J. Chem. Soc., 1960, 3726.

188. B.D. Venetta, Rev. Sci. Instrum., 1959, 30, 450.

189. R. Bauer, Z. Naturforsch., 1963, 18A, 718.

190. L. Brewer, R.A. Berg, G.M. Rosenblatt, J. Chem. Phys., 1963, 38, 1381.

191. S.F. Kilin, Opt. Spektrosk., 1962, 12, 414.

192. R. Carbone, P. Longaker, Appl. Phys. Lett., 1964, 4, No. 2.

193. R.A. Myers, P.S. Pershan, J. Appl. Phys., 1965, 36, 22.

194. E. Fink, K.H. Welge, Z. Naturforsch., 1964, 19A, 1193.

195. J.B. Birks, D.J. Dyson, T.A. King, Proc. Roy. Soc., 1964, A277, 270.

196. W.R. Falk, L. Katz, Can. J. Phys., 1962, 40, 978.

197. I.B. Berlman, O.J. Steingraber, J. Chem. Phys., 1965, 43, 2140.

198. F.P. Schafer, K. Rollig, Z. Phys. Chem., 1964, 40, 198.

199. G.B. Zarowin, Rev. Sci. Instrum., 1963, 34, 1051.

200. R.G. Bennett, Rev. Sci. Instrum., 1960, 31, 1275.

201. M. Burton, H. Dreeskamp, Z. Elektrochem., 1960, 64, 165.

202. J.T. D'Alessio, P.K. Ludwig, M. Burton, Rev. Sci. Instrum., 1964, 35, 1015.

203. R. Henck, A. Coche, J. Phys. (Paris), 1963, 24, 166.

204. Y. Koechlin, A. Raviart, Nucl. Instrum. Methods, 1964, 29, 45.

205. G. Laustriat, G. Pfeffer, H. Lami, A. Coche, Compt. Rend., 1963, 257, 434.

206. R.L. McGuire, E.C. Yates, D.G. Crandall, C.R. Hatcher, I.E.E.E. Trans. Nucl. Sci., 1965, NS-12, 24.

207. R.H. Müller, H.J. Stolten, Anal. Chem., 1953, 25, 1103.

208. W.I. Higuchi, M.A. Schwartz, E.G. Rippie, T. Higuchi, J. Phys. Chem., 1959, 63, 996.

209. R.H. Holm, F.A. Cotton, J. Amer. Chem. Soc., 1958, 80, 5658.

210. D.W. Barnum, J. Inorg. Nucl. Chem., 1961, 21, 221.

211. K. Yamasaki, K. Sone, Nature, 1950, 166, 998.

212. T.D. Brown, Ph.D. Thesis, (St. Andrews), 1973.

213. D.C. Luehrs, R.T. Iwamoto, J. Kleinberg, Inorg. Chem., 1965, 4, 1739.

214. R.M. Izatt, W.C. Fernelius, B.P. Block, J. Phys. Chem., 1955, 59, 80.

215. R.M. Izatt, W.C. Fernelius, C.G. Hass , B.P. Block, J. Phys. Chem., 1955, 59, 170.

216. I. Grenthe, W.C. Fernelius, J. Amer. Chem. Soc., 1960, 82, 6258.

217. R.G. Bates, H.B. Hetzer, J. Res. Nat. Bur. Stand., 1960, 64A, 427.

218. J. Barthel, R. Wachter, M. Knerr, Electochim. Acta, 1971, 16, 723.

219. J.R. Jones, Chem. Commun., 1968, 513.

220. R. Schaal, F. Peure, Bull. Soc. Chim. Fra., 1963, 2636.

221. J.J. Freemann, G.A. Crosby, J. Phys. Chem., 1963, 67, 2717.

222. G.A. Crosby, R.J. Watts, S.J. Westlake, J. Chem. Phys., 1971, 55, 4663.

223. R.H. Clarke, R.E. Connors, Spectrochim. Acta, 1974, 30A, 2063.

224. P. Sinha, " Complexes of the Rare Earths ", Pergamon, 1966.

225. K. De Armond, L.S. Forster, Spectrochim. Acta, 1963, 19, 1687.

226. M.K. De Armond, J.E. Hillis, J. Chem. Phys., 1968, 49, 466.

227. J.S. Brinen, F. Halverson, J.R. Leto, J. Chem. Phys., 1965, 42, 4213.

228. K. Nakamoto, C. Udovich, J. Takemoto, J. Amer. Chem. Soc., 1970, 92, 3973.

229. G.S. Hammond, P.A. Leermakers, J. Amer. Chem. Soc., 1962, 84, 207.

230. P. Yuster, S.I. Weissman, J. Chem. Phys., 1949, 17, 1182.

231. D.S. McClure, J. Chem. Phys., 1949, 17, 905.

232. E.H. Gilmour, G.E. Gibson, D.S. McClure, J. Chem. Phys., 1952, 20, 829.

233. E.H. Gilmour, G.E. Gibson, D.S. McClure, J. Chem. Phys., 1955, 23, 399.

234. H. Levanon, Chem. Phys. Lett., 1971, 9, 257.

235. R.C. Weast, " Handbook of Chemistry and Physics ", Chemical Rubber Company, 1971.

236. C.A. Fleming, D.A. Thornton, J. Mol. Struct., 1975, 25, 271.

237. J.P. Fackler, Jr., F.A. Cotton, Inorg. Chem., 1963, 2, 102.

238. D.R. Eaton, J. Amer. Chem. Soc., 1965, 87, 3097.

239. H.G. Brittain, Inorg. Chem., 1975, 14, 2858.

240. A.J. Carty, D.G. Tuck, E. Bullock, Can. J. Chem., 1965, 43, 2559.

241. R.G. Linck, R.E. Sievers, Inorg. Chem., 1966, 5, 806.

242. R.C. Fay, T.S. Piper, Inorg. Chem., 1964, 3, 348.

243. J.J. Fortman, R.E. Sievers, Coord. Chem. Rev., 1971, 6, 331.

244. N. Serpone, D.G. Bickley, Prog. Inorg. Chem., 1972, 17, 391.

245. B. Jurado, C.S. Springer, Chem. Commun., 1971, 85.

246. J.J. Fortman, R.E. Sievers, Inorg. Chem., 1967, 6, 2022.

247. T.J. Pinnavaia, J.M. Sebeson, D.A. Case, Inorg. Chem., 1969, 8, 644.

248. J.R. Hutchison, J.G. Gordon, R.H. Holm, Inorg. Chem., 1971, 10, 1004.

249. C. Kutal, R.E. Sievers, Inorg. Chem., 1974, 13, 897.

250. R. Langley, " Practical Statistics ", Pan Piper, 1968.

251. A.H. Bruder, S.R. Tanny, H.A. Rockefeller, C.S. Springer, Inorg. Chem., 1974, 13, 880.

252. W. Biltz, Ann. Phys., 1904, 331, 334.

253. S. Freed, S.I. Weissman, F.E. Fortess, J. Amer. Chem. Soc., 1941, 63, 1079.

254. T. Moeller, W.F. Ulrich, J. Inorg. Nucl. Chem., 1956, 2, 164.

255. J.C.A. Boeyens, J.P.R. De Villiers, J. Cryst. Mol. Struct., 1971, 1, 2971.

256. E.F. Caldin, " Fast Reactions in Solution ", Blackwell (Oxford), 1964, 237.

257. J.D. Neilson, T.M. Shepherd, J. Chem. Soc. Faraday II, 1976, 72, 557.

258. F. Wilkinson, Pure Appl. Chem., 1975, 41, 661.

259. M. Kasha, J. Chem. Phys., 1952, 20, 71.

260. J. Najbar, J. Luminescence, 1975, 11, 207.

261. T. Förster, Disc. Faraday Soc., 1959, 27, 7.

262. H.F. Wagestian, G.S. Hammond, Theor. Chim. Acta, 1971, 20, 186.

263. F. Wilkinson, A. Farmilo, J. Chem. Soc. Faraday II, 1976, 604.

264. K.H. Grellmann, A.R. Watkins, A. Weller, J. Phys. Chem., 1972, 76, 469.

265. P. Bortolus, S. Dellonte, J. Chem. Soc. Faraday II, 1975, 1338.

266. M.T. McCall, G.S. Hammond, O. Yonemitsu, B. Witkop, J. Amer. Chem. Soc., 1970, 92, 6991.

267. R.C. Powell, Z.G. Soos, J. Luminescence, 1975, 11, 1.

268. V. Breuninger, A. Weller, Chem. Phys. Lett., 1973, 23, 40.

269. A.W. Varnes, R.B. Dodson, E.L. Wehry, J. Amer. Chem. Soc., 1972, 94, 946.

270. A. Adamczyk, F. Wilkinson, J. Chem. Soc. Faraday II, 1972, 68, 2031.

271. T.L. Banfield, D. Hussain, Trans. Faraday Soc., 1969, 63, 1985.

272. J. Weiss, Trans. Faraday Soc., 1946, 42, 133.

273. I. Tollert, Z. Phys. Chem. (Leipzig), 1939, 184A, 165.

274. S.P. McGlynn, M.J. Reynolds, G.W. Daigre, N.D. Christodouleas, J. Phys. Chem., 1962, 66, 2499.

275. D. Rehm, A. Weller, Ber. Bunsenges. Phys. Chem., 1969, 73, 834.

276. B.S. Solomon, C. Steel, A. Weller, Chem. Commun., 1969, 927.

277. R. Sahai, R.H. Hofeldt, S.H. Lin, Trans. Faraday Soc., 1971, 67, 1690.

278. K.C. Lin, S.H. Lin, Mol. Phys., 1971, 21, 1105.

279. V. Balzani, R. Ballardini, M.T. Gandolfi, L. Moggi, J. Amer. Chem. Soc., 1971, 93, 339.

280. E. Wigner, Nachr. Ges. Wiss. Gottingen Math. Phys. K1, 1927, 355.

281. D.L. Dexter, J. Chem. Phys., 1953, 21, 836.

282. D.J. Binet, E.L. Goldberg, L.S. Forster, J. Phys. Chem., 1968, 72, 3017.

283. R.N. Napier, Ph.D. Thesis, (St. Andrews), 1976.

284. R.D. Shannon, C.I. Prewitt, Acta Cryst., 1970, 26B, 1076.

285. A.R. Watkins, J. Phys. Chem., 1973, 77, 1207.

286. A.R. Watkins, J. Phys. Chem., 1974, 78, 1885.

287. A.R. Watkins, J. Phys. Chem., 1974, 78, 2555.

288. P. Debye, Trans. Electrochem. Soc., 1942, 82, 265.